ISSN 0385-2520

Rock Magnetism and Paleogeophysics

Volume 15
December 1988

DELP Publication No. 23

Edited by Rock Magnetism and Paleogeophysics Research Group in Japan

Published by the Japanese National Committee for the Dynamics and Evolution of the Lithosphere Project (DELP)

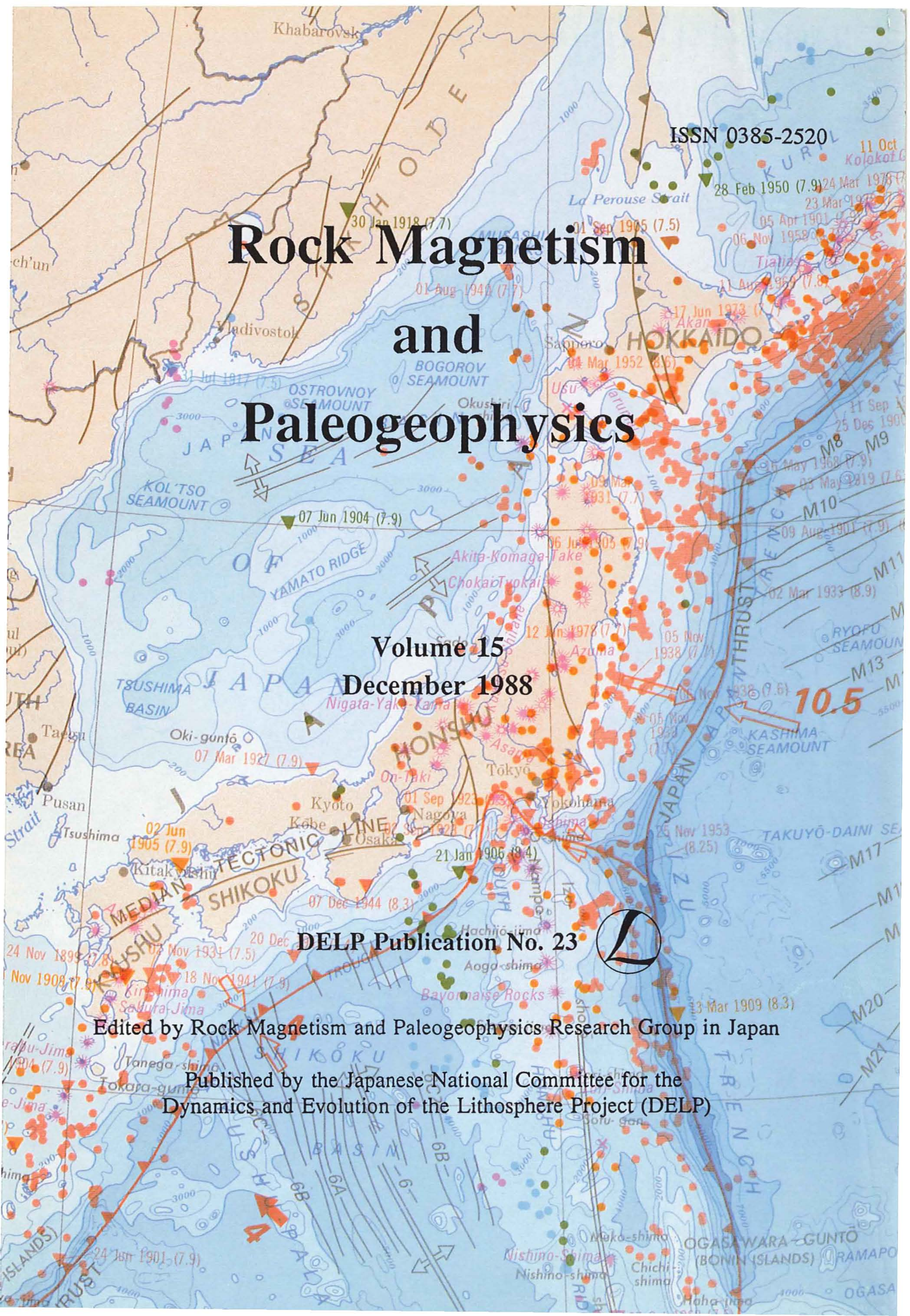

ISSN 0385-2520

Rock Magnetism and Paleogeophysics

Volume 15
December 1988

DELP Publication No. 23

Edited by Rock Magnetism and Paleogeophysics Research Group in Japan

Published by the Japanese National Committee for the
Dynamics and Evolution of the Lithosphere Project (DELP)

まえがき

本書は岩石磁気学・古地磁気学研究グループの１９８８年度の年次研究報告書であり、「国際リソスフェア計画フェア探査開発計画（Dynamics and Evolution of the Lithosphere Project, DELP）」の成果報告（DELP Publication）第２３号として刊行されるものである。

岩石磁気学・古地磁気学研究グループでは、以前から Annual Report として英文の報文集を刊行してきた。（Annual Progress Report of the Rock Magnetism (Paleogeophysics) Reseach Group in Japan, 1963, 1964 1965, 1969; Rock Magnetism and Paleogeophysics, 1973-present）。本巻は Annual Report の第１５巻である。これらの報文集は図書館などからの寄贈要請も多く、諸外国の関連分野の研究者によってかなり広く利用されている。このような経過からこの報文集もすべて英文によって編集された。日本国内の方々には幾分不自由をおかけすることになると思うが、以上の事情によることをご理解いただきたい。

ＤＥＬＰ計画は昭和６０年度から開始されすでに４年が経過した。我々の研究グループは課題５「日本列島の構造発達」に参加し、日本列島及びその周辺のテクトニックな発展の歴史を解明しようと努力を続けている。課題５の研究成果の一部は、７月２２日～２５日に京都府で開かれた研究会で発表された。この研究会のプログラムは目次の後に示されており、また、ここで発表された論文の多くは本研究報告に収められている。

なお、本書はあくまでも extended abstract 集であり、ここに収録された研究はいずれ正式の論文として発表されることになる。投稿中のものや投稿予定のはっきりしているものについては、各報文の最後にそのことが示されているので、引用される場合にはできるだけ正式の論文を参照していただくようお願いしたい。

本書の刊行及び研究会の開催については、文部省国際共同研究等経費「リソスフェア探査開発計画（ＤＥＬＰ）」（代表：秋本俊一）より援助を受けた。ここに記して感謝の意を表する。

１９８８年１２月

岩石磁気学・古地磁気学研究グループ

PREFACE

This volume is the annual progress report of the Rock Magnetism and Paleogeophysics Research Group in Japan for the year 1988. We have published annual reports with a title *Annual Progress Report of the Rock Magnetism (Paleogeophysics) Research Groups in Japan* in 1963, 1964, 1965, and 1967. Since 1973, the title changed to *Rock Magnetism and Paleogeophysics* and the reports were published annually (except 1976).

As the previous reports were so, this volume contains a collection of summaries, extended abstracts or brief notes of the research works carried out in our group this year. Many of the reports contain materials which may undergo a significant change or may be revised as the research activity continues. In this respect, readers are warned to regard them as tentative, and are also requested to refer from a complete paper if such is published as a final result. (Names of journals appear at the end of individual articles if they are in press, submitted, or in preparation for submission to some scientific journals).

This volume is published with a financial aid from Ministry of Education, Science and Culture for the Dynamics and Evolution of the Lithosphere Project (DELP). It is Publication No. 23 of the Japanese DELP Program. We thank other members of the Lithosphere Project for help and encouragements.

Tokyo
December 1988

Masaru Kono
Editor

Rock Magnetism and Paleogeophysics
Research Group in Japan

Table of Contents

まえがき ii

Preface iii

Table of Contents iv

Rock Magnetism and Paleogeophysics Symposium 20 vi

ROCK MAGNETISM

T. Nishitani and S. Sasaki 1
Measurement of Remanent Magnetization of Izu Oshima Lava Flow in 1986

Y. Itoh, M. Araki, I. Katsura, and T. Danhara 4
Magnetic Properties of the Azuki Tuff in Pleistocene Osaka Group, Southwest Japan

T. Yamazaki and I. Katsura 7
Magnetic Grain Size and Viscous Remanent Magnetization of Pelagic Clay

H. Morinaga, H. Imamura, H. Inokuchi, and K. Yaskawa 11
Anomalous Natural Remanent Magnetization of Surface Soils Found in a Pre-Ceramic Site

MAGNETOSTRATIGRAPHY, SECULAR VARIATION

H. Morinaga, I. Horie, H. Murayama, Y.Y. Liu, T. Kuramoto, and K. Yaskawa 15
Age Determination of Collapse in Limestone Cave by Paleomagnetism of Speleothems – An Example for Yuri-no-ana Cave –

Y.Y. Liu, H. Morinaga, I. Horie, H. Maruyama, and Y. Yaskawa 21
Preliminary Report on Paleomagnetism of a Stalagmite, in Ping Le, South China

T. Nakajima 23
Isomagnetic Chart over the Japanese Islands for 25,000 Y.B.P.

M. Miki, H. Inokuchi, J. Matsuda, S. Yamaguchi, N. Isezaki, and K. Yaskawa 25
Preliminary Study of Geomagnetic Paleosecular Variation and K-Ar Ages in Easter Island, the Southeast Pacific

J.E.T. Channell and M. Torii 28
Two "Events" Recorded in the Brunhes Chron at Hole 650 (Leg 107, Tyrrhenian Sea): Geomagnetic, Sedimentological or Deformational Phenomena?

M. Hyodo, W. Sunata, E.E. Susanto, and H. Wahyono 31
Paleomagnetism of Plio-Pleistocene Sediments in Sangiran, Central Java

PALEOMAGNETISM AND TECTONICS, JAPAN

M. Koyama and H. Kitazato 35
Paleomagnetic Evidence for Pleistocene Clockwise Rotation in the Oiso Hills: A Possible Record of Interaction between the Philippine Sea Plate and Northeast Japan

M. Koyama 39
Paleomagnetic Studies in the South Fossa Magna and Adjacent Areas, Japan – Present Status and a Data Base for Future Studies

H. Ueno, K. Hayashi, and M. Nedachi 41
Magnetic Polarity Sequence of the Furutobe Kuroko Mining Area, Akita Prefecture, Japan

T. Yamazaki 47
Paleomagnetism of Miocene Sedimentary Rocks around Matsushima Bay, Northeast Japan and Its Implication to the Time of the Rotation of Northeast Japan

N. Shima, K. Matsumoto, M. Furukawa, and N. Isezaki 50
The Distribution of Magnetization in the Eastern Part of the Japan Basin

I. Kaneoka and M. Yuasa 53
^{40}Ar–^{39}Ar Age Studies on Igneous Rocks Dredged from the Central Part of the Japan Sea During GH78-2 Cruise

H. Tanaka and H. Tsunakawa 56
Paleomagnetic Constraint on the Northern and Southern Borders of Northeast Japan Block and the Timing of Its Rotation

PALEOMAGNETISM AND TECTONICS, WORLD

Y. Otofuji, Y. Inoue, S. Funahara, F. Murata, and X. Zheng 59
Paleomagnetic Study of Eastern Tibet – Deformation of the Three Rivers Region –

A. Hayashida and H. Suzuki 64
Preliminary Paleomagnetic Data from the Paleozoic and Mesozoic Rocks of the Billefjorden Area, Southwest Spitsbergen

Y. Fukao, A. Yamamoto, and M. Kono 65
Gravity Anomaly across the Peruvian Andes

M. Kono, Y. Fukao, and A. Yamamoto 73
Mountain Building in the Central Andes

Author Index 81

ROCK MAGNETISM AND PALEOGEOPHYSICS SYMPOSIUM 20

The 20th Annual Symposium of Rock Magnetism and Paleogeophysics was held between 22nd and 25th of July, 1988, at Kyoto Seminar House in Keihoku-cho, Kyoto 601-05.

Friday 22 July

1. H. Morinaga (Kobe University)
   Anomalous secular variation of the geomagnetic field during 10,000–15,000 yr BP
2. S. Sasajima (Hanazono College of Zen)
   On the reliability of Eurasian APWP for east Asian assembled continental blocks – an improved APWP –
3. M. Funaki (National Polar Research Institute)
   Measurement of magnetic directions of the St. Severin chondrite using magnetotactic bacteria
4. T. Yamazaki (Geological Survey of Japan)
   Magnetic grain size variation and VRM acquisition of pelagic red clay: Characterization by suspension method
5. S. Funahara (Kobe University)
   Paleomagnetic study of the western Tibet: Deformation of the narrow zone along the Indus-Zangbo suture between India and Asia
6. Y. Tatsumi (Kyoto University)
   Opening of the Japan Sea by asthenospheric injection

Saturday 24 July

Special Session: the Earth's Deep Interior and Geodynamo

7. M. Torii (Kyoto Univeristy)
   Opening remarks
8. M. Kono (Tokyo Institute of Technology)
   Geomagnetic dynamo problems
9. M. Ando (Kyoto University)
   Seismic tomography and the structure of the Earth's deep interior
10. Y. Tatsumi (Kyoto University)
    CMB and magma genesis
11. T. Yukutake (Univeristy of Tokyo)
    Study on the Earth's deep interior: Reports on SEDI
12. M. Hoshi (Tokyo Institute of Technology)
    Disk dynamo: A review
13. Y. Yokoyama (University of Tokyo)
    Models of geomagnetic secular variation
14. H. Tsunakawa (Tokai University)

Paleosecular variation: A brief review

15. K. Hirooka (Toyama Univeristy)
    Regional anomaly of Japanese archaeomagnetic declination and Mongolian anomaly

16. T. Yamazaki (Geological Survey of Japan)
    Long-term non-dipole component from the deep-sea sediment core

17. M. Hyodo (Kobe University)
    Pacific dipole window inferred from the Holocene geomagnetic secular variation

18. M. Okada (Shizuoka University)
    Review of Brunges-Matsuyama geomagnetic reversal

19. H. Tanaka (Tokyo Institute of Technology)
    Review of paleointensity studies – Hint to the geodynamo –

Sunday 24 July

20. N. Ishikawa (Kyoto University)
    Paleomagnetic study of Pohang area, southeastern coast of the Korean peninsula

21. Z. Zheng (Tokyo Institute of Technology)
    Preliminary paleomagnetic results from Jingle, Shanxi, North China

22. A. Hayashida (Doshisha University)
    Paleomagnetism of ODP Leg 117 sediments

23. N. Niitsuma (Shizuoka University)
    Results of ODP Leg 117, Neogene Package

24. E. Kikawa (Geological Survey of Japan)
    Secondary magnetization of oceanic gabbros drilled at Atlantis II fracture zone, Southwest Indian Ridge

25. K. Tamaki (University of Tokyo)
    ODP Leg 121 –Broken RIdge–, Ninety East Ridge/Hot spot and rifting

26. T. Furuta (University of Tokyo)
    Rock magnetsim of oceanic basalts

MEASUREMENTS OF REMANENT MAGNETIZATION OF IZU OSHIMA LAVA FLOW IN 1986

Tadashi NISHITANI and Senichi SASAKI

Institute of Mining Geology, Mining College
Akita University, Akita 010

Paleomagnetic directions have been determined on lave flows in Izu Oshima Island which erupted in November, 1986. Sample locations are shown in Fig.1. Eighty-six specimens (30 sites) from LCI lava and 105 specimens (35 sites) from LAII lava flow were collected.

The direction of remanence was almost constant against alternating field and thermal demagnetizations. Mean intensity of remanent magnetization was 1.08 x 10^{-2} Am^2/kg.

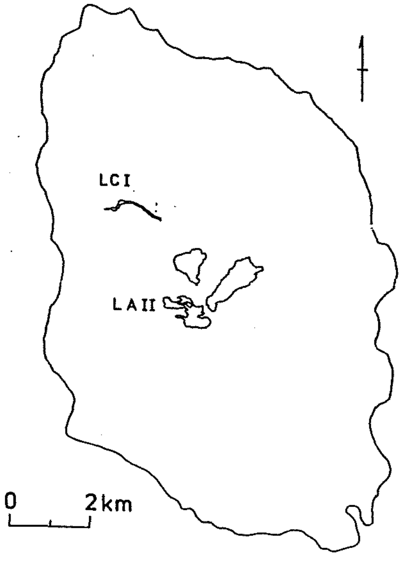

Fig.1(a) Location of Izu Oshima lava flow.

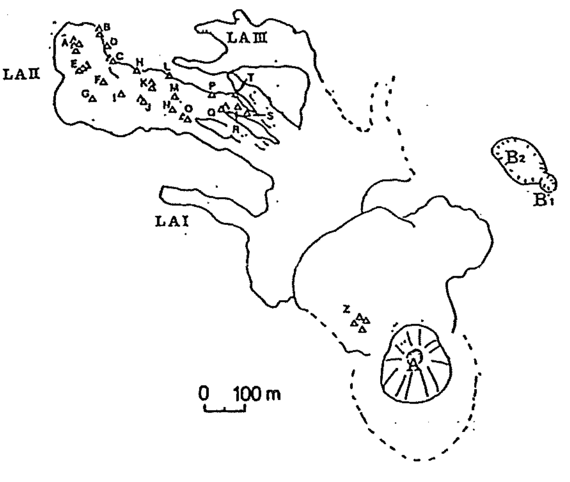

Fig.1(b) Sampling sites at LAII lava flow.

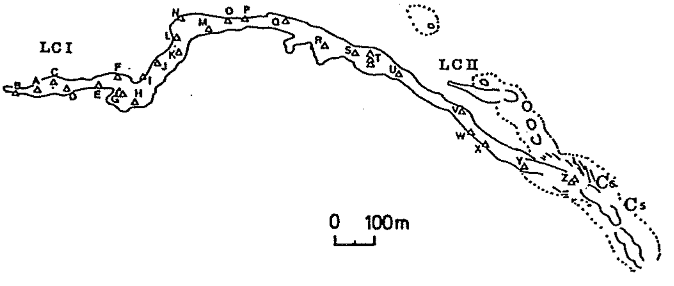

Fig.1(c) Sampling sites at LCI lava flow.

Fig.2(a) and Fig.2(b) show NRM declinations for LAII and LCI lava flows. M.N. means the magnetic north direction. These declinations are widely dispersed.

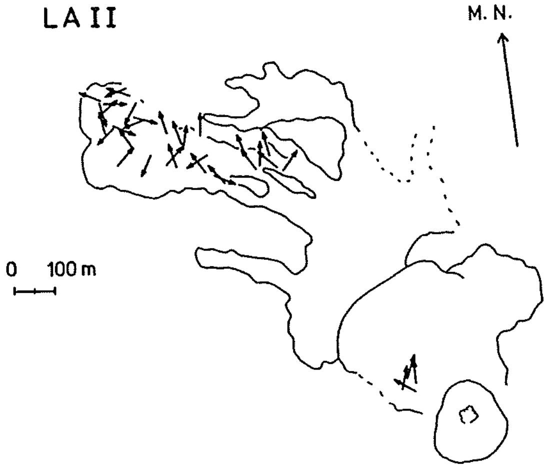

Fig.2(a) Declinations for samples in LAII.
M.N. means magnetic north direction.

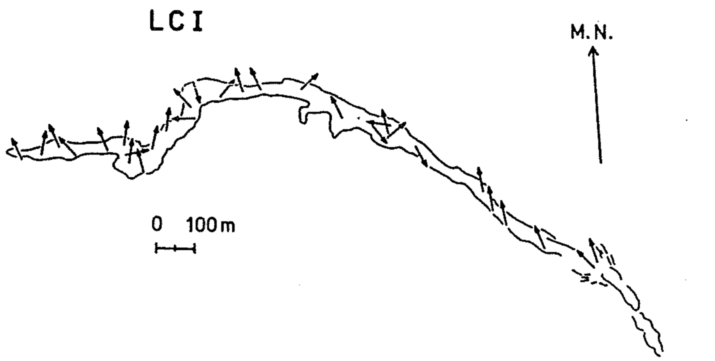

Fig.2(b) Declinations for samples in LCI.

Inclinations for samples LCI and LAII are shown in Fig. 3(a) and Fig.3(b) respectively. In this figure arrows are indicate only inclinations and do not represent the projection of NRM against horizontal plane. Simple mean inclination values are 46.9 ± 12.2^{o} for LAII and 45.4 ± 13.5^{o} for LCI. According to chronological Scientific Tables (1988) the inclination for the Earth's magnetic field around LAII and LCI lavas is 47.1^{o}. Observed inclination is near the direction of the present magnetic field. It can be said from this observation that the horizontal displacement after the remanence was fixed was not so large but rotations were occurred even after the remanence was fixed.

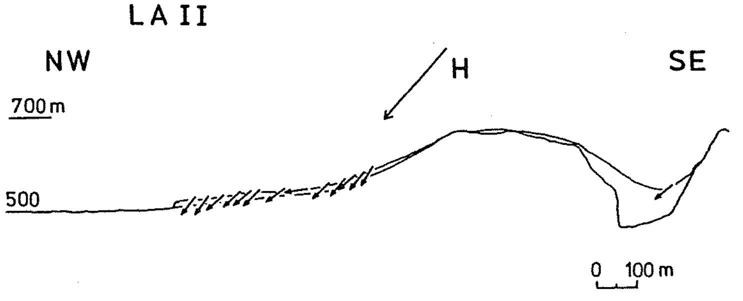

Fig.3(a) Inclination for samples in LAII lava flow. H stands for the direction of Earth's magnetic field.

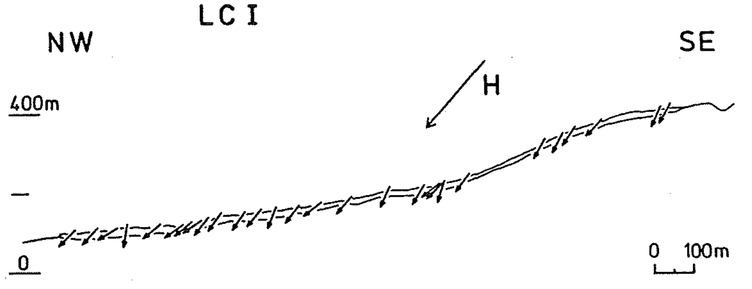

Fig.3(b) Inclination for samples in LCI lava flow.

References

Chronological Scientific Tables (1988), National Astronomical Observatory, Maruzen.

MAGNETIC PROPERTIES OF THE AZUKI TUFF IN PLEISTOCENE OSAKA GROUP, SOUTHWEST JAPAN

Yasuto ITOH*, Makoto ARAKI**, Ikuo KATSURA* and Tohru DANHARA**

* Department of Geology and Mineralogy, Kyoto University, Kyoto 606, Japan
** Kyoto Fission-Track Co., Ltd., Kyoto 615, Japan

The Azuki tuff layer, which shows characteristic lithofacies and mineral assemblage, is the most extensive and important key bed in the Plio-Pleistocene Osaka Group in Southwest Japan. Using thermomagnetic balance, Yokoyama (1975) showed the possibility that the Azuki tuff was distinguished from other tuff layers by its specific Curie temperature spectrum. On the basis of closer investigation, the present authors attempt to describe magnetic properties of the Azuki tuff which are useful in stratigraphic correlation, and to identify magnetic minerals in the tuff layer.

In this study, we collected a block sample (15x15x35 cm) from an outcrop along the Kisen River, west of the Lake Biwa (35°9.61' N, 135°54.73' E). In the Kisen River section, the Azuki tuff is intercalated in non-marine siltstone and divided into four units based on lithofacies. In ascending order, the lithofacies of the units are as follows (see Fig. 1 for thickness of each unit); Unit 1 is white fine tuff, Unit 2 is light gray normal-graded tuff, Unit 3 is brownish light gray normal-graded tuff, and Unit 4 is dark gray bioturbated tuff. The block sample was oriented using a magnetic compass.

As shown in Fig. 1, cubic specimens (22x22x22 mm) were prepared from six horizons of the block sample for paleomagnetic measurements. No specimen was obtained from the thin and fragile Unit 1 layer. Natural remanent magnetizations (NRMs) of the specimens were measured with a ScT C-112 cryogenic magnetometer or a Schonstedt SSM-1A magnetometer in the Kyoto University. Magnetic stability of specimens for each horizon was tested by means of progressive demagnetization with both thermal and alternating field methods. Fig. 2 shows a typical result of progressive thermal demagnetization (PThD) of the Azuki tuff. Acquisition of viscous remanence was negligible during the course

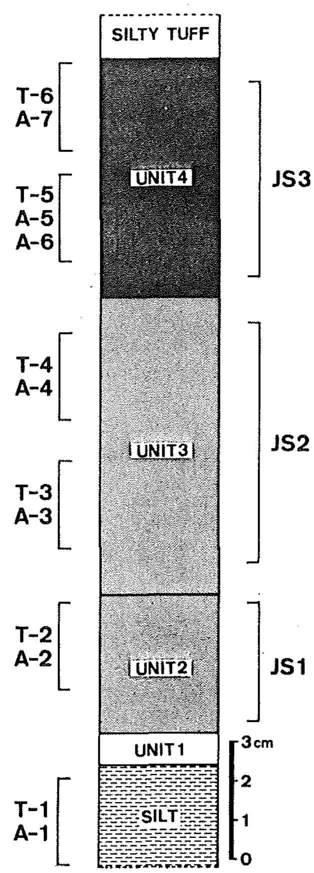

Fig. 1. Simplified columnar section of the Azuki tuff along the Kisen River route, west of the Lake Biwa. Horizons of specimens for paleo-magnetic measurements are shown on the left side of the column. T-series and A-series indicate specimens for progressive thermal and alternating field demagnetizations, respectively. Horizons of separated glass samples for thermomagnetic analysis are shown on the right side of the column. See text for the lithofacies of the four units.

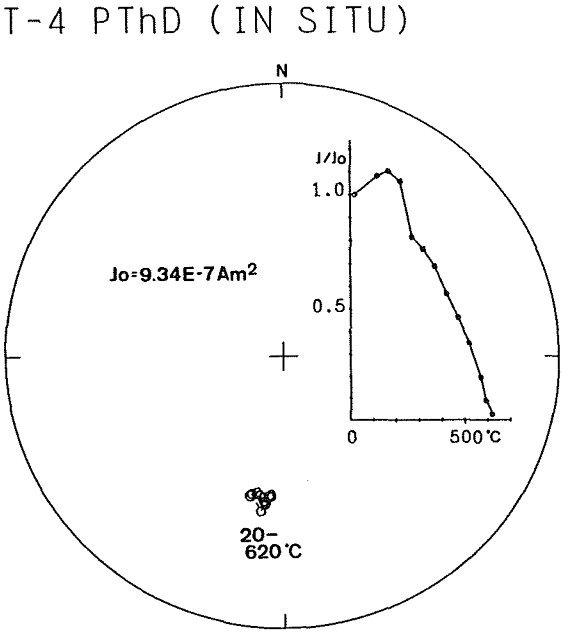

Fig. 2. Equal-area projection of magnetic directions of T-4 during progressive thermal demagnetization in in-situ coordinates. All the directions are plotted on the upper hemisphere. Normalized intensity decay is also shown.

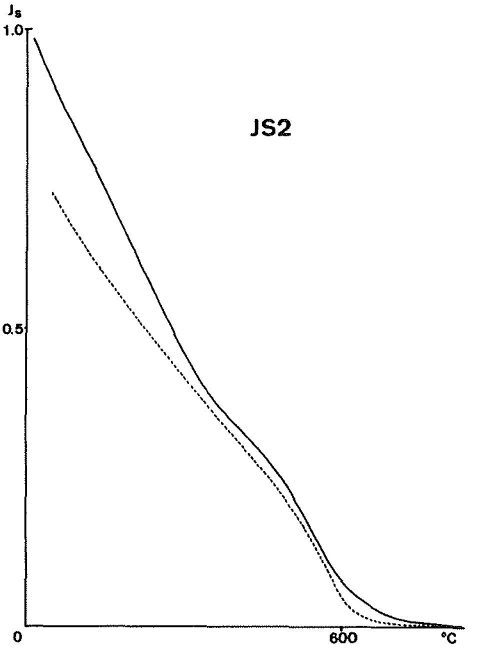

Fig. 3. Thermomagnetic curves for JS2 (separated glasses in Unit 3). The solid and dotted lines indicate heating and cooling processes, respectively.

of thermal treatment. Specimens obtained from other units of the tuff layer showed similar paleomagnetic direction and blocking temperature spectrum. The specimen obtained from underlying siltstone had reversed primary component although the magnetization turned unstable after demagnetization above 300°C.

Preliminary electron microprobe analysis was made for polished thin sections of the Azuki tuff. It has been shown that the volcanic glasses in the Units 3 and 4 contain many sub-micron particles of iron-titanium oxides though they are too small to determine chemical composition using microprobe. Therefore we prepared separated samples of volcanic glasses of the Azuki tuff (see Fig. 1 for sampled horizons) for thermomagnetic analysis. The tuff samples were loosened in water by agitating in an ultrasonic bath and dispersed with aid of peptizer, sodium hexametaphosphate. Heavy minerals were excluded using heavy solution, bromoform. As for the lowermost Unit 1, separating procedure was not carried out because the unit almost consisted of glass shards. A weight of 60-100 mg of sample was heated in the thermomagnetic balance in air at temperatures up to 700°C.

Fig. 3 is the thermomagnetic curves for glass sample in the Unit 3 of the Azuki tuff. As shown in the figure, the heating and cooling curves are almost the same, and Curie temperature estimated from them is consistent with blocking temperature of NRM estimated from J/Jo curve obtained from the same unit (see Fig. 2). Moreover, bulk tuff sample obtained from the Unit 3 showed the same thermomagnetic curves as those in Fig. 3, and had weaker saturation magnetization than separated glass

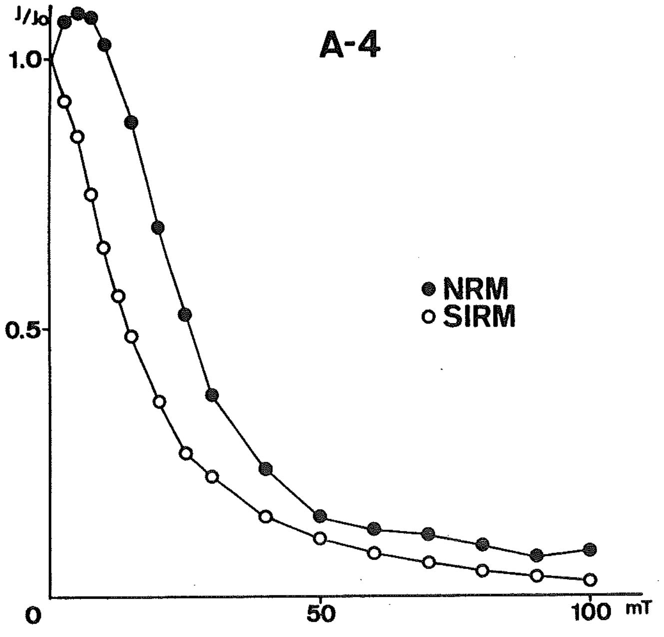

Fig. 4. Normalized intensity of NRM and SIRM during progressive alternating field demagnetization for A-4 in Unit 3.

sample. Samples in the Units 2 and 4 also showed a similar tendency to that of the Unit 3. As for the Unit 1, saturation magnetization was too weak to draw reliable thermomagnetic curves. These results indicate that the stable NRMs of the Units 2 to 4 of the Azuki tuff are carried by sub-micron particles of titanomagnetite contained in volcanic glasses.

The acquisition experiment of isothermal remanent magnetization (IRM) was also performed in fields up to 200 mT for cubic specimens in the Units 2 to 4. The results show that the IRM saturates its intensity in fields of 100 to 150 mT. Subsequently, progressive alternating field demagnetization (PAFD) of the saturation IRM (SIRM) was carried out for the specimens. Fig. 4 delineates the normalized intensity decay of NRM and SIRM of the same specimen obtained from the Unit 3. It is clear that the SIRM is less resistant to the course of PAFD than the NRM, which are also the tendency observed in the Units 2 and 4. Because the NRM of each sub-micron titanomagnetite in volcanic glasses is considered to be the thermal remanence acquired just after the eruption, these data suggest that the carrier of remanence of the Azuki tuff is single-domain titanomagnetite (Lowrie and Fuller, 1971). Thus it has been confirmed that the primary magnetization of the water-laid Azuki tuff is carried by sub-micron magnetic minerals contained in volcanic glasses. Each glass shard would behave as a magnetic particle during the acquisition of depositional remanent magnetization.

References

Lowrie, W. and M. Fuller (1971) J. Geophys. Res., 76, 6339-6349.
Yokoyama, T. (1975) Paleolim. Lake Biwa Japan. Pleist., 3, 114-137.

MAGNETIC GRAIN SIZE AND VISCOUS REMANENT MAGNETIZATION OF PELAGIC CLAY

Toshitsugu YAMAZAKI [1] and Ikuo KATSURA [2]

[1] Marine Geology Department, Geological Survey of Japan, Tsukuba, Ibaraki 305, Japan
[2] Department of Geology and Mineralogy, Kyoto University, Kyoto 606, Japan

Unfossiliferous pelagic clay (red clay) cores from the Pacific generally have unstable remanent magnetization except for tens of centimeters to several meters below the surface [e.g. Kent and Lowrie, 1974; Johnson et al., 1975]. Origin of the instability has been considered to be viscous remanent magnetization (VRM) [Kent and Lowrie, 1974; Yamazaki, 1986]. We conducted a rock-magnetic study of a pelagic clay core from the South Pacific (Core P411, 13°06.16'S, 159°18.01'W). The result of paleomagnetic measurements of this core [Yamazaki, 1986] showed that the unstable-to-stable transition exists at about 1.5 m below the surface, and the secondary ('unstable') component can be removed by the thermal demagnetization at 300°C (Fig. 1).

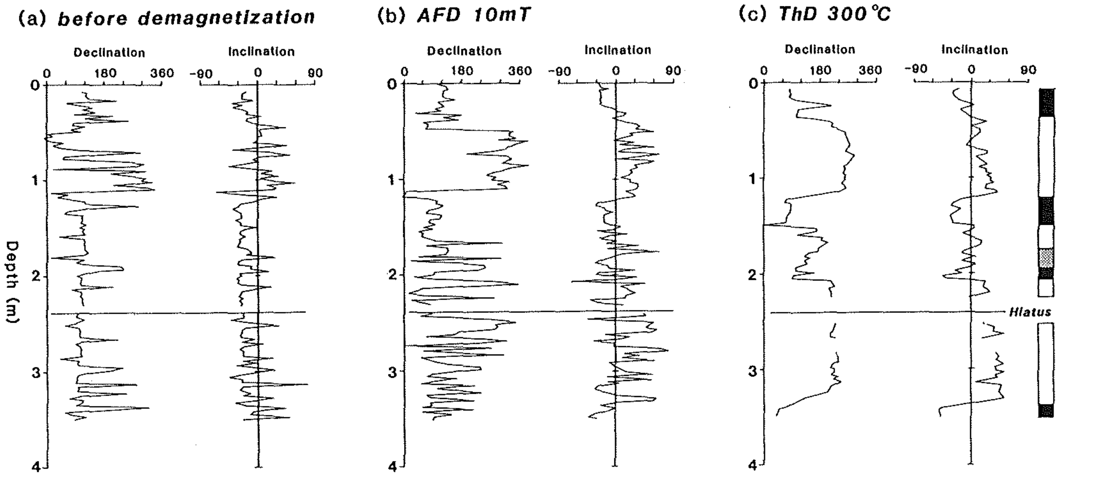

Fig. 1. The direction of remanent magnetization of core P411 (after Yamazaki [1986]). (a) NRM direction before demagnetization, (b) after alternating-field (AF) demagnetization with a peak field of 10 mT, and (c) after thermal demagnetization at 300 °C. Declination is relative because the core was not oriented azimuthally. The unstable-to-stable transition of remanence exists at about 1.5 m.

Using the suspension method of Yoshida and Katsura [1985], we determined down-core variation of complete alignment magnetization (CAM) and magnetic moment distribution (geometric-mean moment (m_G) and log-standard deviation) assuming a log-normal distribution. The mean magnetic-grain diameter (Fig. 2) was calculated from the m_G using the saturation magnetization of magnetite, 4.8 x 10^5 Am^{-1}, on the assumption that all the magnetic grains are SD (single-domain) magnetites of spherical shape. This assumption is supported by strong-field thermomagnetic analyses (Curie temperature of about 580°C), IRM (isothermal remanent magnetization) acquisition experiments (saturated at fields of 0.3T or less) and the ratio of CAM to SIRM (0.25 to 0.35). The diameter ranges from about 0.02 to 0.15 μm, which is roughly equivalent to the SD grain-size range of magnetite [Dunlop, 1973; Butler and Banerjee, 1975]. The diameter decreases remarkably with depth below about 1 m (Fig. 2). The derived grain size holds even when

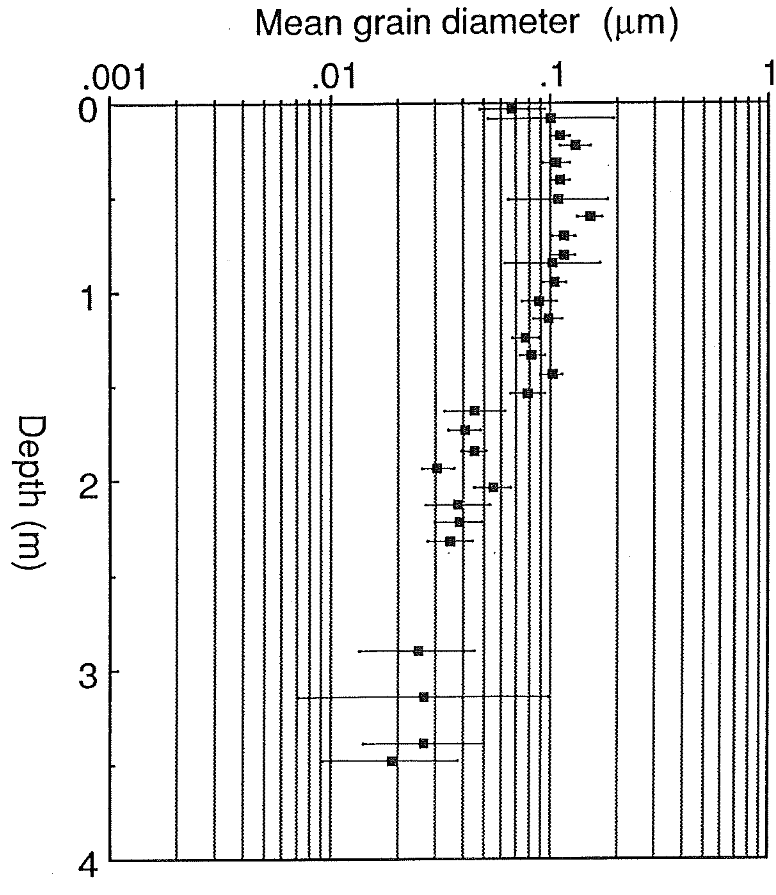

Fig. 2. The mean magnetic-grain diameter of the core calculated from the mean magnetic moment on the assumption that all magnetic grains are SD magnetite of spherical shape. The bar attached to the mean represents its uncertainty which propagated from the uncertainty of the mean magnetic moment.

the magnetites in the sediments suffered oxidation because the saturation magnetization of maghemite is close to that of magnetite. The frequency dependence of susceptibility increased downward (Fig. 3). This indicates the increase of the amount of superparamagnetic (SP) grains with depth [Mullins and Tite, 1973; Bloemendal et al., 1985], which is in accordance with the above grain-size estimation.

On the other hand, the viscosity acquisition coefficient normalized by the CAM increases with depth (Fig. 4). This agrees well with the experimental results of Tivey and Johnson [1981] and Dunlop [1983] that for the synthetic magnetite grains from 0.02 to 0.35 μm in diameter, the magnetic viscosity coefficient increases with decrease of grain diameter. We concluded that the magnetic grain size mainly controls the magnitude of the secondary magnetization, VRM, of pelagic clay.

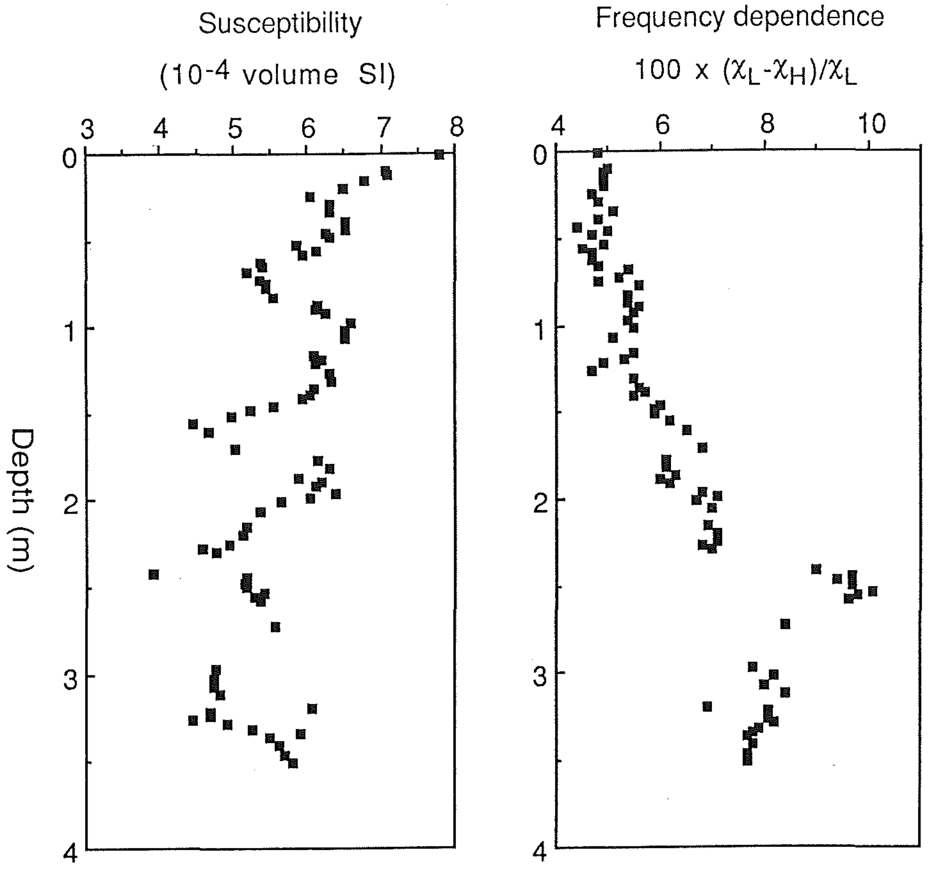

Fig. 3 Low-field low-frequency (0.47 kHz) susceptibility (left), and frequency dependence of susceptibility (right). The frequency dependence is defined as 100 x $(\chi_L-\chi_H)/\chi_L$, where χ_L and χ_H are low-frequency (0.47 kHz) and high-frequency (4.7 kHz) susceptibility, respectively.

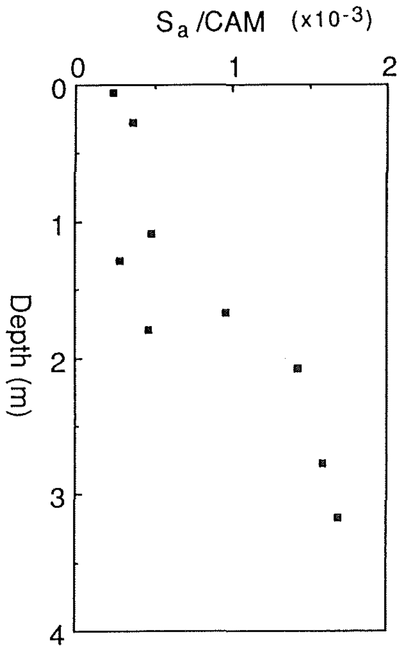

Fig. 4 Down-core variation of the magnetic viscosity coefficient for VRM acquisition (S_a) normalized by CAM.

Origin of pelagic clay has been considered to be mainly eolian dust [e.g. Rex and Goldberg, 1858; Janecek and Rea, 1983]. We believe that the intensified global atmospheric circulation by the change of climate causes the growth of grain size of magnetic minerals, which leads the unstable-to-stable transition of remanence.

References

Bloemendal, J., C.E. Barton, and C. Radhakrishnamurthy (1985) *J. Geophys. Res., 90,* 8789.

Butler, R.F. and S.K. Banerjee (1975) *J. Geophys. Res., 80,* 4049.

Dunlop, D.J. (1973) *J. Geophys. Res., 78,* 1780.

Dunlop, D.J. (1983) *Geophys. J. R. astr. Soc., 74,* 667.

Janecek, T.R., and D.K. Rea (1983) *Geol. Soc. Amer. Bull., 94,* 730.

Johnson, H.P., H. Kinoshita, and R.T. Merrill (1975) *Geol. Soc. Amer. Bull., 86,* 412.

Kent, D.V., and W. Lowrie (1974) *J. Geophys. Res., 79,* 2987.

Mullins, C.E., and M.S. Tite (1973) *J. Geophys. Res., 78,* 804.

Rex, R.W., and E.D. Goldberg (1958) *Tellus, 10,* 153.

Tivey, M., and H.P. Johnson (1981) *Geophys. Res. Lett., 8,* 217.

Yamazaki, T. (1986) *Geophys. Res. Lett., 13,* 1438.

Yoshida, S., and I. Katsura (1985) *Geophys. J. R. astr. Soc., 82,* 301.

(Submitted to *J. Geophys. Res.*)

ANOMALOUS NATURAL REMANENT MAGNETIZATION OF SURFACE SOILS FOUND IN A PRE-CERAMIC SITE

Hayao MORINAGA[1], Hiroshi IMAMURA[2], Hiroo INOKUCHI[2], and Katsumi YASKAWA[2]

1. The Graduate School of Science and Technology, Kobe University, Nada, Kobe 657, Japan
2. Faculty of Science, Kobe University, Nada, Kobe 657, Japan

1. Introduction

It is possible for lightning to strike surface soils and rocks and impart a complex magnetization. The effects of lightning tend to be superficial as the current is usually dissipated in the wet upper layers and the magnetic effects on soils and rocks usually decrease rapidly with depth, to be generally negligible below some 20 m (Tarling, 1983). Anomalous and strong magnetization caused by lightning has been reported for volcanic rocks by Matsuzaki et al. (1954), Cox (1961) and Nakajima and Hirooka (1980). The remanent directions of each small area in rocks struck by lightning were either scattered in direction (Matsuzaki et al., 1954) or rather tangential in declination, on circles centering around a certain point (Nakajima and Hirooka, 1980). The tangentially directed declinations distributed in the rocks imply that the remanences were acquired under a circular magnetic field due to line electric current of lightning discharge (Nakajima and Hirooka, 1980). The complex remanence by lightning is of isothermal origin, determined through an acquisition experiment and an alternating-field (AF) demagnetization study (Matsuzaki et al., 1954; Cox, 1961; Nakajima and Hirooka, 1980).

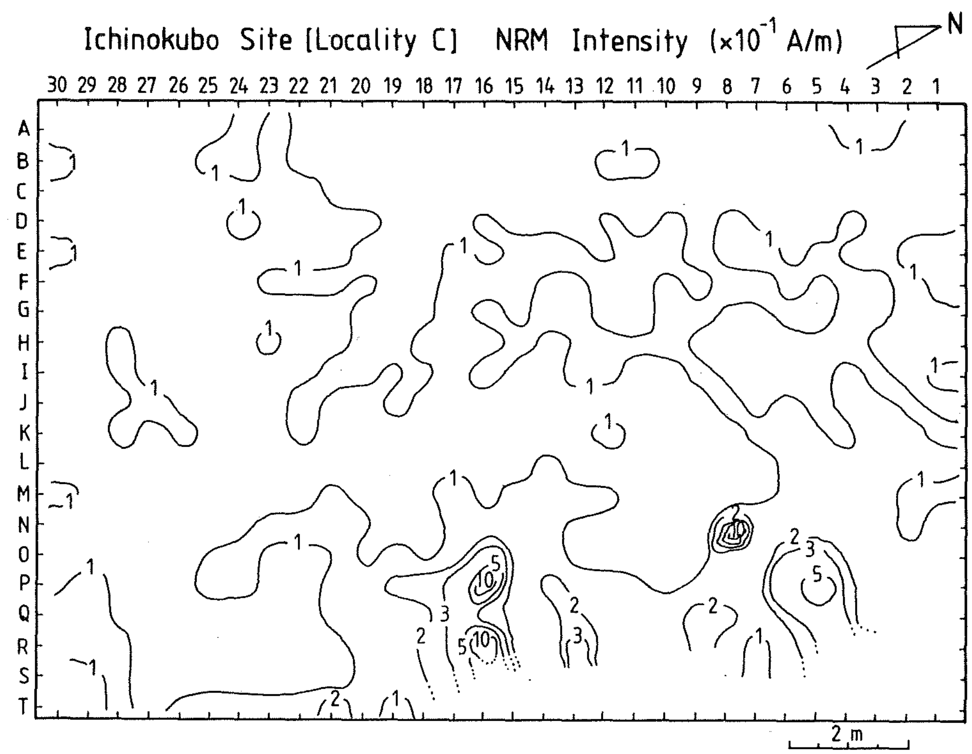

Figure 1 Distribution chart of NRM intensities on the surface of Ichi-no-kubo paleolithic site [Locality C].

This paper describes an anomalous natural remanent magnetization (NRM) of surface soils containing volcanic ashes, which were detected at Ichi-no-kubo site in Oita Prefecture. This site is dated from the early Pre-ceramic age (about 9,000 years ago), by the features of stone implements. In order to estimate positions of the past fireplaces, paleomagnetic investigation was carried out at three localities in this site. The anomalous NRM, which can not be ascribed to thermal events, was detected only in one [locality C] of these three localities. Only the results from locality C are reported here in detail.

2. Sampling and magnetic measurement

Locality C covered an area of 150 (10× 15) m^2 and was divided by mutually perpendicular strings stretched every 50 cm. The strings aligned with NW55° direction were numbered in order of progression from geographic north, while the strings aligned with NE25° direction were alphabetized in order of progression from geographic north (Figs.1 and 2). Paleomagnetic soil samples were then obtained at intersections of two mutually perpendicular strings, by pressing 2.2× 2.2× 2.2 cm^3 non-magnetic polycarbonate boxes vertically into the flat face of the exposed soil, taking care to align certain sides parallel to reference strings. The orientation is therefore considered accurate to within ± 5° in inclination and declination. We collected 510 samples and named them after two mutually perpendicular strings stretched on the sampling positions; for example, 1-A, 15-D, 25-P, and so on.

NRM of the soil samples was measured using a cryogenic magnetometer, whose sensitivity is 10^{-11} Am^2. The NRM intensities before AF demagnetization ranged from 0.25 to 10.94 $\times 10^{-1}$ A/m. Distribution charts

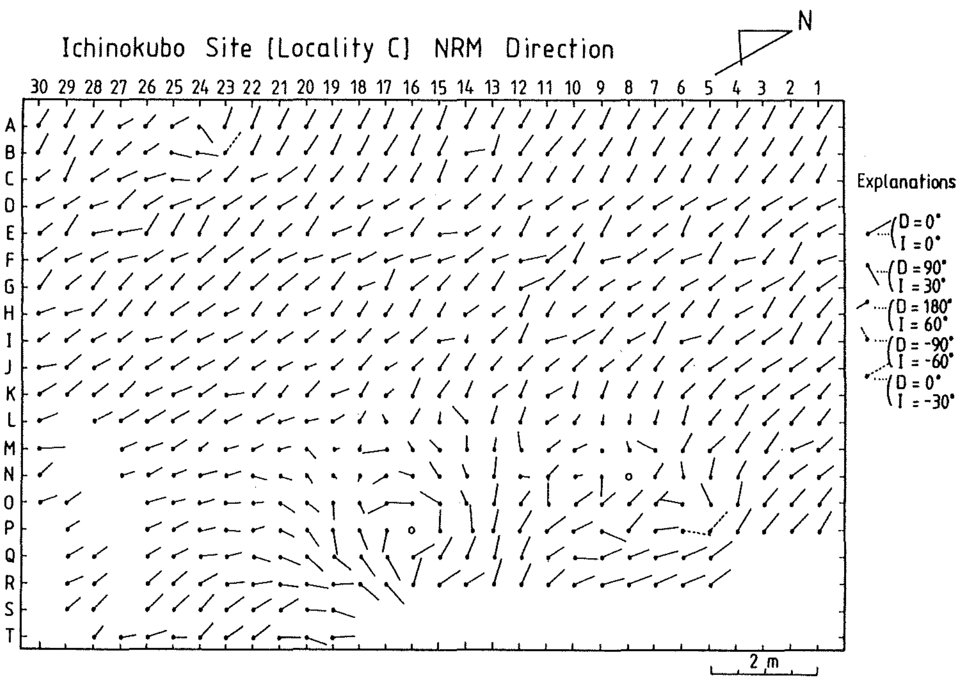

Figure 2 Distribution chart of NRM directions on the surface of Ichi-no-kubo paleolithic site [Locality C]. Solid and broken lines, which are projections of magnetization vectors drawn from the sampling points on to the horizontal plane, show positive and negative inclinations respectively. The two open circles indicate sampling positions of immeasurable samples.

of the NRM intensity and direction on the surface of the site are shown in Figure 1 and Figure 2, respectively. The NRM directions are indicated by lines, which are projections of magnetization vectors drawn from the sampling points (dots), on to the horizontal plane (Fig.2). Solid and broken lines show positive and negative NRM inclinations respectively. Two samples, 8-N and 16-P (open circles in Fig.2) had too strong NRM to be measured with the cryogenic magnetometer. Therefore, only the minimum intensities could be estimated and their directions could not be calculated. The minimum intensities are used in case of drawing the magnitude contour lines (Fig.1).

Four samples (5-P, 8-N, 16-P, and 16-R) containing the two immeasurable ones have very strong NRM (> 5.00×10^{-1} A/m), which show values of more than ten times those of the other samples. The strong NRM, however, did not show enough magnitude to rotate the needle of the magnetic compass during sampling. The other samples distributed around these four have NRM of rather strong intensity and declination directed tangentially on circles centering around the four sample positions; particularly around positions of the two samples 8-N and 16-P. The samples distributed over the southwestern regions from these positions have NRM of rather normal intensity and declination fairly trailed in the tangential direction.

3. Discussions and conclusions

The anomalous NRM found in Ichinokubo site is IRM, and is ascribed to lightning. A study of progressive AF demagnetization was conducted on two samples (5-P and 16-R), of the anomalously strong NRM in locality C (Fig.3-a and 3-b), in order to judge what they were caused by . In Figure

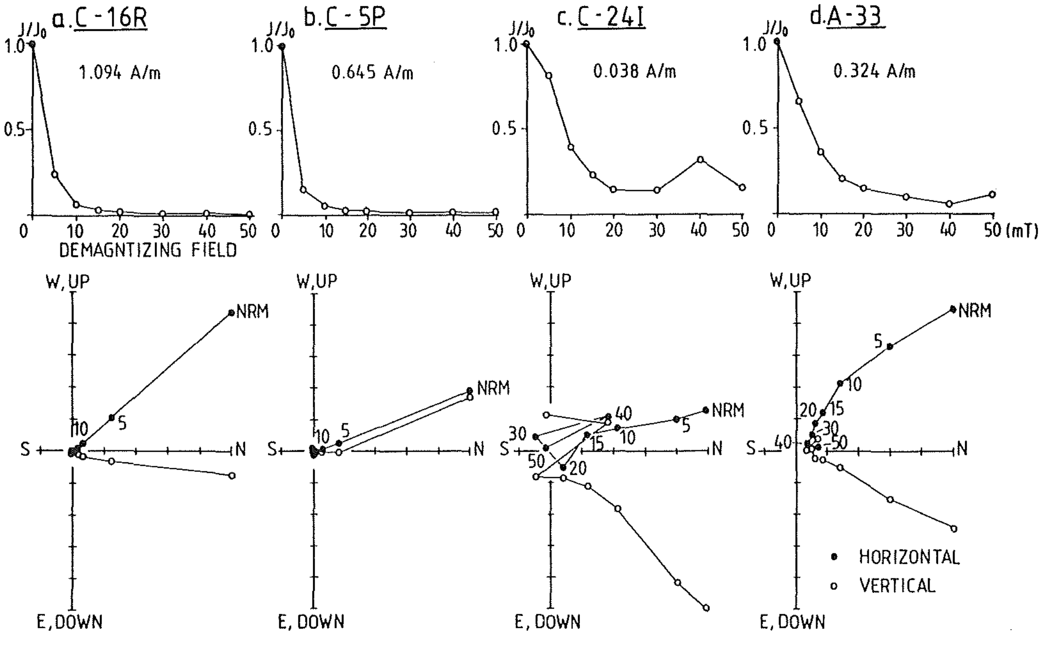

Figure 3 Intensity decay curves (upper figures) and orthogonal vector diagrams for typical samples; a and b are anomalously strong NRM samples in locality C, c is a normal NRM sample in locality C, and d is a detectably baked sample collected from a different locality in Ichi-no-kubo site.

3, the results for a normal NRM sample in the identical locality (c) and a detectably baked sample collected from a different locality in this site (d) are also shown. Intensity decay curves for the two anomalous NRM samples differ obviously from the other ones. The anomalous NRM shows a very strong intensity, but its intensity decays more quickly than the other ones (Fig.3-a and 3-b). The normal NRM sample has much a weaker intensity than the anomalous ones (Fig.3-c). The baked sample has not only rather strong but also stable NRM (Fig.3-d). The anomalous strong NRM can not be explained as having been baked. Such a magnetic behavior of the anomalous NRM during the progressive AF demagnetization is very similar to those of rocks affected by lightning (Matsuzaki et al., 1954; Cox, 1961; Nakajima and Hirooka, 1980). The obviously tangential and tangentially trailed NRM declinations (Fig.2) also suggest that the soils distributed over a portion of this locality were remagnetized by a circular magnetic field due to line electric current of lightning discharge. This is strong evidence that the remagnetized NRM is of isothermal origin.

On closer investigation of the anomalous NRM directions, it is shown that the NRM also has a component relating to either the past or the nearly present geomagnetic field. The anomalous NRM seems to be composed of IRM acquired by the circular magnetic field due to lightning, and remanence acquired under the past or the nearly present geomagnetic field. The quick intensity decay of the anomalous NRM due to thunderbolts implies that the remagnetized NRM is not so stable, and hence that the remagnetization event occurred almost recently. This may demonstrate that the anomalous NRM is not related to the paleolithic site itself. It is necessary to distinguish carefully between the anomalous NRM due to lightning, and that of the baked earth.

References

Cox, A. (1961) *US Geol. Surv. Bull.*, **1083E**, 131.

Matsuzaki, H., K. Kobayashi, and K. Momose (1954) *J. Geomag. Geoelectr.*, **6**, 53.

Nakajima, T. and K. Hirooka (1980) *Rock Mag. Paleogeophys.*, **7**, 52.

Tarling, D. H. (1983) *Palaeomagnetism* (Chapman and Hall, London), 379.

(To be submitted to J. Geomag. Geoelectr.)

AGE DETERMINATION OF COLLAPSE IN LIMESTONE CAVE BY PALEOMAGNETISM OF SPELEOTHEMS - AN EXAMPLE FOR YURI-NO-ANA CAVE -

Hayao MORINAGA[1], Ikuko HORIE[2], Haruko MURAYAMA[2], Yu Yan LIU[2], Tadashi KURAMOTO[3], Katsumi YASKAWA[2]

[1]The Graduate School of Science and Technology, Kobe University, Nada, Kobe 657, Japan
[2]Faculty of Science, Kobe University, Nada, Kobe 657, Japan
[3]Akiyoshi-dai Museum of Natural History, Akiyoshi, Yamaguchi 754-05, Japan

1. Introduction

The aspect of geomagnetic secular variation has been clarified by archeomagnetism and paleomagnetism of lake and shallow marine unconsolidated sediments (Creer et al., 1983). The main aim of these works is to understand the origin of the geomagnetic field and its variation as well as geophysical processes at core-mantle boundary, by using periodicity of the available geomagnetic secular variation. Another aim is to determine ages of archeo-sites and stratigraphic units and of activity for ancient earthquakes and faults, by utilizing the variation curve as time-scale. If a standard curve, which expresses more-completely the true behavior of the geomagnetic field can be established, it will be possible to determine ages with a small amount of paleomagnetic data. Under the existing circumstance, however it is possible to determine their rather-accurate ages only by a method comparing variation records for a certain period with the existing paleo-secular variation. We report here one example of dating by this method.

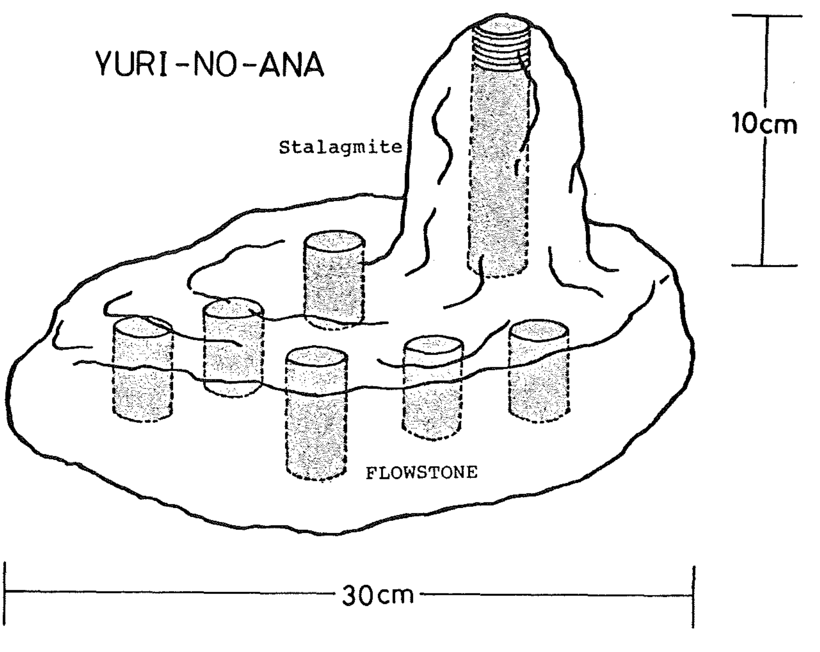

Fig.1 Schematic view of a flowstone block and a stalagmite growing on the block. These speleothems were existed on the cave floor as it is. Core samples 2.5 cm in diameter were drilled out in the laboratory.

Some limestone caves distributed over West Japan, Akiyoshi-do cave and Yuri-no-ana cave in the Akiyoshi Plateau, Yamaguchi and Seiryu-kutsu cave in the Hirao Plateau, Fukuoka, both present a site of base rocks and secondary concretions (speleothems) collapsed from their ceiling and walls. In Yuri-no-ana cave, stalagmites and stalactites about 1 m in diameter have been broken off, and now lie on the cave floor. In Akiyoshi-do cave and Seiryu-kutsu cave, some meter thick base rocks and speleothems have slided down, making chasms.

Speleothems, particularly stalagmites and flowstones generally have fairly stable natural remanent magnetization (NRM). They also continuously record the geomagnetic field in the same way as unconsolidated sediments because of their continuous growth (Latham et al., 1979, 1982, 1986 & 1987; Inokuchi et al., 1981; Morinaga et al., 1985, 1986 & 1988). We estimate here the age of a collapse comparing the continuous records kept in speleothems with the existing geomagnetic secular variation curve deduced from paleomagnetism of unconsolidated sediments in Japan.

2. Samples and Magnetic Results

A flowstone block, and a stalagmite growing on the block were collected from Yuri-no-ana cave in West Akiyoshi Plateau. The flowstone block is 5 to 10 cm in thickness, about 30 cm long diameter and about 15 cm short diameter (Fig.1), and existed on the cave floor as it is. This flowstone must record the geomagnetic field possibly before its emplacement. The stalagmite is 10 cm or less in height and 5 to 10 cm in diameter (Fig.1). This stalagmite may have been grown until the time of sampling, because ground water was being supplied to its top at the time. This suggests the possibility of recording the geomagnetic field from after emplacement of the flowstone to the present.

As the sample was not oriented at the time of sampling, no information is available on direction of the sample within a horizontal plane. However, it was confirmed that growth (extension) direction of the stalagmite is coincident with

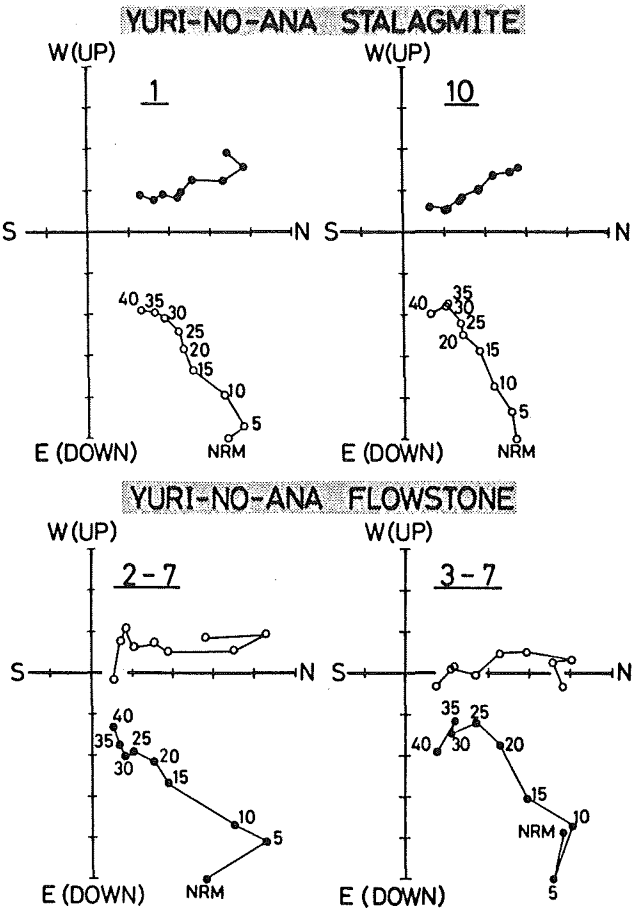

Fig.2 Typical orthogonal vector component diagrams for progressive AF demagnetization of subsamples from the stalagmite (upper) and the flowstone (lower). Numbers adjacent to circles denote peak demagnetizing AF in mT. closed circles, projection on horizontal plane; open circles, projection on vertical plane.

a vertical axis. That is, declination values from the stalagmite are relative and the inclination values are against the Earth's coordinate system.

Six core samples 2.5 cm in diameter were drilled out in the laboratory from the flowstone and one from the stalagmite, and then were cut by a diamond blade into thin disk subsamples of 2.5 mm thick (Fig.1). The natural remanent magnetization (NRM) of subsamples was measured in a cryogenic magnetometer whose sensitivity is 10^{-11} Am^2.

The NRM intensities of subsamples ranged from 10^{-5} to 10^{-6} A/m. After the NRM measurement, all the subsamples were cleaned by progressive alternating field (AF) demagnetization at 5 mT intervals, then remeasured for remanence (Fig.2). The stalagmite subsamples generally had very stable remanences and showed only one component after viscous remanent magnetization was removed at an AF level of 5 mT. The flowstone subsamples usually had less stable remanences than the stalagmite ones. Some of the flowstone subsamples did not show any stable components at all. Except for these unstable subsamples, characteristic directions of the rest all subsamples were obtained by averaging measured values after AF demagnetization at the levels showing a stable component. In case of a stalagmite subsample 1, for example, the characteristic direction was obtained by averaging measured values after the demagnetization at the levels from 5 to 35 mT. This procedure is effective to eliminate an error

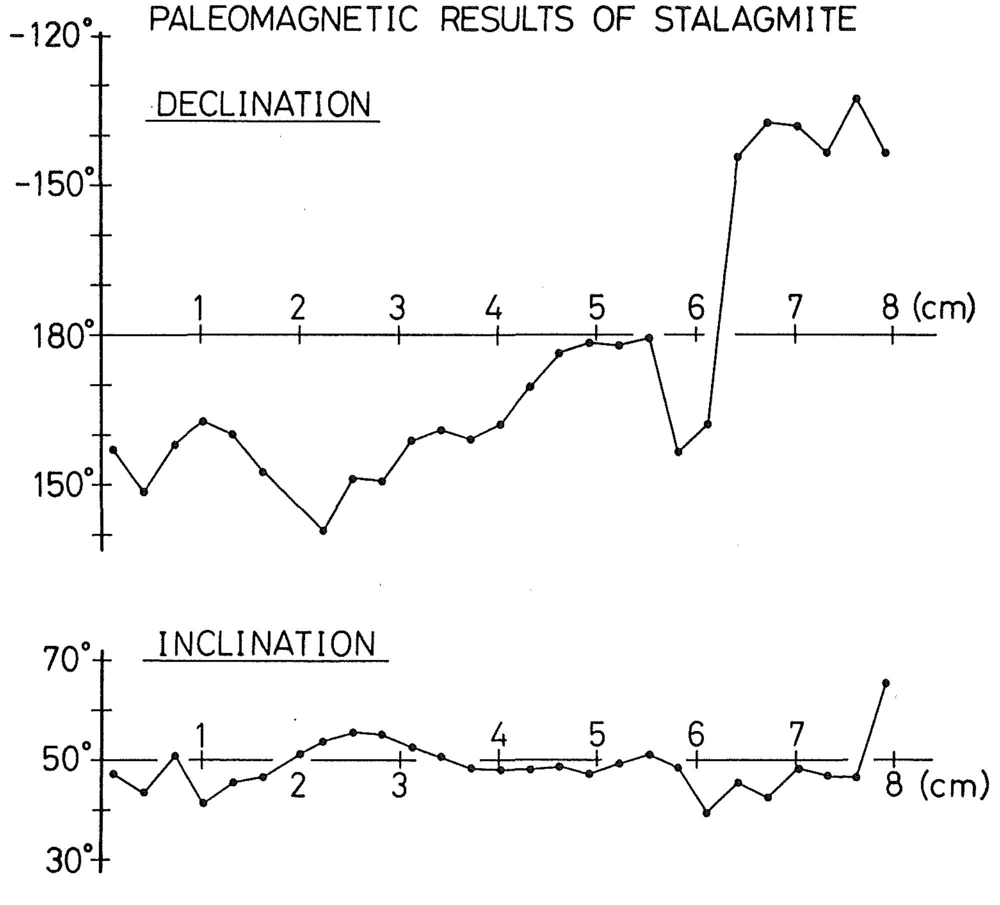

Fig.3 Relative declination and inclination of the stalagmite versus distance from the top.

at the time of magnetic measurements.

Characteristic directions of the stalagmite subsamples are plotted against their distance from the top (Fig.3). Characteristic directions of all six parallel samples from the flowstone are plotted against their distance from the surface, after stretching and compressing the records to adjust positions of the subsamples to their distance from the surface of a "master" sample (Fig.4-dots). The average curves are also shown in figure 4.

3. Discussion and Conclusions

The characteristic directions of stalagmite subsamples do not agree at all with those of flowstone subsamples. Roughly averaged direction for the stalagmite subsamples is 180° in relative declination and 50° in inclination, and for the flowstone subsamples is 40° and 0° in relative declination and inclination, respectively. The difference of averaged values is evidence that each speleothem has grown under different conditions. Taking into consideration the condition at the time of sampling; namely that the flowstone had been broken into blocks, and a growth axis of the stalagmite coincides with a vertical axis, the difference confirms that the flowstone block had obviously collapsed and the stalagmite have grown on the block *in situ*.

We compared the paleomagnetic direction record for the stalagmite with a provisional secular variation curves deduced from paleomagnetism of a sediment core from Yogo Lake (M. Hyodo, personal communication, 1988) (Fig.5). The Yogo Lake record spans 12 ka to the present. According to paleomagnetism of a stalagmite collected from Komori-ana cave, East Akiyoshi Plateau, it is known that its upward growth rate is about 5 cm per 1,000 years (Morinaga et al., 1986). The Yuri-no-ana stalagmite may have a similar growth rate to that of the Komori-ana stalagmite. As the height of the Yuri-no-ana stalagmite is less than 10 cm, the age of its lowest part may be several thousand years BP. Hence, it is very reasonable to compare this stalagmite record with Yogo Lake record. If we note in particular a large swing in relative declination for the stalagmite, we can conclude to the best of our comparison that the stalagmite record corresponds to the shaded part of the Yogo Lake record. This correspondence shows that the stalagmite started to grow about 4,500 years ago.

If the flowstone block is restored to the original state, more

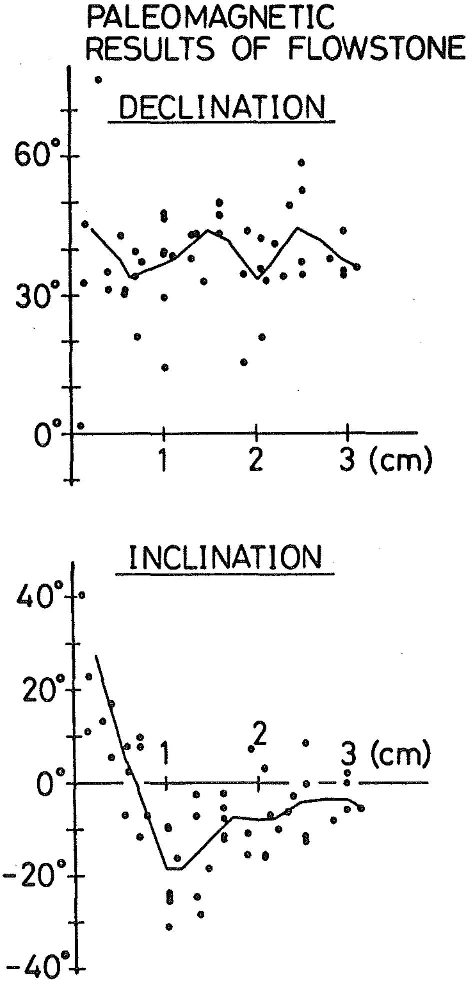

Fig.4 Relative declination and relative inclination of the six flowstone core samples versus distance from the surface (dots). Vector averages are also shown (lines).

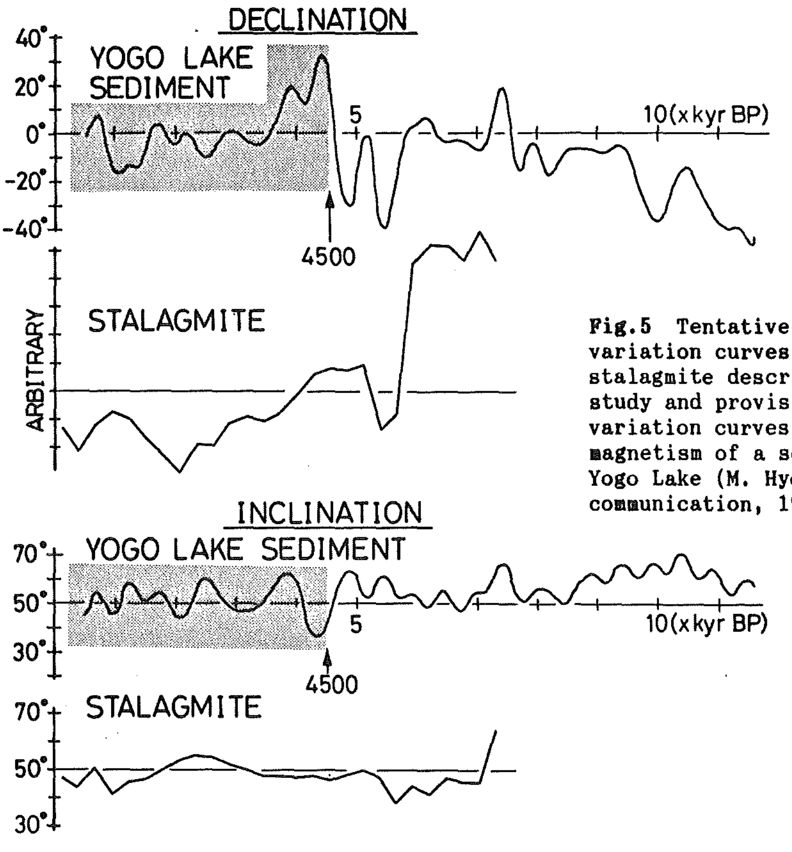

Fig.5 Tentative correlation between variation curves obtained from the stalagmite described in the present study and provisional secular variation curves deduced from paleomagnetism of a sediment core from Yogo Lake (M. Hyodo, personal communication, 1988).

precise age of the collapse can be determined by a similar comparison using its paleomagnetic record. However, as such a restoration is not feasible, we can consider the collapse age only on the basis of the above mentioned correspondence. If the stalagmite started to grow just after the collapse, it can be concluded that the collapse occurred about 4,500 years ago. If ground water was not supplied to the flowstone block after the collapse and sometime later the stalagmite started to grow, the minimum age of collapse is shown as being about 4,500 years BP. In this case, however, we believe that the collapse occurred near about 4,500 years BP.

We believe, judging from scale of the collapse in Yuri-no-ana cave, that the collapse that occurred about 4,500 years ago was not attributed to a free fall by its gravitation or animal/human works. The collapse may have occurred following a catastrophic event, probably an enormous earthquake. However, the result of this paper gives only one collapse age. It may be premature to conclude that all collapses seen in caves distributed around Akiyoshi and Hirao Plateaus occurred simultaneously as a result of the hypothetic earthquake about 4,500 years BP. For example, a collapse seen at Senjojiki site in Akiyoshi-do cave is thought to have occurred since 22,000 years BP, because it is observed over a layer containing Aira-Tn ash (A. Fujii, personal communication, 1988). It is therefore hardly possible to conclude from geological viewpoints, that the collapse at Senjojiki site occurred about 4,500 years ago. Such collapses may have occurred repeatedly in the past. It is necessary to date more samples by the method proposed in this paper. If we can obtain more data, we can clarify the history of catastrophic events in this region.

The precision of the ages obtained by the proposed method depends on the magnetic stability of investigated samples and the accuracy of the geomagnetic secular variation curve as a time scale. Speleothems having more intense remanent magnetization tend to show higher magnetic stability (Morinaga et al., 1988) and their paleomagnetic records are therefore very effective to date by this method. Many efforts are being made at present to establish a reliable paleo-secular variation curve.

References

Creer, K. M., P. Tucholka, and C. E. Barton (1983) *Geomagnetism of Baked Clays and Recent Sediments* (Elsevier, Amsterdam), 324.

Inokuchi, H., H. Morinaga, and K. Yaskawa (1981) *J. Geomag. Geoelectr.*, **33**, 325.

Latham, A. G., H. P. Schwarcz, and D. C. Ford (1986) *Earth Planet. Sci. Lett.*, **79**, 195.

Latham, A. G., H. P. Schwarcz, and D. C. Ford (1987) *Can. J. Earth Sci.*, **24**, 1235.

Latham, A. G., H. P. Schwarcz, D. C. Ford, and G. W. Pearce (1979) *NATURE*, **280**, 383.

Latham, A. G., H. P. Schwarcz, D. C. Ford, and G. W. Pearce (1982) *Can. J. Earth Sci.*, **19**, 1985.

Morinaga, H., H. Inokuchi, and K. Yaskawa (1985) *J. Geomag. Geoelectr.*, **37**, 823.

Morinaga, H., H. Inokuchi, and K. Yaskawa (1986) *J. Geomag. Geoelectr.*, **38**, 27.

Morinaga, H., H. Inokuchi, and K. Yaskawa (1989) *in press in Geophys. J.*

(In press in J. speleol. Soc. Japan, in Japanese with English abstract)

PRELIMINARY REPORT ON PALEOMAGNETISM OF A STALAGMITE IN PING LE, SOUTH CHINA

Yu Yan LIU[1], Hayao MORINAGA[2], Ikuko HORIE[1], Haruko MURAYAMA[1], and Katsumi YASKAWA[1]

[1]Faculty of Science, Kobe University, Nada, Kobe 657, Japan
[2]The Graduate School of Science and Technology, Kobe University, Nada, Kobe 657, Japan

Six stalagmites were taken from Luo Hu Zi cave, Ping Le (24°40'N, 110°39'E) located 85 km south-southeast of Gui Lin with the aim of clarifying paleomagnetic secular variation in South China. All the stalagmites were actively growing at the time of sampling. They were oriented with a magnetic compass prior to removal *in situ*. Here we describe preliminary paleomagnetic results for one of them.

The stalagmite sample, LHZ-1, was about 35 cm in length and 4 cm to 12.5 cm in diameter for near the top to near the bottom, respectively. It was divided into blocks of 5 cm long along a long axis. Seven successive (time-serial) core samples were extracted from each block. Then, they were sliced into 131 disk subsamples of 2 to 2.5 mm thick.

A ScT cryogenic magnetometer was used to measure natural remanent magnetizations (NRMs) and alternating-field cleaned magnetizations for disk subsamples. Progressive AF demagnetization was carried out on all the subsamples up to 50 mT at 5 mT intervals, using a three-axis tumbler in a field-free space. The NRM intensities of disk subsamples before AF demagnetization were in the range 10^{-7} to 10^{-5} Am^2/kg. Most subsamples had a very stable component and only weak, low coercivity component, which could be eliminated at AF levels up to 10 mT (Fig.1-a). Medium

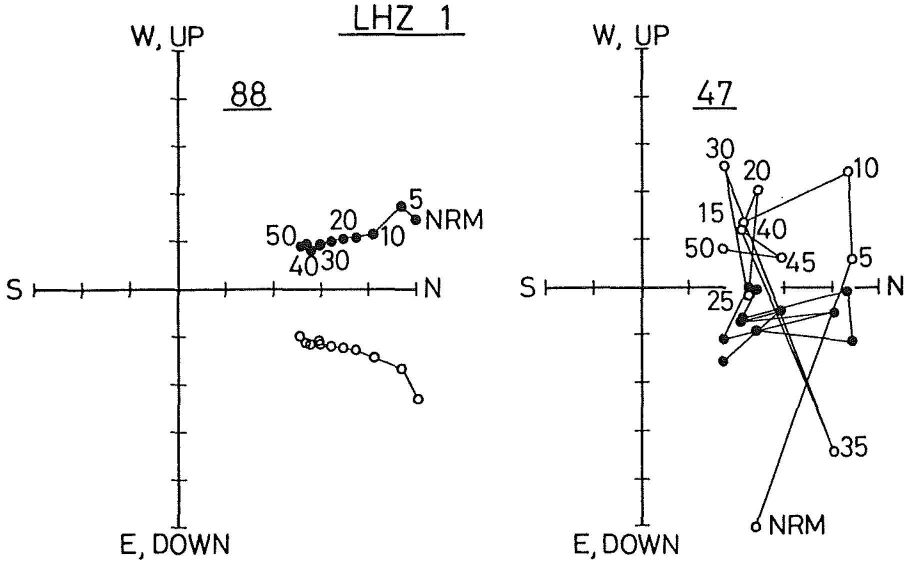

Figure 1 Behavior of two typical subsamples from the LHZ-1 stalagmite during alternating field demagnetization. The subsample 88 shows a stable component (left figure). The subsample 47 shows no stable component (right figure). The closed circles represent the projection of the paleomagnetic vector onto a horizontal plane (N-S and E-W axes). The open circles represent the projection of the vector onto a vertical plane (up-down and N-S axes).

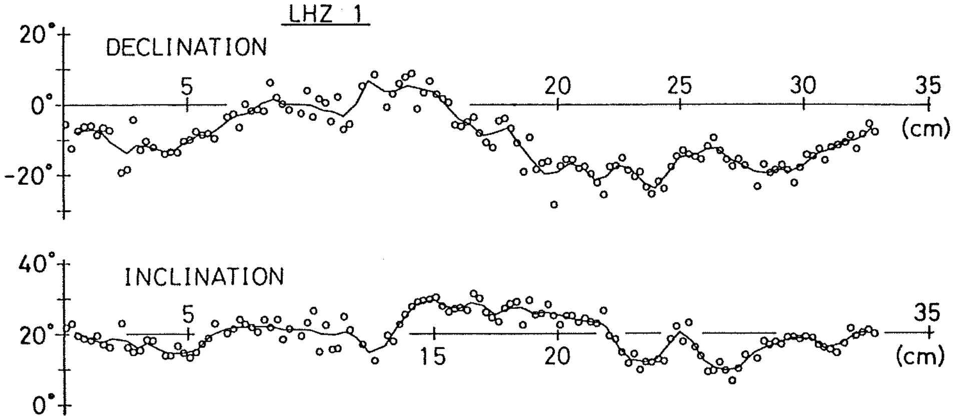

Figure 2 Paleomagnetic results of the LHZ-1 stalagmite. The values of declination and inclination are unit-vectorial averages for AF-demagnetized data selected by visual inspection (open circles). The average curves are also shown (lines).

destructive fields (MDFs) over 40 mT for almost all the subsamples. These MDF values are higher than those reported for Japanese speleothems (Morinaga et al., 1986, 1989). Possibly primary, characteristic directions were obtained as unit-vectorial averages for AF-demagnetized data selected by visual inspection, because these selected data are in Fisherian distribution. Some subsamples (N=7) showed no stable components (Fig.1-b).

Characteristic directions (declinations and inclinations)for the LHZ-1 stalagmite are plotted against their distance from the top (Fig.2-dots). The curves of the declination and the inclination were drawn with average values calculated in range every 10 mm at 5 mm intervals (Fig.2-lines). The curves are firstly proposed variation curves of declination and inclination probably for the last ten-thousands of years in South China, although dating of the stalagmite has not yet performed. The present declination and inclination at Gui Lin are approximately D=0° and I=30°, which are somewhat different from the values at the top of the LHZ-1 stalagmite. The paleomagnetic data had better to be somewhat transformed, because the orientation of the sample might have been slightly incorrect.

References

Morinaga, H., H. Inokuchi, and K. Yaskawa (1986) *J. Geomag. Geoelectr.*, **38**, 27.

Morinaga, H., H. Inokuchi, and K. Yaskawa (1989) in press in *Geophys. J.*

(To be submitted to Geophys. J.)

ISOMAGNETIC CHART OVER THE JAPANESE ISLANDS FOR 25,000 Y.B.P.

Tadashi NAKAJIMA

Geological Laboratory, Faculty of Education,
Fukui University, Fukui 910, Japan

Paleomagnetic measurements have been carried out on the Aira-Tn ash (AT) derived from Aira caldera in Kagoshima Prefecture, Kyusyu. AT is exposed in a widespread area of the Japanese islands, forming the important time-marker in the upper Quaternary sequences (Machida and Arai, 1976). The eruption age of AT was determined to be 24,720 ± 290 y.B.P. with radiocarbon dating by Matsumoto *et al.* (1987).

Paleomagnetic samples were collected from five sites as shown in Fig. 1 and Table 1. These samples have stable remanent magnetizations with respect to the progressive alternating field cleaning up to 50 mT. The optimum demagnetization field (ODF) to produce minimum dispersion was selected from four pilot samples for each site, and the other samples were demagnetized at this field. The results of the magnetic measurement at ODF are tabulated in Table 2.

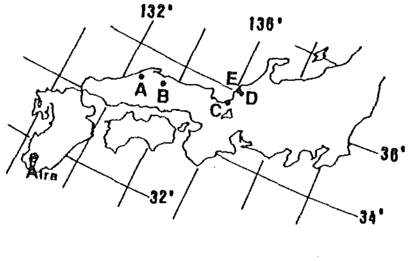

Fig. 1 Sampling sites (A,B,C,D,E).

The VGPs obtained from different sites agree well with one another. It means that their remanent magnetizations were acquired under the same geomagnetic dipole field in about 25,000 y.B.P. Figure 2 shows a tentative isomagnetic chart over the Japanese islands for about 25,000 y.B.P., assuming that the earth's magnetic pole at the time was located on the mean VGP (Long.=101.3°W, Lat.=76.1 °N, A_{95}=2.4°) calculated from the VGP data in Table 2. Paleomagnetic studies on the Aira-Tn ash from many other sites are being undertaken to improve the isomagnetic chart.

Table 1 Localities of the sampling site.

Site	Locality	Longitude	Latitude
A Iinohara	Sada-cho, Shimane Pref.	132.68° E,	35.24° N
B Shimofukuda	Kawakamimura, Okayama Pref.	133.68° E,	35.28° N
C Koudouji	Mihama-cho, Fukui Pref.	135.94° E,	35.59° N
D Ieyoshi	Awara-cho, Fukui Pref.	136.21° E,	36.22° N
E Jyoushinden	Awara-cho, Fukui Pref.	136.18° E,	36.25° N

Table 2 Results of the paleomagnetic measurements.

			Site-mean direction				V.G.P.			
Site	ODF (mT)	N	Dec. (°E)	Inc. (°)	α_{95} (°)	k	Long. (°E)	Lat. (°N)	dp (°)	dm (°)
A	7.5	9	11.7	43.9	5.9	76.6	263.0	76.1	4.6	7.4
B	5.0	15	8.9	44.6	1.6	565.4	271.0	78.2	1.3	2.0
C	5.0	13	12.2	46.4	2.4	310.6	259.7	77.0	2.0	3.1
D	5.0	11	16.0	47.3	2.6	302.6	251.6	74.4	2.2	3.4
E	10.0	10	16.2	47.0	8.8	31.4	252.1	74.1	7.3	11.4

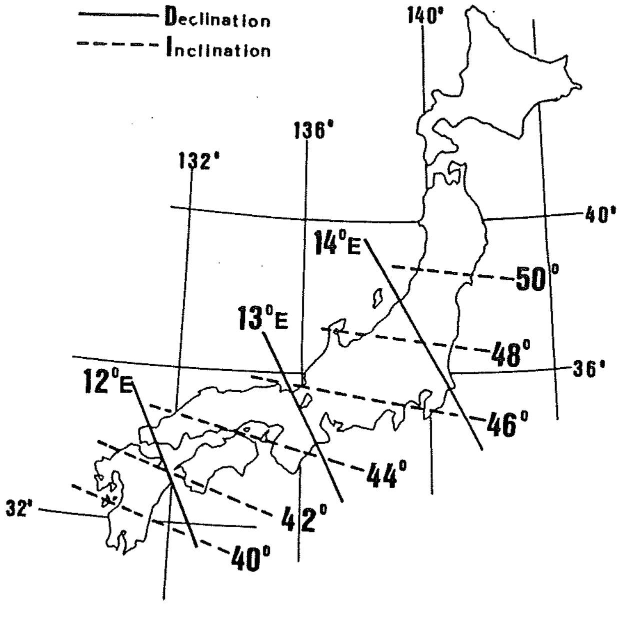

Fig. 2 Isomagneic chart over the Japanese islands for about 25,000 y.B.P.

REFERENCES

Machida, H. and F. Arai (1976) *Kagaku*, **46**, 339 (in Japanese).

Matsumoto, E., Y. Maeda, K. Takemura, and S. Nishida, *Quaternary Research*, **26**, 79 (in Japanese).

PRELIMINARY STUDY OF GEOMAGNETIC PALEOSECULAR VARIATION AND K-Ar AGES IN EASTER ISLAND, THE SOUTHEAST PACIFIC

Masako MIKI[1], Hiroo INOKUCHI[2*], Jun-ichi MATSUDA[2], Satoru YAMAGUCHI[1**], Nobuhiro ISEZAKI[2] and Katsumi YASKAWA[2]

1. The Graduate School of Science and Technology, Kobe University, Kobe 657, Japan
2. Department of Earth Sciences, Fuculty of Science, Kobe University, Kobe 657, Japan

Anomalously low geomagnetic secular variation for the last few million years has been recognized in Central Pacific, and this secular variation low is due to the Pacific dipole window (e.g., Doell and Cox, 1971, 1972; Doell, 1972a, 1972b). The paleomagnetic and geochronological study was carried out on Easter Island in an attempt to determine the southeastward extent of the Pacific dipole window.

Easter Island (27.1°S, 109.2°W) is a small volcanic island in the southeast Pacific. The island is a part of the seamount chain generated by a hot spot during last 10 m.y. in the Nazca Plate (Herron, 1972). The island consists of three volcanoes; Poike, Rano Kau and Terevaka. We collected more than 250 samples for paleomagnetism and geochronological study from the lava flows of three volcanoes (Fig.1).

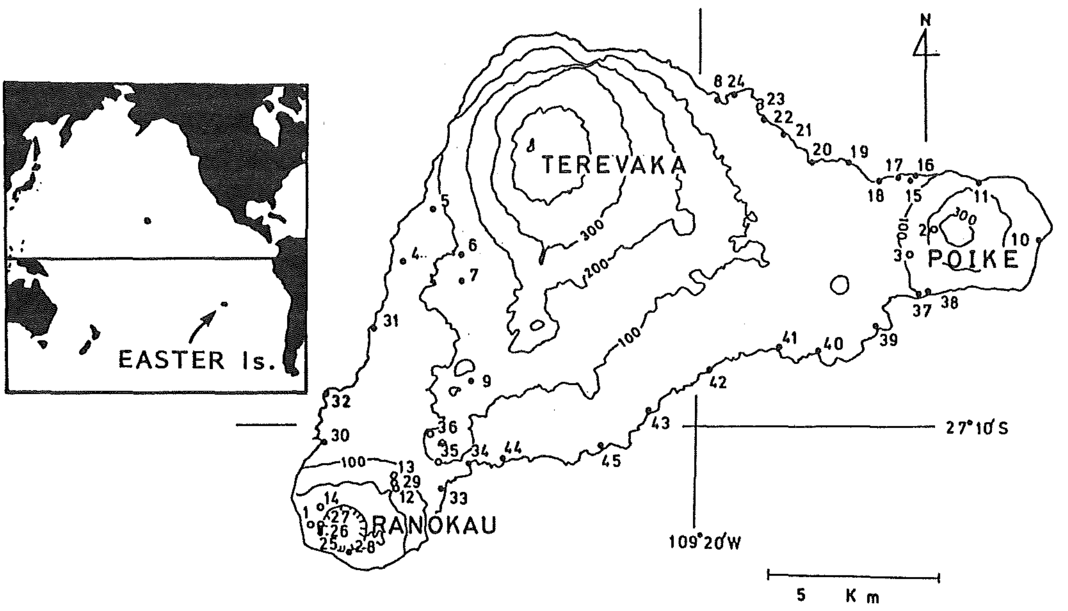

Fig.1. The map of Easter Island with sampling sites. The solid circles show the sites for paleomagnetic study. The open circles show the sites for geochemical study. Contour interval is 100 m.

* Present adress: Marine Biological Station, Fuculty of Science, Kobe University, Tsuna, Hyogo, 665-24, Japan
** Present adress: Teikoku Women's Junior College, Moriguchi, Osaka, 570, Japan

Stability of remanent magnetization was examined through progressive demagnetization experiments of both alternating field and thermal technique. Three or more pilot samples were chosen from each site for the experiments. The remanent magnetization was measured using a spinner magnetometer. The stable component of magnetization was isolated from almost all sites during both alternating field demagnetization in the field up to 30 mT and thermal demagnetization at the temperature up to 300°C.

Five or less samples from each site were demagnetized in the field up to 30 mT for the preliminary study of paleomagnetism. Reliable paleomagnetic directions were obtained from eight sites of Poike, six sites of Rano Kau and nineteen sites of Terevaka. All of the directions have normal polarity. The mean paleomagnetic directions of the three volcanoes are as follows; D=6.9°, I=-41.2° and α_{95}= 12.5° for Poike; D=-9.7°, I=-46.2° and α_{95}=10.9° for Rano Kau and D=4.2°, I=-44.0° and α_{95}=5.7° for Terevaka respectively. There is no significant difference among the three directions of remanent magnetization.

The K-Ar whole rock dating was attempted on lava flows from three sites of Poike, one site of Rano Kau and four sites of Terevaka. The rock samples were fresh enough for K-Ar dating. The amount of radiogenic ^{40}Ar was measured at the chronological laboratory in Okayama University of Science (with help of Dr. Nagao). We obtained the age of 0.14±0.10 Ma from a site of Poike and the age of 0.34±0.03 Ma from a site of Rano Kau. In other sites, the upper limits of the ages were determined preliminarily. All of the ages obtained are younger than 0.8 Ma. The ages are much younger than that reported by Clark and Dymond (1974). The activities of three volcanoes on Easter Island appear to have occurred during Brunhes polarity chron because of the young K-Ar ages and the normal polarity of paleomagnetic directions. The time interval of the samples is probably a few times of 10^5 years and long enough for the estimate of the paleosecular variation.

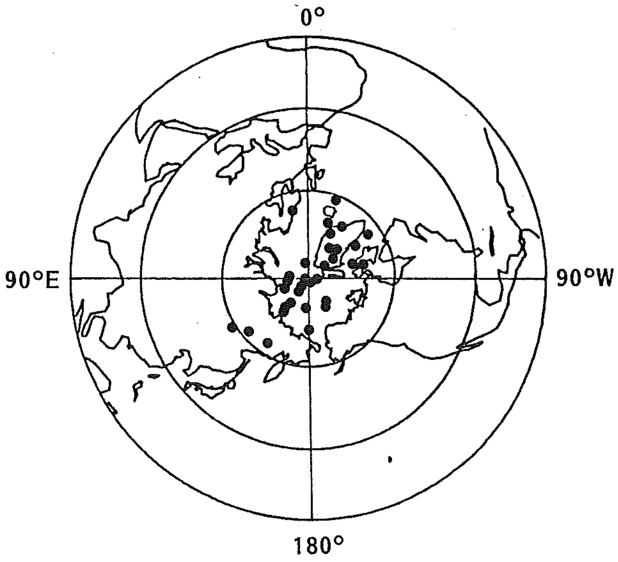

Fig.2. VGP positions for Easter Island lava flows. All symbols are on the northern hemisphere of the equal area projection.

The VGP positions were calculated from the paleomagnetic results of all 33 sites on Easter Island (Fig.2). The mean VGP position is 88.3°N and 316.2°E with an α_{95} value of 4.7°. The geographic pole is contained within the 95% confidence limit circle.

The angular dispersion value of Easter Island calculated after McElhinny and Merrill (1975) is 15.0° with upper limit of 18.0° and lower limit of 12.8°. The value is larger than that calculated from Terevaka

Fig.3. VGP angular dispersions in the Pacific Ocean: Garapagos (Doell and Cox, 1972), Hiva-Oa (Katao et al., 1988), Society (Duncan, 1975), Easter (Isaacson and Heinrichs, 1976), Pagan (U.S.-Japan P.C.P.M., 1975), Hawaii (McWilliams et al., 1982), Model C (Cox, 1962), Model D (Cox, 1970) and Model F (McFadden and McElhinny, 1984). The star shows the angular dispersion in Easter Island calculated from the results of this study.

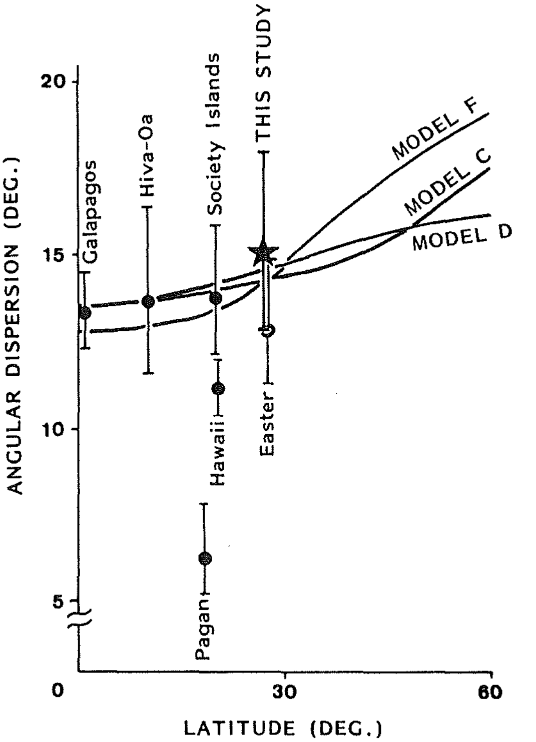

volcano by Isaacson and Heinrichs (1976). The angular dispersion value of Easter Island is consistent with the values predicted by secular variation models (Fig.3); e.g., Model C(Cox,1962), Model D(Cox, 1970) and Model F(Mcfadden and McElhinny, 1984). The preliminary results of this study indicate that Pacific dipole window has not been exist in the Easter Island during the past some 10^5 years.

References

Clark, J. and J.Dymond (1974) EOS Trans. AGU, 55, 300.
Cox, A. (1962) J. Geomag. Geoelectr., 13, 101.
Cox, A. (1970) Geophys. J. R. Astr. Soc., 20, 253.
Doell, R.R. (1972a) J. Geophys. Res., 77, 862.
Doell, R.R. (1972b) J. Geophys. Res., 77, 2129.
Doell, R.R. and A.Cox (1971), Science, 171, 248.
Doell, R.R. and A.Cox (1972) In: The Nature of the Solid Earth (eds E.C. Robertson, McGraw-Hill, New York), 245.
Duncan, R.A. (1975) Geophys. J. R. Astr. Soc., 41, 245.
Herron, E.M. (1972) Geol. Soc. Amer. Bull., 83, 1671.
Isaacson, L.B. and D.F. Heinrichs (1976) J. Geophys. Res., 81, 1476.
Katao, H., H.Morinaga, M.Hyodo, H.Inokuchi, J.Matsuda and K.Yaskawa (1988), J. Geomag. Geoelectr., 40, 703
McElhinny, M.W. and R.T.Merrill (1975) Rev. Geophys. Space Phys., 13, 687.
McFadden, P.L. and M.W.McElhinny (1984) Geophys. J. R. Astr. Soc., 78,809.
McWilliams, M.O., R.T.Holcomb and D.E.Champion (1982) Phill. Trans. R. Soc. Lond. A., 306, 211.
U.S.-Japan Paleomagnetic Cooperation Program in Micronesia (1975) J. Geomag. Geoelectr., 28, 57.

TWO "EVENTS" RECORDED IN THE BRUNHES CHRON AT HOLE 650 (LEG 107, TYRRHENIAN SEA): GEOMAGNETIC, SEDIMENTOLOGICAL OR DEFORMATIONAL PHENOMENA?

James E.T. Channell* and Masayuki Torii**

*Department of Geology, University of Florida, Gainesville, FL 32611, USA
**Department of Geology & Mineralogy, Kyoto University, Kyoto 606, Japan

Abstract

The Brunhes Chron at Hole 650A is represented by about 415 m of volcaniclastic turbidites. Two intervals (11 ~ 20 mbsf and 99 ~ 100 mbsf) where the remanent magnetization has negative inclination are recognized in the Brunhes (Fig. 1). All samples were progressively thermally demagnetized on shore. Orthogonal projection of thermal demagnetization data from these APC-cored intervals indicate that a well-defined single magnetization component can be resolved. "Event A" is recorded over a stratigraphic thickness of about 9 m, and "Event B" over a stratigraphic thickness of about 1.5 m. The record of "Event A" spans more than one core (from 2H to 3H). Biostratigraphic and stable isotope data help to constrain the age of these "events". "Event A" is inferred to occur in oxygen isotopic Stage 2 (12 ~ 24 ka), and "Event B" in isotopic Stage 5 (73 ~ 130 ka).

In these particular intervals, the color and compositional banding indicates that the cores are relatively undeformed (Fig. 2). The presence of a steep downward magnetic overprint at this Hole indicates that the negative inclinations cannot be explained by inadvertent flipping of cores or core sections. Negative inclinations of magnetic remanence associated with "Event A" and "Event B" are recorded entirely within fine grained calcareous muds, that may constitute the upper parts of distal turbidite flows. Due to failure of the "multishot" core orientation device, the remanence declination values are relative.

For "Event A", there are several broadly synchronous "events" such as the Mono Lake and Summer Lake excursions (20 ~ 30 ka). For "Event B", which appears to occur in isotopic stage 5, there are several correlative "events" which are well documented in several piston cores from the Tyrrhenian Sea and eastern Mediterranean. This "event" may correlate to the Blake Event recorded in Atlantic and Caribbean cores. However the lack of azimuthal orientation of the core at this Site, and the general scatter in relative declination values limit the resolution of the dataset. Additional oriented piston cores from exceptionally thick records of the Brunhes Chronozone are necessary to confirm the nature of these "events".

(submitted to *Proceedings of the Ocean Drilling Program*, Part B., vol. 107, 1989)

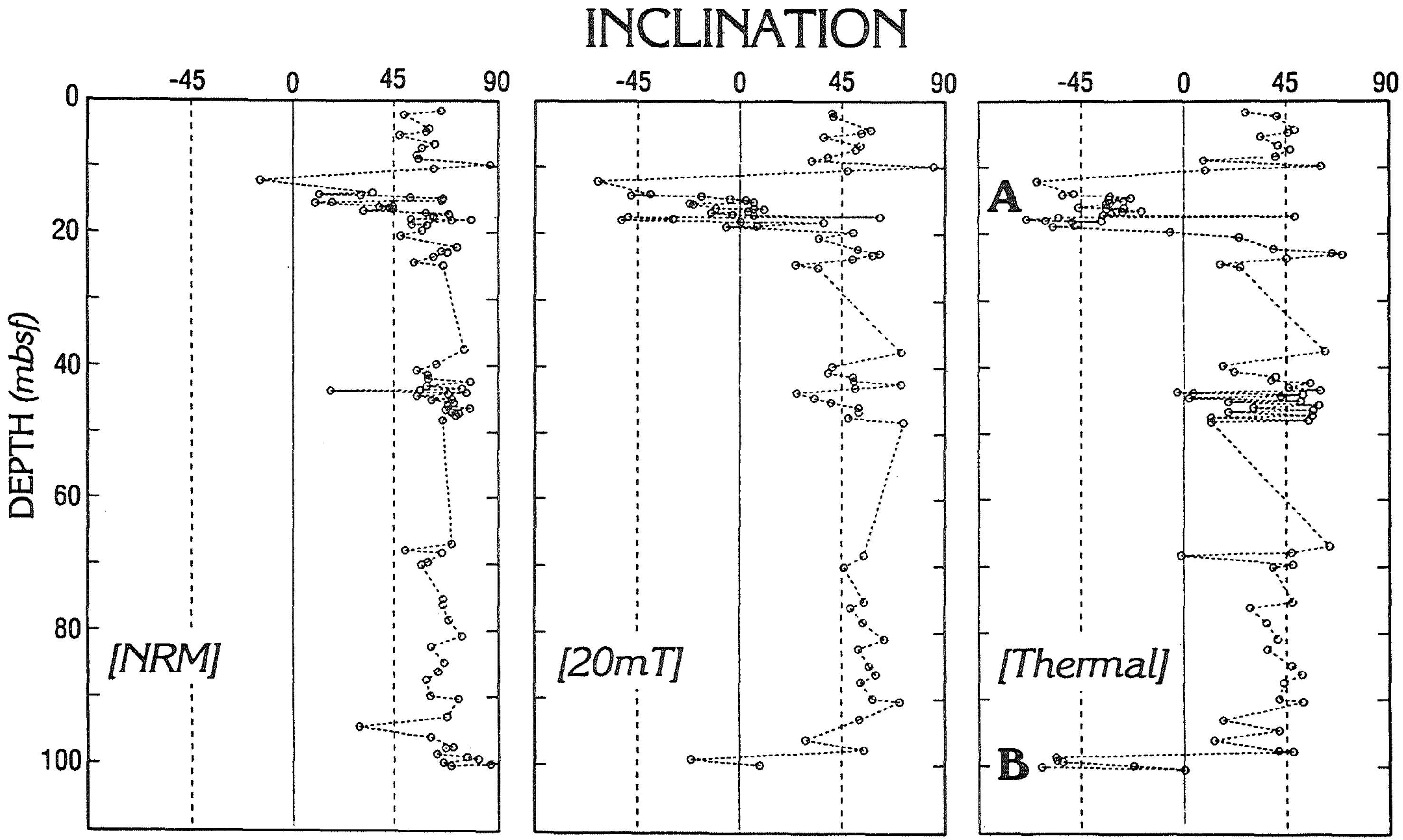

Fig. 1. Inclinations of the natural remanent magnetization (NRM), inclinations of remanence after demagnetization at peak fields of 20 mT, and inclinations of the high blocking temperature component resolved by thermal demagnetization, for the upper 100 mbsf at Hole 650A.

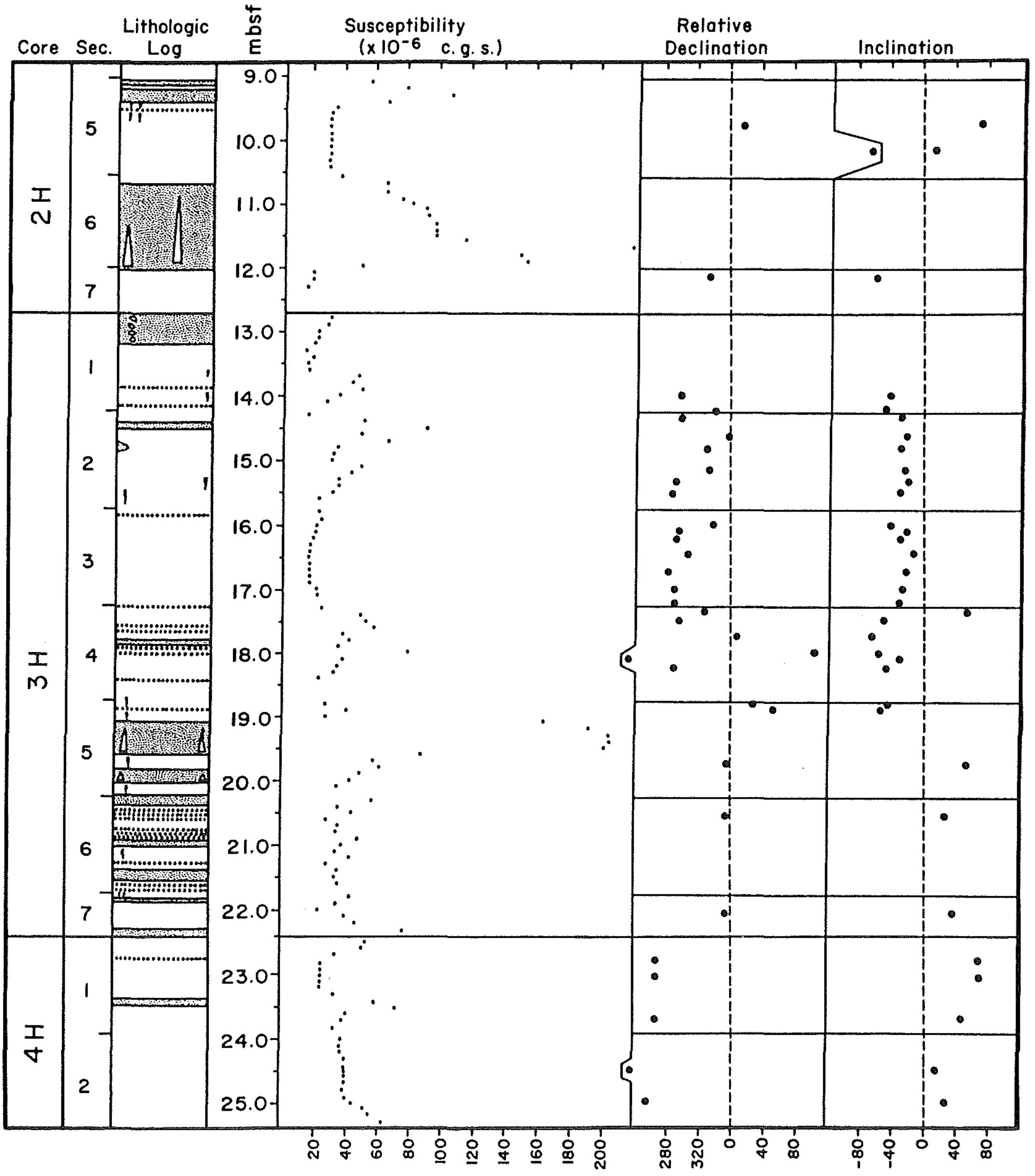

Fig. 2. Lithologic log, magnetic susceptibility, and the well defined remanence component directions for the interval at Hole 650A which records "Event A". Standard ODP symbols are used in the lithologic log. Core section breaks are indicated on the declination and inclination plots. Note that the coarser grained layers correspond to highs in the susceptibility values, and that these layers were generally avoided during sampling.

PALEOMAGNETISM OF PLIO-PLEISTOCENE SEDIMENTS IN SANGIRAN, CENTRAL JAVA

Masayuki HYODO[1], Wahyu SUNATA[2], Eko Edi SUSANTO[2], Hendro WAHYONO[2]

1) Department of Earth Sciences, Faculty of Science, Kobe University, Kobe 657, Japan
2) Geological Research and Development Centre, Bandung, Indonesia

1. Introduction

Central to East Java has been attracting a number of geologists, anthropologists and other scientists since the discovery of Pithecantropus fossils at the end of 19th century. Especially Sangiran area has been investigated by many research groups (Koenigswald, 1940 ; Watanabe & Kadar, 1985) because numerous hominid fossils were excavated in the area from the 1930s. In spite of such intensive study, no reliable chronology is still obtained. Our paleomagnetic investigation of the Plio - Pleistocene sediments in Sangiran aims at establishing magnetostratigraphy and then at deducing the paleomagnetic secular variation.

2. Geology

The Sangiran area is located to the north of Surakarta City, Central Java at about 7.5°S in latitude and 110°E in longitude. The area, which extends 6 km from north to south and 3 km from east to west, is characterized by a dome structure which was truncated by erosion. Because of the structure, older sediments are exposed concentrically on the truncated surface, the oldest sediment being located at the center. The exposed sediments are subdivided into four main stratigraphical units by three marked key beds. The Kalibeng Formation is laid at the bottom mainly consisting of marine bluish gray clay and silty clay. The marine clay is overlain by the Pucangan Formation which is formed by a black clay layer. Depositional environment of this formation gradually changed from shallow marine to lagoonal and then to lacustrine. The Pucangan Formation is overlain by the Kabuh Formation above which the Notopuro Formation lies. The Kabuh Formation is mainly composed of clay, silt, sand and gravel layers of fresh water origin. The base of the Kabuh Formation is formed by the so-called Grenzbank zone (Koenigswalt, 1940), a pebbly sand bed with interbeds of hard sand and pebbles. Hominid and mammalian fossils are contained in the Kabuh as well as the Pucangan Formations.

3. Sampling and experiments

Paleomagnetic sampling was made at fourteen localities covering the all formations. Fine clay and tuff were preferentially sampled, but when they were unobtainable, silty clay was sampled. From one sampling level, at least five 2.5 cm cubic specimens or one large block sample were collected by hand sampling and in laboratory seven 2.5 cm cubic specimens were cut from each block sample. Specimens were put in acrylic cubic capsules. In total, 654 specimens from 106 horizons were prepared.

All the specimens were subjected to progressive demagnetization in alternating fields (AF) up to 80-100 mT at intervals of 5-20 mT. The NRM of specimens in the same horizon displays similar pattern of intensity decay and directional change in the course of progressive AF demagnetization. Demagnetization pattern of reverse NRM clarifies that NRM is intensively affected by secondary viscous remanent magnetization (VRM). The secondary VRM is usually more than 90 % of total NRM and sometimes remains unremoved even by the demagnetization in AF of 50 mT. The reverse NRM affected by such large

VRM is often found in somewhat silty clays from the Kabuh Formation. On the other hand, very fine clay from the Pucangan Formation revealed the very stable reverse NRM throughout the progressive AF demagnetization up to 80 mT. Total intensity of these two types of NRM is also different ; the former is larger by one or two order of magnitude.

4. Results and discussion

[Magnetostratigraphy]

Stable component of NRM isolated by demagnetization in higher AFs clearly defines the boundary of the geomagnetic polarity change. Average magnetization of each horizon calculated with most converged magnetization after demagnetization in AFs of 50-100 mT was classified as normal, reverse and intermediate. The intermediate was defined as a direction which departed from the geocentric axial dipole field by more than 50°. The sequence of the horizon average magnetization is subdivided into five kinds of zone ; (1) normal, (2) reverse, (3) intermediate, (4) normal mixed with intermediate and (5) reverse mixed with intermediate (Fig.1).

The clear polarity change just below the Upper Tuff in the Kabuh Formation would be the Brunhes / Matuyama boundary at the age 0.73 m.y.. At three localities in the southern part, the boundary was determined in the zone about 1 m thick below the Upper Tuff. The level of the Brunhes / Matuyama boundary is quite higher than that reported by earlier investigators who located it in the Pucangan Formation (Yokoyama et al., 1980 ; Semah, 1982) or unsuccessfully determined (Shimizu et al., 1985). It may be because they failed to obtain the succession of reverse polarity in the lower part of the Kabuh Formation owing to insufficient removal of VRM. The Jaramillo event, which ranges in age between 0.90 and 0.97 m.y., can be assigned to the normal zone mixed with intermediate magnetic vectors between the Grenzbank zone and the tuff layer T11. The another normal zone with intermediate around the Balanus Limestone in the Kalibeng Formation can be assigned to the Olduvai event, between 1.67 and 1.87 m.y.. This event ranges in level between 1-3 m above and 7-10 m below Balanus Limestone near Pablengan. The succession of normal polarity below the nodule layer in the Kalibeng Formation would belong to the Gauss normal epoch. The Gauss / Matuyama boundary at 2.48 m.y. in age may be situated somewhere between the Upper Tuff and the nodule layer. No paleomagnetic sample was available in the range due to the lack of good outcrop. Below the Lower Tuff 3 in the Kalibeng Formation are two mixed zones of reverse and intermediate, separated by a stout normal layer just below the Lower Tuff 1. The Kaena event, between 2.92 and 3.01 m.y., may be assigned to the Upper zone and the Mammoth event, between 3.05 and 3.15 m.y., to the lower zone. While a lot of Fission - track ages have been determined with regard to the Sangiran area, the result of magnetostratigraphy is consistent with those published recently (Suzuki, 1983 ; Suzuki et al., 1985) rather than those reported previously (Nishimura et al., 1980). Fossils of Pithecantropus skull, Pithecantropus mandible and Megantropus mandible have been found from the stratigraphic levels which range from the tuff layer T11 in the Pucangan Formation up to the Upper Tuff in the Kabuh Formation (Watanabe & Kadar, 1985). These levels range from the lower boundary of the Jaramillo event to the Brunhes / Matuyama boundary in magnetostratigraphy.

[Paleomagnetic secular variation]

The Paleomagnetic secular variation revealed by our study shows that the geomagnetic field must have been unstable during the time of magnetic events. Magnetization in intermediate eastely direction has frequently been observed in those magnetic events. In addition, the normal or reversed magnetic vector deviates from the geocentric axial dipole field. Even a reversed vector is contained in the Olduvai event. Such unstable geomagnetic field during events

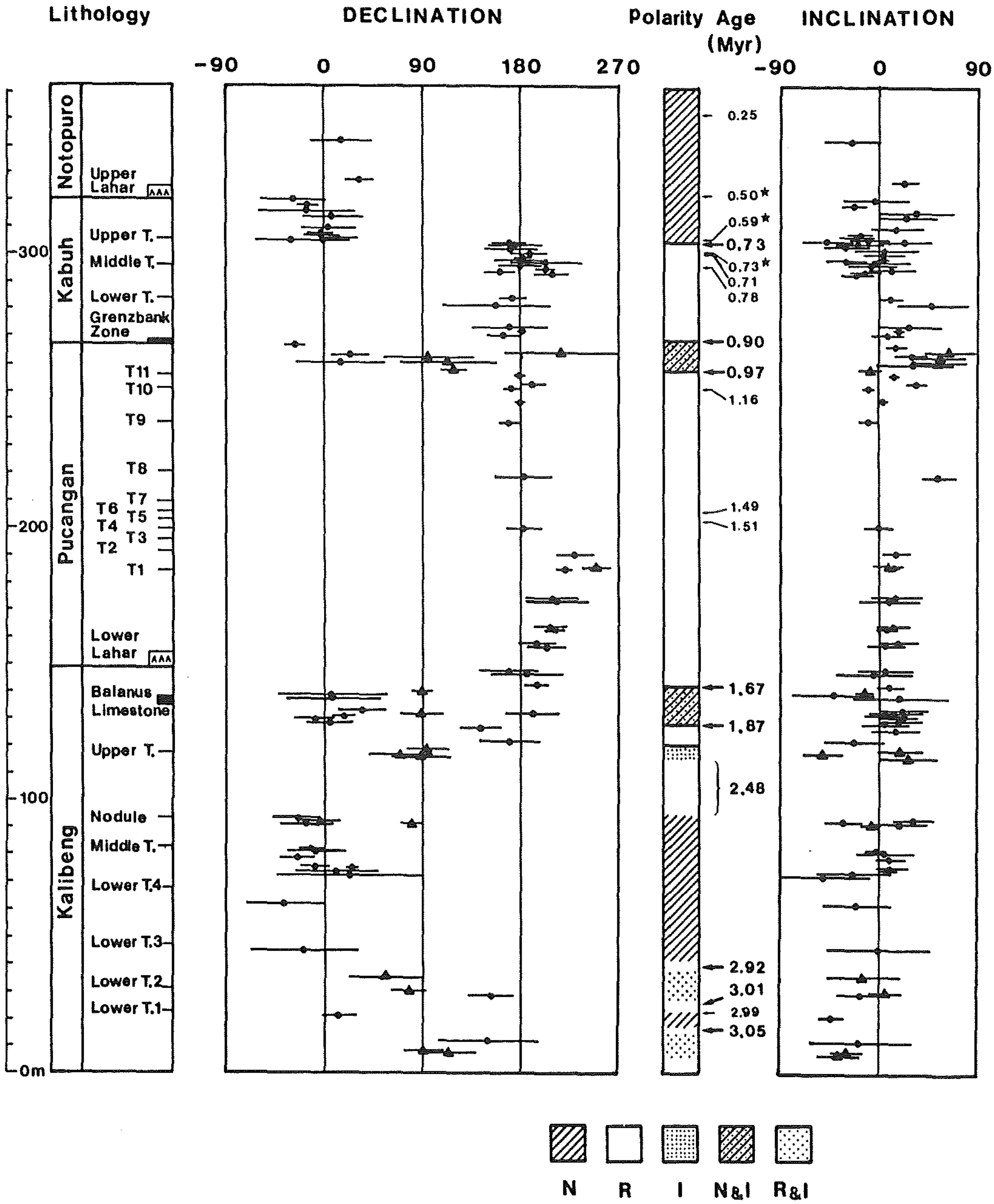

Fig. 1 Paleomagnetic secular variation for the past 3 million years from Sangiran. The key beds in lithology are according to Watanabe and Kadar (1985). Declination and inclination are those of horizon averages of the most converged NRM's after demagnetization in AF's of 50 - 100 mT. Closed triangles show intermediate directions and error bars show the limits of α^{95} confidence circle. The ages of polarity boundaries (see text) are given by large letters. Fission - track ages given by small letters are according to Suzuki et al. (1985) and those by small letters with star to Suzuki (1983).

is also suggested by the results of paleomagnetic studies with igneous rocks which have been compiled for construction of a polarity time scale (Mankinen & Dalrymple, 1979). During the Jaramillo event, intermediate paleomagnetic field has been observed in Tahiti and New Mexico and during the Olduvai event reverse paleomagnetic field has been observed in California and Madeira. During the Mammoth event, normal paleomagnetic field has been observed at three different places. Globally, polarization of the geomagnetic field may have been incomplete during events, governed by locally spaced nondipole fields. The dominance of easterly geomagnetic vectors in Java may suggest that around Java the geomagnetic field during events have been governed by a standing nondipole source (Yukutake & Tachinaka, 1968) which has lasted at least from the Mammoth to the Jaramillo events. According to these considerations, the short sequence of intermediate easterly vectors around the Upper Tuff in the Kalibeng Formation can be assigned to the Reunion event. Long sequence of magnetic vectors which have quite westerly declination was found in the lower part of the Pucangan Formation. The duration of this westerly swing, which may be as long as more than one hundred thousands years, suggests a dipole wobble.

5. Conclusions

Our investigation established a magnetostratigraphy throughout the exposed sediments in the Sangiran area. Nine polarity boundaries were located in the stratigraphy. The stratigraphic levels of Pithecantropus fossils range from the lower boundary of the Jaramillo event at 0.97 m.y. to the Brunhes / Matuyama boundary at 0.73 m.y.. Paleomagnetic secular variation obtained in this study suggests that the geomagnetic field during events was unpolarized in contrast to the stable state of normal or reversed polarity during epochs.

References

Koenigswald, G.H.R. von, Dienst. Mijnb. Ned. 28, 232p (1940)

Nishimura, S., Thio, K.H. & Hefuwat, F. in Physical Geology of Indonesian Island Arcs. Kyoto Univ. (ed. Nishimura, S.) 72-80 (1980)

Mankinen, E.A. & Dalrymple, G.B. J. Geophys. Res. 84, 615-626 (1980)

Semah, F. Mod. Quaternary Res. SE Asia 7, 151-164 (1982)

Shimizu, Y., Mubroto, B., Siagian, H., & Untung, M. in Quaternary Geology of the Hominid Fossil Bearing Formations in Java (eds. Watanabe, N. & Kadar, D.) Geol. Res. Dev. Centre, Spec. Publ. 4. 275-308 (1985)

Suzuki, M., J. Anthr. Soc. Nippon, 92, 2, 112-113 (1983)

Suzuki, M., Wikarno, Budisantoso, Saefudin, I. & Itihara, M. in Quaternary Geology of the Hominid Fossil Bearing Formation in Java (eds. Watanabe, N. & Kadar, D.) Geol. Res. Dev. Centre, Spec. Publ. 4, 309-375 (1985)

Yokoyama, T., Hadiwisastra, S., Hayashida, A. & Hantono, W. in Physical Geology of Indonesian Island Arcs. Kyoto Univ. (ed. Nishimura, S.) 88-96 (1980)

Yukutake, T. & Tachinaka, H. Bull. Earthquake Res. Inst. 46, 1027-1074 (1968)

Watanabe, N. & Kadar, D. (eds.) Quaternary Geology of the Hominid Fossil Bearing Formations in Java. Geol. Res. Dev. Centre, Spec. Publ.. 4, 378p (1985)

(To be submitted to the Quaternary Research)

PALEOMAGNETIC EVIDENCE FOR PLEISTOCENE CLOCKWISE ROTATION IN THE OISO HILLS: A POSSIBLE RECORD OF INTERACTION BETWEEN THE PHILIPPINE SEA PLATE AND NORTHEAST JAPAN

Masato KOYAMA and Hiroshi KITAZATO

Institute of Geosciences, Shizuoka University
Oya, Shizuoka 422, Japan

A paleomagnetic study was made on the Pleistocene strata in the Oiso Hills located along the boundary between the Philippine Sea plate and the northeast Japan arc. This study evaluates the sense and amount of the Quaternary deformation associated with the interaction between the plates. About 170 sedimentary rock samples ranging in age from 0.2 to 1.0 Ma were measured. We used alternating field and thermal demagnetization to examine the stability of the natural remanent magnetizations. The mean field directions from the Numashiro, the Ninomiya, and the Haneo Formations, which range in age from 0.2 to 0.7 Ma, are nearly aligned with the present axial geocentric dipole field. In contrast, the directions from the Maekawa Formation, which ranges in age from 0.8 to 1.0 Ma, show on average 50° clockwise deflections of declination. These deflections are probably caused by clockwise tectonic rotation between 0.6 and 0.9 Ma. We propose and discuss three models of the rotation mechanism, (1) local drag along a major strike-slip fault, (2) regional dextral shear along the plate boundary, and (3) oroclinal bending caused by collision of a buoyant terrane.

References

Geological Survey of Japan (1978) Geological map of Japan, 2nd. ed., 1:1,000,000.

Japan Association of Quaternary Research (1987) Quaternary maps of Japan.

Nakamura, K., K. Shimazaki, and N. Yonekura (1984) Bull. Soc. Geol. France, 26, 221.

Okada, H. (1987) Fossils, 43, 5.

Seno, T. (1985) J. Geod. Soc. Japan, 31, 106.

Yano, S. (1986) Geosci. Repts. Shizuoka Univ., 12, 191.

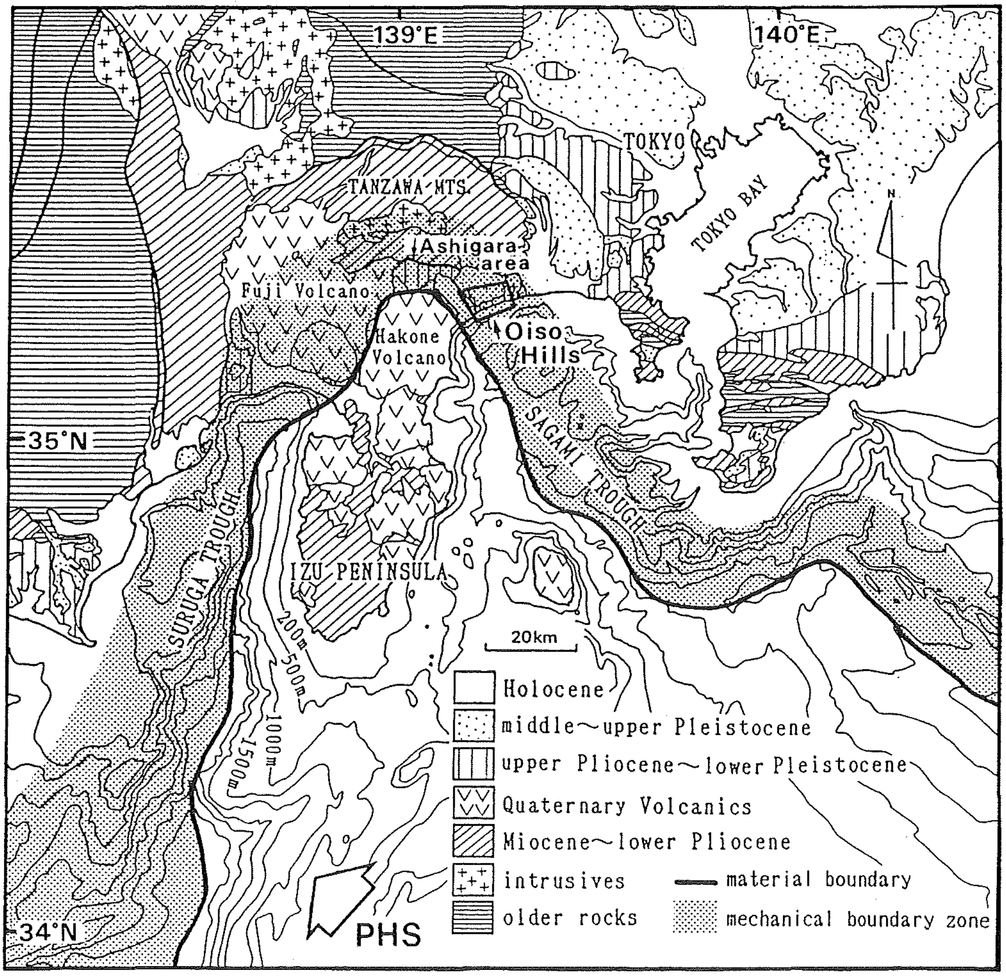

Fig. 1. Geologic sketch map of the Oiso Hills and adjacent areas modified from Geological Survey of Japan (1978) and Japan Association of Quaternary Research (1987). Thick solid line and shaded belt: material boundary and mechanical boundary zone between the Philippine Sea plate and Honshu, respectively, after Nakamura et al. (1984). Large arrow: estimated convergence direction between the Philippine Sea plate and northeast Japan in the early Quaternary before 0.5 Ma (Seno, 1985). Solid frame: study area in the southern part of the Oiso Hills.

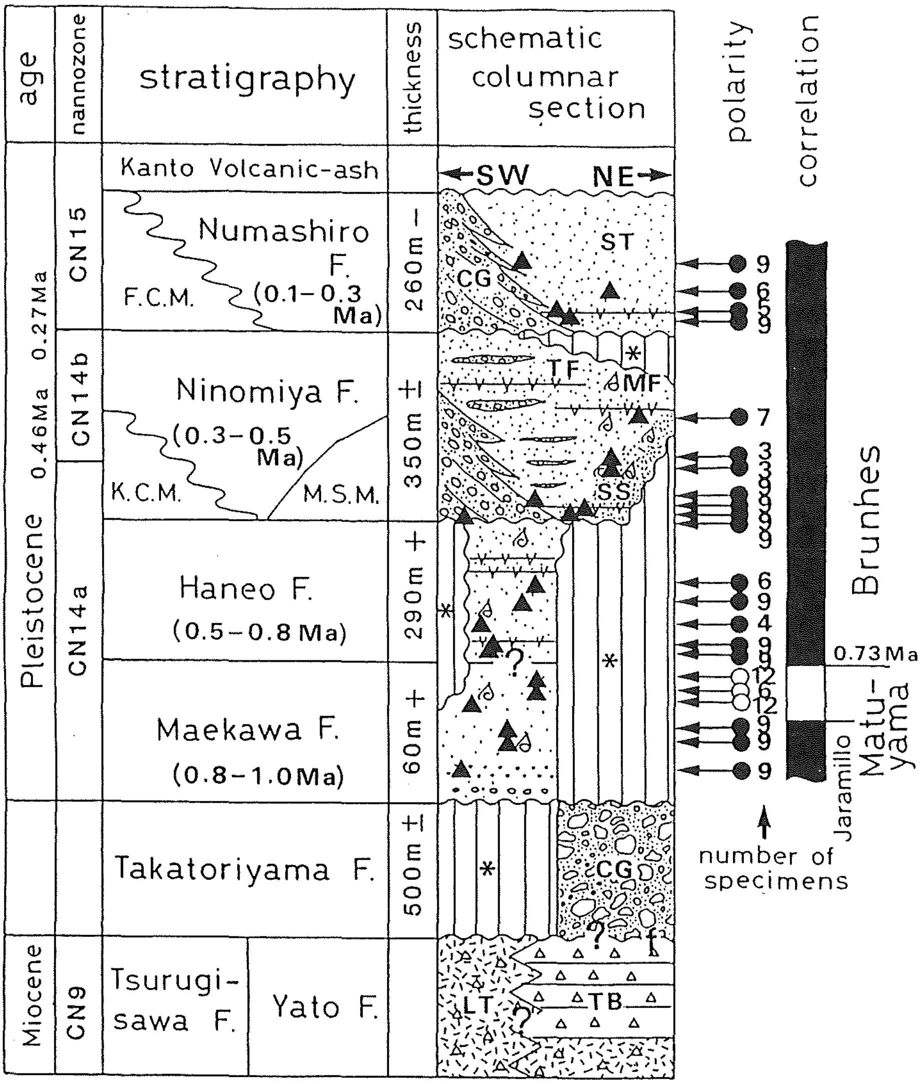

F.C.M. : Fudosan Conglomerate Member
K.C.M. : Kozu Conglomerate Member
M.S.M. : Myoken Sandstone Member
F. : Formation

Fig. 2. Summary of stratigraphy, lithology, and magnetostratigraphy of the southern part of the Oiso Hills. Age ranges in parentheses in the column of stratigraphy are the nannofossil ages estimated by Okada (1987). In the column of schematic columnar section, solid triangles show the horizons of sampling sites. Rock patterns are CG, conglomerate; ST, siltstone; TF, key tuff bed; MF, molluscan fossils; SS, sandstone; LT, lapilli tuff; TB, tuff breccia. Pattern denoted by asterisk shows the lack of strata by unconformity. The magnetostratigraphic data were obtained in the present study. The other data are by Yano (1986).

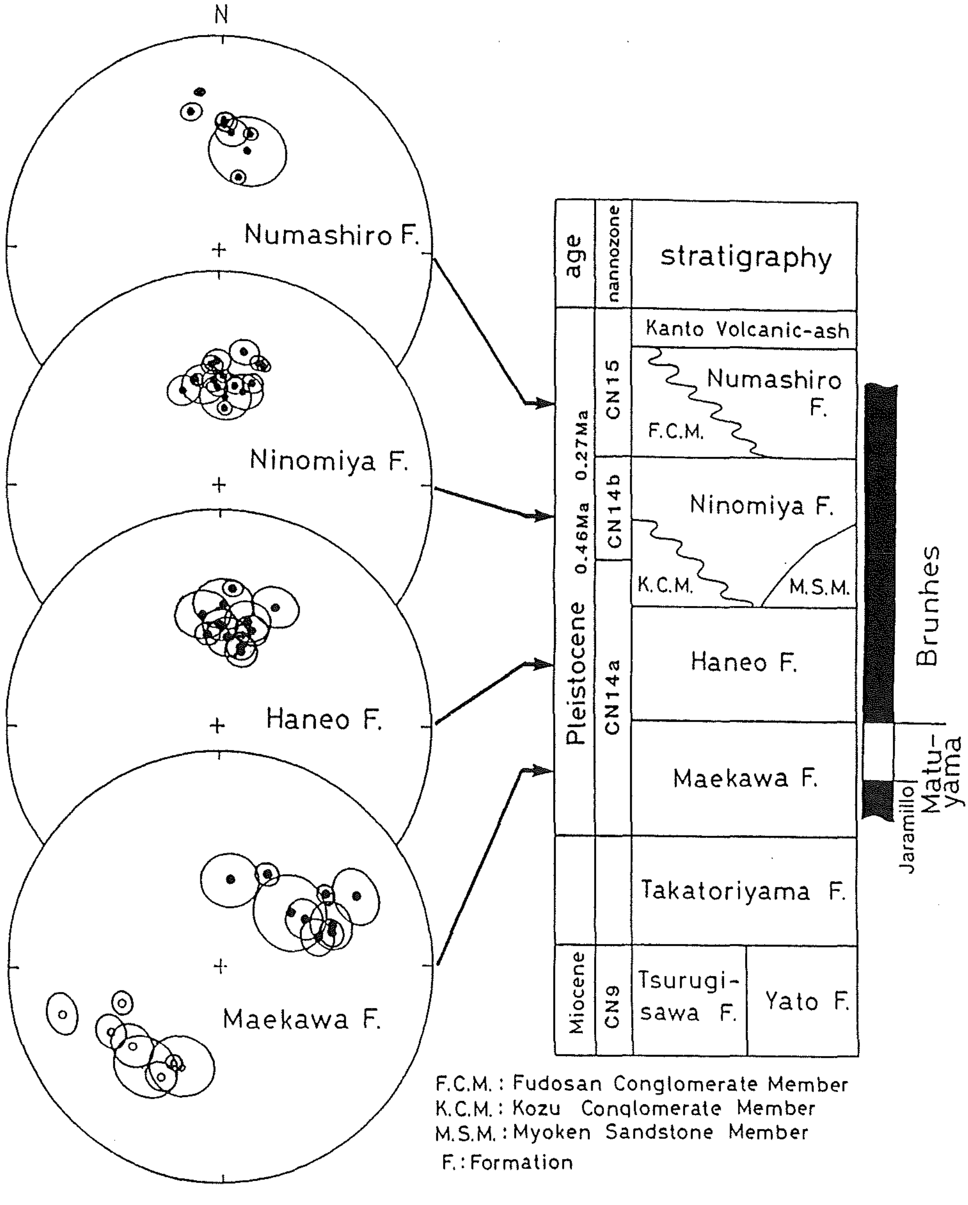

Fig. 3. Horizon-mean directions of remanent magnetization after demagnetization and tilting correction. All directions are plotted on stereonets of equal area projection. Solid circle: direction on lower hemisphere. Open circle: direction on upper hemisphere. Circle around each direction shows the 95% confidence limit.

(In press in Geophys. Monogr. Ser., AGU)

PALEOMAGNETIC STUDIES IN THE SOUTH FOSSA MAGNA AND ADJACENT AREAS, JAPAN -PRESENT STATUS AND A DATA BASE FOR FUTURE STUDIES

Masato KOYAMA

Institute of Geosciences, Shizuoka University, Shizuoka 422, Japan

Paleomagnetic studies in the South Fossa Magna and adjacent areas, central Japan, are reviewed to prepare a data base mainly for tectonic analyses. This paper summarizes 32 paleomagnetic studies, which have been published during 1957 to 1988 and are to be published in 1989. These studies give paleomagnetic data of 1042 sampling horizons. Preliminary reports and associated papers are refered to as well.

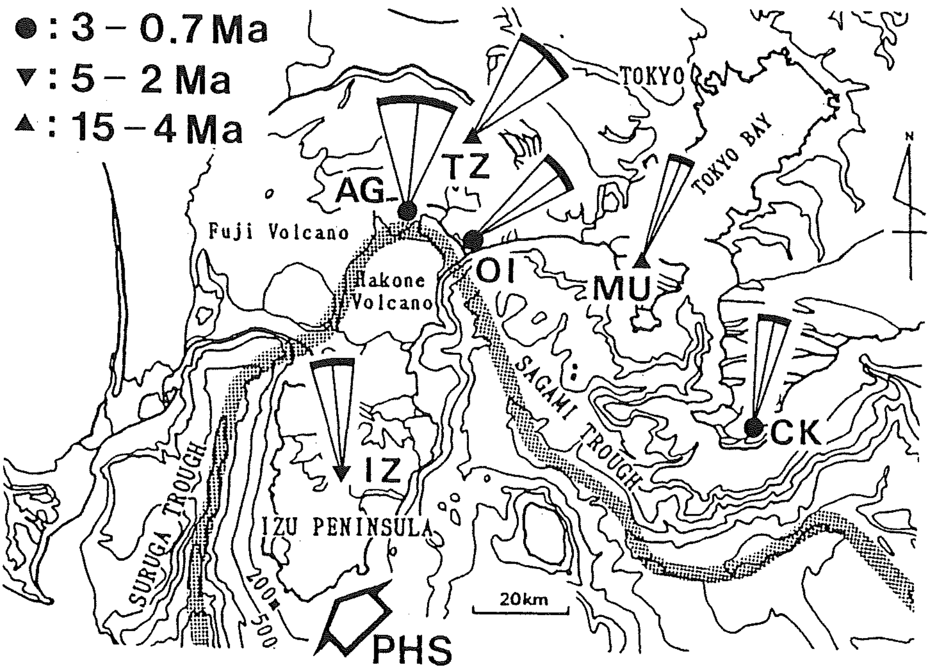

Fig. 1. Map showing the mean direction of paleomagnetic declination from each study area. Fan-shaped arrow shows the area-mean direction and its confidence limit from each study area. The ages of sampled strata are shown with symbols (●: 3～0.7 Ma, ▼: 5～2 Ma, ▲: 15～4 Ma). IZ: upper part of the Shirahama Group in the Izu Peninsula (Koyama, 1986), AG: Ashigara Group in the Ashigara area (Koyama, 1986), OI: Maekawa Formation in the

Oiso Hills (Koyama and Kitazato, 1989), TZ: northeastern Tanzawa Mountains (Ota et al., 1986), MU: Miura Peninsula (Yoshida et al., 1984), CK: Chikura Group in the southern Boso Peninsula (Koyama and Kotake, 1987). All the directions with reversed polarity were converted to those with normal polarity. Shaded belt: material boundary between plates (Nakamura et al., 1984), large arrow: present and late Quaternary convergence direction of the Philippine Sea plate to the Eurasian plate based on Minster and Jordan (1979) (Nakamura et al., 1984). This map only includes the data each of which is thought to be the most reliable and representative one in each area judged from the qualifications explained in text. The directions from the strata younger than 0.7 Ma are not included because all of them are nearly aligned with the present north. The directions from the Fujikawa, Misaka and Koma areas, the Ryuso and Takakusayama areas, and the Tama Hills and the Sagamihara area are also not included because of the lack of reliable data, or of significant directional divergence within the same area, which is probably due to local deformations.

References

Koyama, M. (1986) D. thesis, Geol. Inst., Univ. Tokyo.

Koyama, M. and N. Kotake (1987) in Abstracts, 82th Meet., Soc. Geomag. Earth Planet. Space Sci., I-28.

Koyama, M. and H. Kitazato (1989) (In press in Geophys. Monogr. Ser., AGU).

Minster, J. B. and T. H. Jordan (1979) EOS, 60, 958.

Nakamura, K., K. Shimazaki, and N. Yonekura (1984) Bull. Soc. Geol. France, 26, 221.

Ota, H., H. Ishiguro, S. Iwahashi and N. Niitsuma (1986) Geosci. Rep. Shizuoka Univ., 12, 153.

Yoshida, S., H. Shibuya, M. Torii and S. Sasajima (1984) Geomag. Geoelectr., 36, 579.

(To be published in Modern Geology)

MAGNETIC POLARITY SEQUENCE OF THE FURUTOBE KUROKO MINING AREA, AKITA PREFECTURE, JAPAN

Hirotomo UENO*, Kenichiro HAYASHI**, Munetomo NEDACHI*

* Department of Geology, College of Liberal Arts, Kagoshima University, Kagoshima 890

** Institute of Mineralogy, Petrology and Economic Geology, Faculty of Science, Tohoku University, Sendai 980

Introduction

Kuroko deposits in Japan are of the standard submarine volcanic-hosted massive sulfide deposits. They are lack of deformation and show primary sedimentary features. They were formed a narrow stratigraphic interval of the Middle Miocene.

In this paper, magnetic polarity sequence of a stratigraphic succession of the Furutobe mining area is described, and the Kuroko horizon is ascertained in this sequence.

Geological Setting

The Furutobe mine (40°24'N, 140°42'E) is situated at the north-east end of the Hokuroku basin. The stratigraphic sequence of the mining area is mainly composed of Miocene volcanics, pyroclastics and sediments (Tanaka and Lu, 1966; Metal Mining Agency of Japan, 1978). That is summarized in Figure 1. Each stratigraphic unit is briefly described in ascending order.

<u>Basement</u>

The pre-Miocene basement found only at deep drilling cores consists of black slate and phyllite, and are assumed as Permian in age.

<u>Lower Formation</u>

LR_1 dacite lava: The lava is composed of dacite including visible quartz phenocrysts, and found at drilling cores.

LT_1 dacitic tuff breccia: It consists of lapilli tuff and volcanic breccia, and covers LR_1.

LR_2 dacite lava dome and LT_2 dacitic pyroclastics: LR_2 corresponds to the so-called white rhyolite of Kuroko deposits and has a close relation to mineralization. Its marginal parts are brcciated. Generally hydrothermal alteration is recognized in these rocks. LT_2 composed of tuff breccia is the explosion product from LR_2, and subjected to silicification and mineralization.

Ore deposits: Ore bodies are divided into siliceous ore, yellow ore, black ore and ferruginous chert zones from lower to upper. The former three ore zones are composed mainly of sulfide minerals and barite. The ferruginous chert zone are composed of quartz, barite and hematite.

LR_3 dacite lava dome and LR_3 dacitic pyroclastics: LR_3 covers partly ore bodies, but essentially shows feature of lava dome (Odajima, 1983). Dacite is affected by hydrothermal alteration. LT_3 is the explosion product from LR_3.

Middle Formation

MT_1 basaltic tuff: It consists of basaltic tuff interbedded by lenticular mudstone, and covers directly ore bodies.

AGE, FORMATION			ROCK TYPE	
Quaternary			Pumice flow	
Miocene, Tertiary	Funakawa	Tobe	Accidental tuff breccia	
	On-nagawa	Upper	Dacite	UD
			Pumice tuff	UT
		Middle	Mudstone	MM
			Basalt lava flow & Dolerite	MB_2 DO
			Dacite lava flow	MD
			Pumice tuff	MT_2
			Basalt lava flow	MB_1
			Basaltic tuff	MT_1
	Nishikurosawa	Lower	Dacite lava dome & Dacitic pyroclastics	LR_3 LT_3
			Dacite lava dome & Dacitic pyroclastics	LR_2 LT_2
			Dacitic tuff breccia	LT_1
			Dacite lava	LR_1
Paleozoic	Basement		Slate, Chert & others	

COLUMNAR SECTION

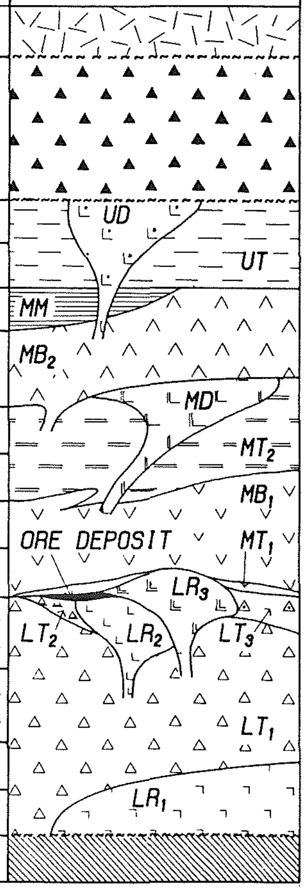

Fig. 1 Stratigraphic succession of the Furutobe mining area.

MB_1 basalt lava flow: It is the so-called Ainai basalt. It consists of massive green basalt flow and shows often pillow structures. Its thickness is 350 meters.
MT_2 pumice tuff: It consist of pumice tuff and tuff breccia, and is well-exposed west of the mining area.
MD dacite lava flow: The rock is compact dacite with columnar joints. Vents of this unit are observed underground.
MB_2 basalt lava flow and DO dolerite: MB_2 is the so-called Yotsukuma basalt and consists of compact basalt flow. DO intrudes into LT_1 and MT_2. The relation between MB_2 and DO is not clear, but assumed that DO is the vent part of MB_2.
MM mudstone: Medium grained mudstone crops out west of the mining area. Foraminiferas of this member indicate Lower Miocene in age.
<u>Upper Formation</u>
UT pumice tuff: It crops out north of the mining area and conformably overlies MM.
UD dacite: Dacite which has flow structures intrudes into MM and also covers MM.
<u>Tobe Formation</u>
This formation consists of accidental tuff breccia and unconformably overlies the Upper Formation.

Magnetic Polarity

Samples are collected on the surface and underground. Remanent magnetizations were measured by an astatic magnetometer and partly a Schonstedt SSM-2A magnetometer. Alternating field (AF) demagnetization was carried out using a three axis tumbling demagnetizer.

Results are summarized in Table 1 and illustrated in Figure 2. The samples of LT_1 have normal polarity magnetizations. The median destructive fields by AF demagnetization are 30 to 35 mT. Samples of LR_2 and LR_3 have normal polarity magnetizations. However, those are hydrothermally altered and opaque oxide minerals examined under an ore microscope are hematite. Magnetite as a rock forming mineral are completely changed to hematite. Those magnetizations may the chemical remanent magnetizations at the period of hydrothermal alteration(Ueno, 1982). In this paper, LR_2 and LR_3 are omitted from Table 1 and Figure 2. Ferruginous chert samples have hard reversed polarity magnetizations and median destructive fields are over 100 mT. The magnetizations of them are due to fine grained hematite(Ueno, 1975). Samples of MT_1 have two magnetic polarities, although magnetic directions are slightly scattered. One is the reversed polarity magnetization from the lower half portion of MT_1. The other is the normal polarity magnetization from the upper half

Table 1. Results of magnetic measurements

Member	Initial Remanence						After AF demag.							
	N	M	D°	I°	k	α°	N	AF	M	D°	I°	k	α°	Pol
LT_1	10	55	037	52	7	16	14	200	47	041	50	5	20	N
Ore	24	218	166	-51	24	6	24	300	137	171	-54	31	5	R
MT_1	25	5.2	167	-42	2	28	25	100	4.2	164	-46	2	28	R
MT_1	8	31	329	51	38	9	8	100	19	326	56	19	13	N
MB_1	31	947	000	52	16	7	31	200	485	003	49	15	7	N
MT_2	14	78	045	54	13	12	14	200	63	044	56	14	11	N
MD	16	11	253	-63	38	6	16	200	9.3	245	-60	50	5	R
DO	22	571	223	-18	7	12	22	150	446	217	-37	21	7	R
MB_2	35	365	179	-41	13	7	36	150	249	181	-40	20	6	R
UT	4	98	190	-9	6	41	4	200	138	187	-42	187	7	R

N is the number of specimens. M is the mean intensity in 10^{-3}A/m(10^{-6} emu/cm^3). AF is the peak alternating field in mT (10 Oe). D° is the declination, clockwise from true north. I° is the inclination, positive downward. k is Fisher's best estimate of precision. α° is the half angle of the cone of confidence at p=0.95 (Fisher, 1953). Polarities are shown in the last column; N (R) is normal (reversed).

portion. The median destructive fields are over 45 mT. It is sure that the geomagnetic field has changed from reversed to normal one during sedimentation of MT_1. Samples of MB_1 have normal polarity magnetizations and the median destructive fields by AF magnetization are 40 mT. Samples from many localities of MT_2 have normal polarity magnetizations and show smooth AF curves with median destructive of 35 mT. Samples of MD have the reversed polarity magnetizations of which destructive fields are over 50 mT. MB_2 magnetized reversely (Table 1) has cooled during a reversed polarity chron in stead of a normal polarity chron of MB_1. Samples of DO have also reversed magnetizations. The median destructive fields of MB_2 and DO samples are 20 mT. These measuring results support that DO is the intrusive phase of MB_2. Measurements for MM are not succeeded. Samples of UT have reversed polarity magnetizations.

As described above, the magnetic polarity sequence of the Furutobe mining area is completed. That is useful as standard one for further paleomagnetical researches of other Kuroko deposits. It is supported that the Kuroko mineralization

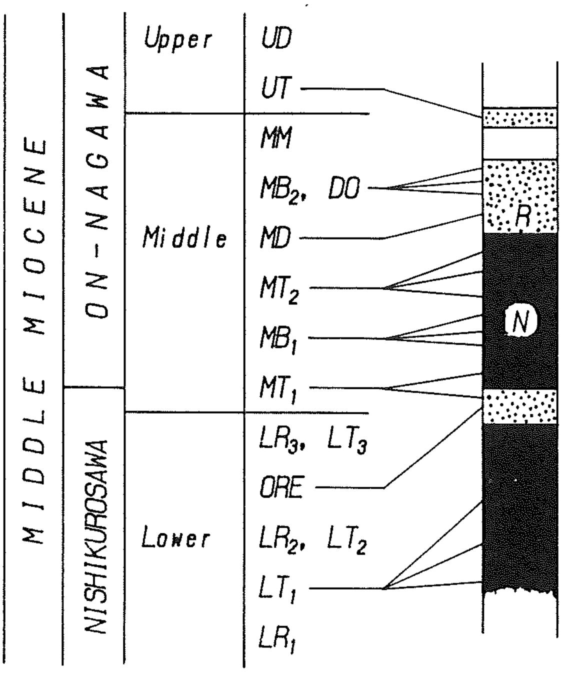

Fig. 2 Magnetic polarity sequence of the Furutobe mining area.

occurred during a short reversed polarity interval at the latest period of the Nishikurosawa age (Ueno, 1975).

References

Fisher, R. A.(1953) Royal Soc. Proc., ser.A, **217**, 295.

Metal Mining Agency of Japan (1978) Rept. on detailed surveys in the Hokuroku district, the 52nd fiscal year of Showa.

Odajima, Y.(1983) Mining Geol., **33**, 201.

Tanaka, T. and Lu, K. I.(1969) Mining Geol., **19**, 312.

Ueno, H.(1975) Nature, **253**, 428.

Ueno, H.(1982) Sci. Rept. Tohoku Vniv., ser.3, **15**, 273.

PALEOMAGNETISM OF MIOCENE SEDIMENTARY ROCKS AROUND MATSUSHIMA BAY, NORTHEAST JAPAN AND ITS IMPLICATION TO THE TIME OF THE ROTATION OF NORTHEAST JAPAN

Toshitsugu YAMAZAKI

Geological Survey of Japan, Higashi, Tsukuba, Ibaraki 305, Japan

A paleomagnetic study of sedimentary rocks distributed in the Matsushima area, Northeast Japan (Fig.1), was conducted. Samples were collected from the Ajiri, Matsushima and Otsuka Formations of the early to middle Miocene Matsushimawan Group. Based on the diatom biostratigraphy (Akiba et al., 1982), the strata from the uppermost part of the Ajiri Formation to the lowermost part of the Otsuka Formation are assigned to the *A. ingens* Zone. The rest of the Otsuka Formation is correlated to the *D. lauta* Zone. Stability of remanence was investigated by the progressive thermal demagnetization method.

The magnetic reversal sequence of the Matsushima and Otsuka Formations is correlative with that of the standard time-scale of around 16 Ma (from the Polarity Chron 5C to 5B of Harland et al. 1982) on the basis of diatom biostratigraphy (Fig. 2). The magnetization of the Matsushima and Otsuka Formations was grouped into two antipodal directions of close to north-south (Fig. 3). The Ajiri Formation, which is overlain be the Matsushima Formation, also showed north or slightly eastward deflected magnetic direction (Fig. 3). However, the suspicion that the magnetization of the Ajiri Formation is of secondary origin still remains.

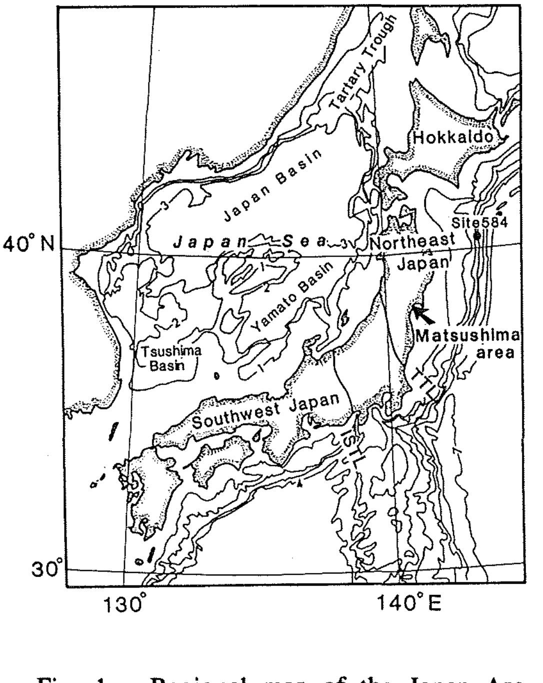

Fig. 1 Regional map of the Japan Arc and the Japan Sea. The location of the Matsushima area is shown by an arrow. Depth contours are at 1000m intervals. Abbreviations are ISTL= the Itoigawa-Shizuoka Tectonic Line, TTL= the Tanakura Tectonic Line.

It has been proposed by previous works that the counter-clockwise rotation of Northeast Japan occurred in early to middle Miocene with the opening of the Japan Sea (Otofuji et al., 1985 ;

Tosha and Hamano, 1988). I conclude that the rotation had been completed before 16 Ma. On the other hand, eastward deflected paleomagnetic directions have been reported from the strata in Southwest Japan which are correlative precisely with the Matsushima and Otsuka Formations by both biostratigraphy and magnetostratigraphy (Hayashida and Ito, 1984; Hayashida, 1986; Itoh, 1988; Itoh and Hayakawa, 1988). This implies that the rotation of Northeast Japan took place earlier than that of Southwest Japan.

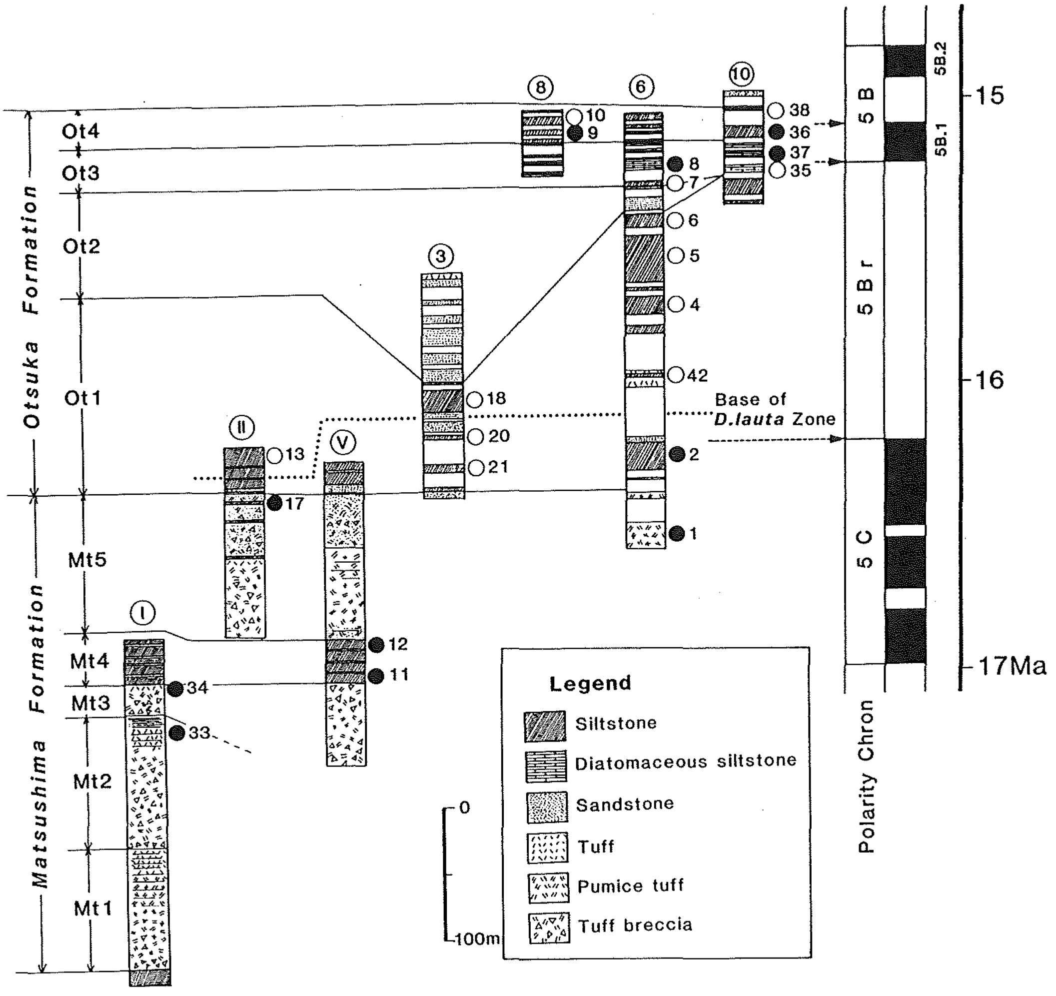

Fig. 2 Summary of the magnetostratigraphy of the Matsushima and Otsuka Formations. Solid (open) circles denote the normal (reversed) polarity. Numbers attached to the symbols represent the names of the sampling sites. Stratigraphic columnar sections are simplified from Ishii et al. (1982). Numbers on the top of the columnar sections correspond to those of Ishii et al. (1982). The boundary of the two diatom zones, *D. lauta* zone and the *A. ingens* zone, is from Akiba et al. (1982). The polarity reversal time scale of Harland et al. (1982) was adopted.

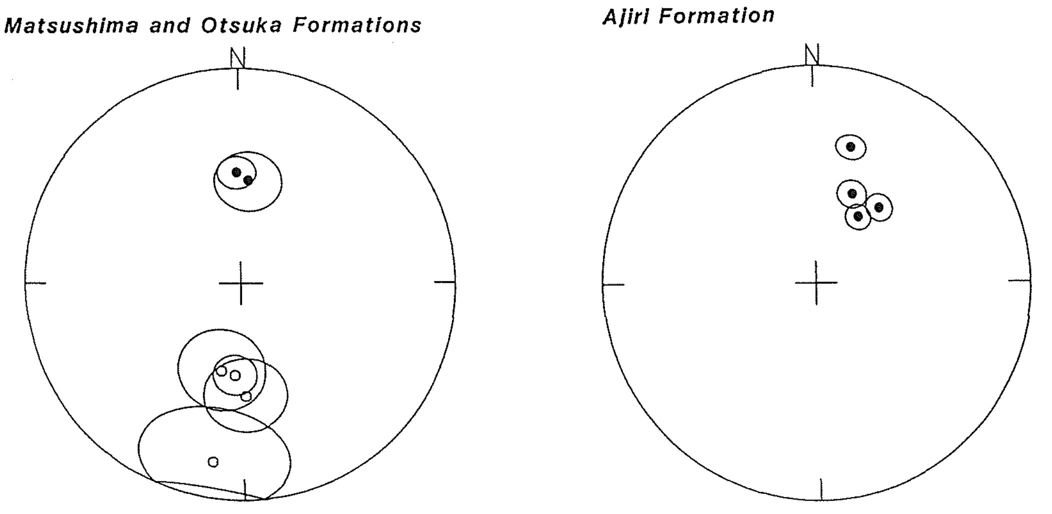

Fig. 3 Equal-area projection of the site-mean directions of (left) the Matsushima and Otsuka Formations and (right) the Ajiri Formation. Only the sites which have five or more independently oriented samples are plotted. Solid(open) circles denote lower (upper) hemisphere directions.

References

Akiba, F., Yanagisawa, Y. and Ishii, T. (1982) *Bull. Geol. Surv. Japan*, **33**, 215 (in Japanese with English abstract).

Harland, W.B., Cox, A.V., Llewellyn, P.G., Pickton, C.A.G., Smith, A.G. and Walters, R. (1982) *A geologic time scale*, (Cambridge University Press, Cambridge), 131pp.

Hayashida, A. (1986) *J. Geomag. Geoelectr.*, **38**, 295.

Hayashida, A. and Ito, Y. (1984) *Earth Planet. Sci. Lett.*, **68**, 335.

Ishii, T., Yanagisawa, Y., Yamaguchi, S., Sangawa, A. and Matsuno, K. (1982) *Geology of the Matsushima district*, with Geological Sheet Map at 1:50,000 (Geol. Surv. Japan), 121pp (in Japanese with English abstract).

Itoh, Y. (1988) *J. Geophys. Res.*, **93**, 3401.

Itoh, Y. and Hayakawa, H. (1988) *Jour. Geol. Soc. Japan*, **94**, 515 (in Japanese with English abstract).

Otofuji, Y., Matsuda, T. and Nohda, S. (1985) *Earth Planet. Sci. Lett.*, **75**, 265.

Tosha, T. and Hamano, Y. (1988) *Tectonics*, **7**, 653.

(In press in *J. Geomag. Geoelecter.*)

THE DISTRIBUTION OF MAGNETIZATION IN THE EASTERN PART OF THE JAPAN BASIN

Nobukazu SHIMA*, Kiyoto MATSUMOTO*, Masahide FURUKAWA** and Nobuhiro ISEZAKI*

* Department of Earth Sciences, Faculty of Science, Kobe University, Kobe 657, Japan
** The Graduate School of Science and Technology, Kobe University, Kobe 657, Japan

The three component geomagnetic data in the eastern part of the Japan Basin were obtained by a Shipboard Three Component Magnetometer (Isezaki 1986) on the expedition of the R/V Hakuho-maru in 1986 and the R/V Tansei-maru in 1987. The total intensity geomagnetic data presented here were gathered not only from these cruises but also from the Geological Survey of Japan, the Lamont-Doherty Geological Observatory, Kumi and Kofu Cruises. The residual anomaly was calculated using IGRF85. Correction of daily variation is made using the land data. Hybrid positioning data by Loran C, NNSS and GPS were used.

We calculated the distribution of magnetization of the sea floor through the following procedure. First, geomagnetic anomaly values were interpolated by Briggs's method (Briggs 1974) over a regular grid (3 km * 3 km) using all the data along the tracks. Then, an inversion technique was used for the calculation of the distribution of magnetization from these grid data. We adopted the rectangular prisms for the magnetized layer (Figure 1). The calculation was based on four assumptions. (1) The direction of magnetization is parallel to the geocentric axial dipole field. Declination is 0 degree and inclination is 60 degrees. (2) The magnetized layer lies at 5 km below the sea level: The surface of this magnetized layer corresponds to the acoustic basement of seismic reflection data (Hilde et al. 1973, Ludwig et al. 1975, Tamaki 1988, Kuramoto et al. 1988). (3) The thickness of magnetized layer is 1 km. (4) The calculation is restricted only in the boxed area in Figure 2a, because this area has fairly flat basement.

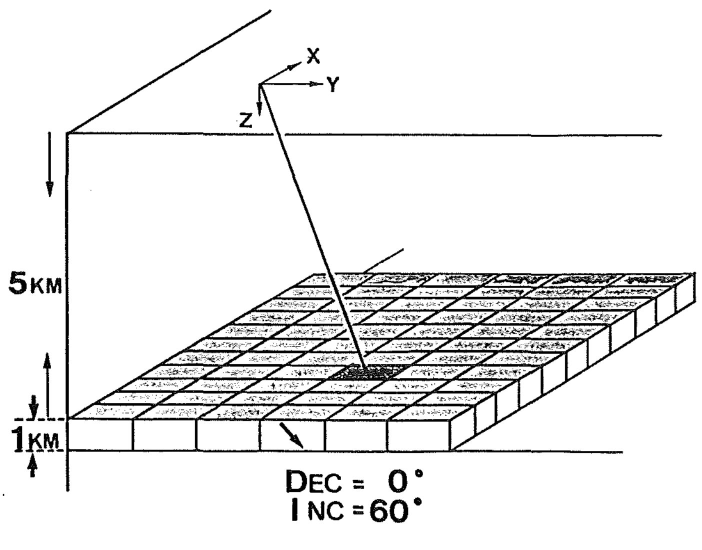

Fig.1 The model for the calculation of the distribution of magnetization

The result of the calculation is presented as magnetization intensity 2.5 A/m contours in Figure 2b. Positive, zero and negative magnetization are shown by dash-dot lines, solid lines and long-dash lines, respectively. Reliability of our result is ascertained by comparison the geomagnetic anomaly field calculated from this distribution with the observed one. They agreed well with each other.

Our results are summarized as follows. The distribution of magnetization is characterized by segmented magnetized bodies. (1) Eight elongated magnetized bodies in the direction of NE-SW with length between 20 km and 70 km. (Those are shown by thick solid lines in Figure 2b.) (2) Five fairly round-shape magnetized bodies with width between 10 km and 30 km. (Those are shown by arrows in Figure 2b.) (3) No long lineations which exist along the typical oceanic ridge such as Mid Atlantic Ridge. These features were kept unchanged whenever we calculated the distribution of magnetization by changing the direction of magnetization and the thickness of the magnetized layer.

This distribution implies the multi-type rifts: Many intrusions occurred when the Japan Basin was opening. Rifts and intrusions probably correspond to the elongated bodies and the round-shape bodies of magnetization, respectively. The elongated direction NE-SW appears to be perpendicular to that of the tectonic tension concerned in opening the Japan Basin.

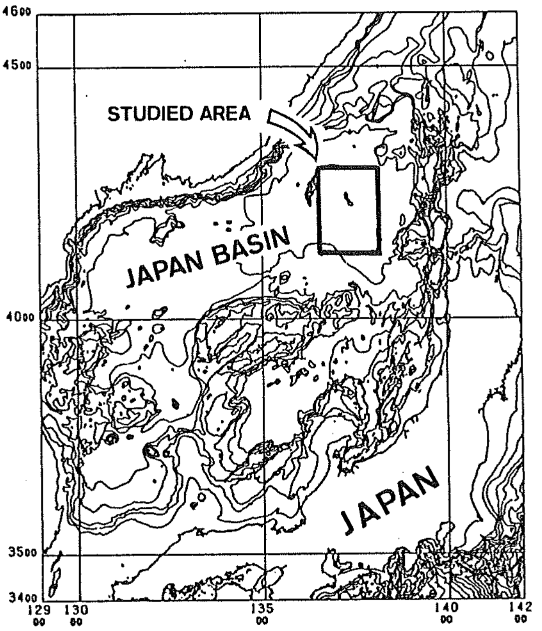

Fig. 2a

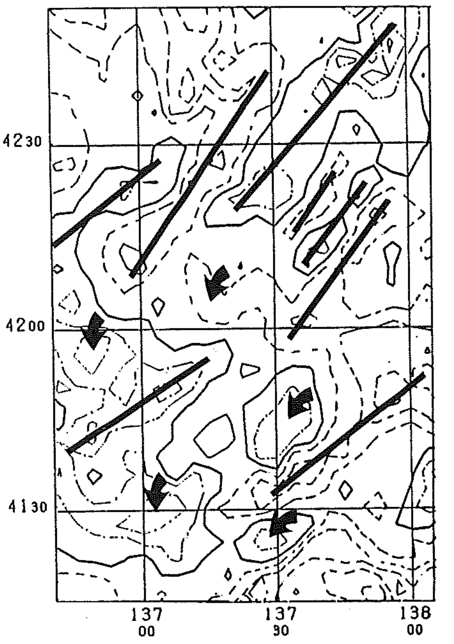

Fig. 2b

Fig. 2a Bathymetry around the Japan Basin based on GEBCO(JODC). The boxed area where we presented the result.

Fig. 2b The distribution of magnetization (contour interval 2.5 A/M) calculated from total intensity geomagnetic anomaly and our interpretation. Dash-dot lines, solid lines and long-dash lines shows positive, zero and negative magnetization, respectively. Thick solid lines show elongated magnetized bodies. Arrows show fairly round-shape magnetized bodies.

We conclude multi-type rifts and many intrusions characterize the eastern part of the Japan Basin. These features are geophysical evidences to show the opening type of the Japan basin. We believe whole the Japan Basin was also created in the same way.

References

Briggs, I.C. (1974) Geophysics, 39, 39-48
Hilde, T.W.C. and J.M.Wageman (1973) The Western Pacific, edited by P.J.Coleman (Univ. Western Australia Press), 415-434
Isezaki, N. (1986) Geophysics, 51, 1992-1998
Kuramoto, S., H.Tokuyama, T.Asanuma and M.Suemasu (1988) Preliminary Report of The Hakuho Maru Cruise KH86-2 (Ocean Research Institute Univ. of Tokyo), 92-109
Ludwig, W.J., S.Murauchi and R.E.Houtz (1975) Geol. Soc. Am. Bull., 86, 651-664
Tamaki, K. (1988) Bulletin of the Geological Survey of Japan, 39, 269-365

$^{40}Ar-^{39}Ar$ AGE STUDIES ON IGNEOUS ROCKS DREDGED FROM THE CENTRAL PART OF THE JAPAN SEA DURING GH78-2 CRUISE

Ichiro KANEOKA* and Makoto YUASA**

* Earthquake Research Institute, University of Tokyo, Bunkyo-ku, Tokyo 113

** Division of Marine Geology, Geological Survey of Japan, Higashi 1-1-3, Tsukuba 305

The GH78-2 Cruise by the research vessel "HAKUREI-MARU" of the Geological Survey of Japan was conducted to investigate the geology of the continental shelves and slopes of the eastern and central parts of the Japan Sea in April-June, 1978. Preliminary results are summarised in the Cruise Report (Honza, ed., 1979). During the cruise, many igneous rocks were dredged. In order to get information on the evolution of the Japan Sea floor, we have performed $^{40}Ar-^{39}Ar$ dating for igneous rocks recovered from five localities.

Samples were chosen on the basis of the interests of their dredging localities and freshness of samples. They include a hypersthene-augite olivine andesite (D277-8) from the southern slope of the Yamato Bank, a hypersthene andesite (D279-1) from the continental slope to the north off the Noto Peninsula, a hornblende-biotite granite (D287-3) from the slope of Mukaise to the north off the Sado Island, an augite-orthopyroxene trachyte (?)(D292-1) from the slope of Oga-Mukose and an olivine basalt (D294-1) from the slope of a high point off the Oga Peninsula.

They were irradiated with fast neutron by the JMTR of the Tohoku University. Experimental procedures are the same as those reported before (Kaneoka, 1980).

Among five samples analysed, three samples show plateau ages. One of the examples is shown in Fig. 1 for D292-1. For this sample, three temperature fractions(1000°-1500°C) show a plateau age of 23.6+0.6Ma with 89% of integrated ^{39}Ar for these

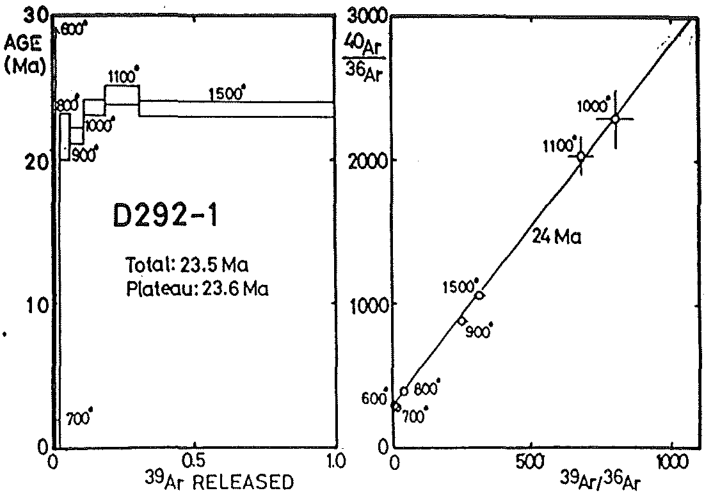

Fig.1 $^{40}Ar-^{39}Ar$ diagram for the sample D292-1.

ranges. The total $^{40}Ar-^{39}Ar$ age (23.5Ma) is quite similar to the plateau age, suggesting that the effect of Ar loss or excess ^{40}Ar is rather small for this sample. The other two samples D279-1 and D287-3 also indicate plateau ages of 23.9± 0.8Ma and 22.0±0.7Ma, respectively. The sample D277-8 shows, however, no plateau in the release patterns of $^{40}Ar-^{39}Ar$ ages and indicate a total $^{40}Ar-^{39}Ar$ age of 26.3Ma. In the case of the sample D294-2, the release patterns of $^{40}Ar-^{39}Ar$ ages are quite scattered, indicating the occurrence of excess ^{40}Ar in this sample.

These results are summarised in Fig. 2. Except for the sample D294-2, all these samples were dredged from continental shelves and slopes and show $^{40}Ar-^{39}Ar$ ages older than 20Ma. A quartz diorite dredged from a site to the east of the sample D279-8 shows a K-Ar age of 26.7Ma (GSJ, unpublished), which is similar to the total $^{40}Ar-^{39}Ar$ age of the sample D277-8. So far, all igneous rocks dredged from the Yamato Bank area show radiometric ages of more than 20Ma. An andesite dredged at a site close to that of the sample D279-1 has been reported to have a K-Ar age of about 8Ma (Ueno et al., 1974). The relatively young K-Ar age might have been caused by radiogenic ^{40}Ar loss due to the alteration of the sample. Another possibility is that these rocks represent different volcanic activities, respectively. Although the K-Ar age would probably indicate the younger limit for its formation age, the discrepancy in the apparent ages is so large. Hence, it is more likely that these volcanic rocks erupted at different times.

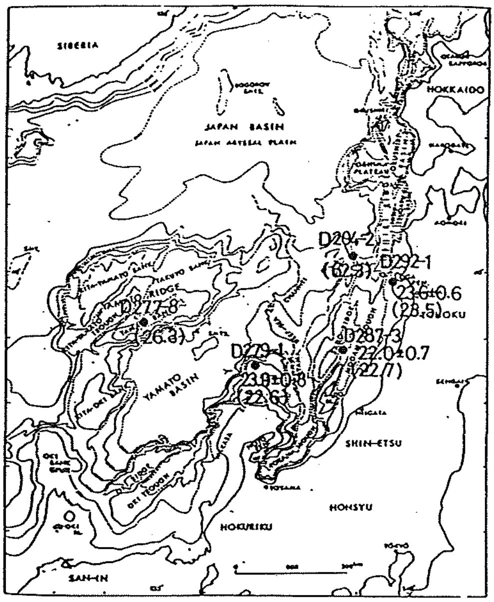

$^{40}Ar-^{39}Ar$ AGE: Plateau Age (Ma) (Total Age)

Fig.2 Dredging sites of analysed rocks and the results of $^{40}Ar-^{39}Ar$ dating.

The $^{40}Ar-^{39}Ar$ age of the sample D287-3 is similar to K-Ar ages of igneous rocks from the Sado Island reported by Konda and Ueda(1980). Hence these igneous activities might have been related each other. The $^{40}Ar-^{39}Ar$ age of the sample D292-1 corresponds to those which belong to the Monzen-layer in the Oga Peninsula. Since this sample was dredged at a relatively shallow depth (about 100m) from the slope of the Oga Peninsula, it is probably a volcanic product which is closely related to those in the Oga Peninsula.

Thus except for the sample D294-2, the other four samples show ages older than 20Ma. However, all samples from the Yamato Seamount chain show ages younger than 20Ma (Kaneoka et al. 1986).

Hence, present samples would probably represent the igneous products which might have occurred before the Yamato Basin was formed, or at least before the Yamato Seamount chain was formed.

References

Honza, E.(ed.)(1979)Cruise Report No.13, 99p., Geol. Surv. Japan.

Kaneoka, I. (1980) Earth Planet. Sci. Lett. 46, 233.

Kaneoka, I., K. Notsu, Y. Takigami,K. Fujioka and H. Sakai (1986) Rock Mag. Paleogeophys., 13, 48.

Konda, T. and Y. Ueda (1980) J. Min. Pet. Econ. Geol., Spec. Issue No.2, 343.

Ueno, N., I. Kaneoka and M. Ozima (1974) Geochem. J., 8, 157.

PALEOMAGNETIC CONSTRAINT ON THE NORTHERN AND SOUTHERN BORDERS OF NORTHEAST JAPAN BLOCK AND THE TIMING OF ITS ROTATION

Hidefumi TANAKA[1)] and Hideo TSUNAKAWA[2)]

1) Earth and Planetary Sciences, Tokyo Institute of Technology, Meguro-ku, Tokyo 152, Japan
2) Institute of Research and Development, Tokai University, Kanagawa 259-12, Japan

Rotation of Northeast Japan clarified by paleomagnetism is interpreted in relation to the opening of the Japan Sea. The extent of the Northeast Japan is usually supposed to be Tohoku Region north of Tanakura Tectonic Line (TTL) including West Hokkaido bordered by Ishikari Low Land (ILL). However, most of paleomagnetic results come from limited parts of Tohoku Region. We need more paleomagnetic informations from other areas especially Hokkaido to confirm the north and south borders of Northeast Japan Block and whether within-block coherency of rotation existed. It is important to know when Northeast Japan rotated to discuss the opening models of the Japan Sea. Paleomagnetic evidences, however, are still not enough to constrain the timing as accurate as in Southwest Japan. For better understanding of the rotation history of Northeast Japan we made two paleomagnetic studies from northernmost and southernmost parts. We here present the results of the paleomagnetic studies (one of the two is very preliminary) and summarize available Northeast Japan poles since Oligocene.

Paleomagnetic study was made on Oligocene to Pliocene sedimentary and volcanic rocks from Shakotan Peninsula, West Hokkaido. Out of 18 successful sites, two oldest rhyolite (35 Ma) showed, unfortunately, very abnormal directions which might be caused by incorrect tilting data. Omitting the oldest two, all other sites give almost north-south directions. A paleomagnetic pole of (77.9°N, 249.5°E, A_{95}=9.5°) is concluded for 5-15 Ma which indicates no tectonic movement of Shakotan Peninsula since 15 Ma.

Another paleomagnetic study is in progress for Oligocene and Miocene sedimentary rocks near Tsukuba all of which are within 50 km from the TTL including both east and west sides. Preliminary result shows westerly deflected normal direction (I=52°, D=324°, α_{95}=21°) for Upper Miocene. This direction should be regarded as very tentative because three sites sampled from Tanokura Formation cover only 1-2 m thickness of the mudstone, and this might be insufficient to average out the effect of the geomagnetic secular variation.

Several paleomagnetic results are now available for Northeast Japan including West Hokkaido if we limit the time to the last 40 Ma (Fig.1). Poles A, B, C, and D by Fujiwara and Sugiyama (1986) from Oshima Peninsula of West Hokkaido cover the time back to 25 Ma and indicate counterclockwise rotation of that region at around 15 Ma. A mean pole W for 5-15 Ma from West Hokkaido was calculated from three poles of A, B, and S (Shakotan Peninsula, this study). Poles W, C, and D make up an apparent polar wander path (APWP) for West Hokkaido since 25

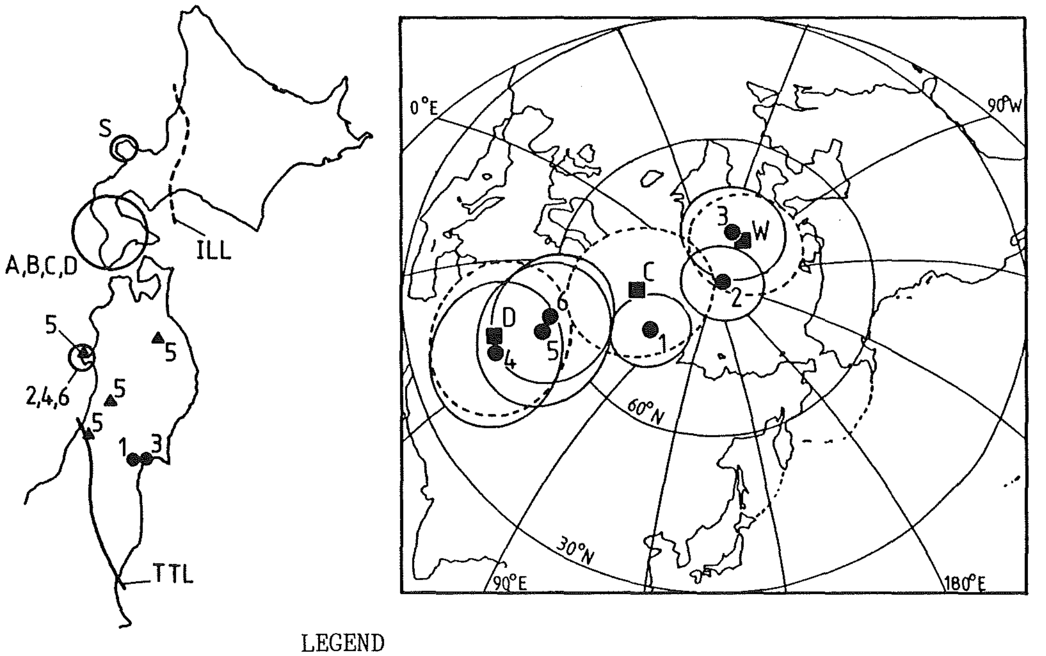

LEGEND

Pole	Age	Formation	Reference
		-- West Hokkaido --	
S	5-15	Shakotan Peninsula	This study
A	7-11	Oshima Peninsula	Fujiwara & Sugiyama (1986)
B	11-14.5	Oshima Peninsula	Fujiwara & Sugiyama (1986)
(W	5-15	Mean of S, A, B)	
C	14.5-17	Oshima Peninsula	Fujiwara & Sugiyama (1986)
D	20-25	Oshima Peninsula	Fujiwara & Sugiyama (1986)
		-- Tohoku Region --	
1	8	Shimokura dikes	Tsunakawa et al. (1985)
2	12-15	Nishikurosawa and Onagawa Formation	Tosha & Hamano (1988)
3	16	Matsushima and Otsuka Formation	Yamazaki (1989)
4	22	Daijima Formation	Tosha & Hamano (1988)
5	20-32	Volcanic Rocks	Otofuji et al. (1985)
6	35	Monzen Formation	Tosha & Hamano (1988)

Fig.1 Comparison of two groups of poles from Tohoku region (circles) and West Hokkaido (squares).

Ma. These poles (squares with α_{95} of dotted line) were compared with Tohoku Region poles since 35 Ma (circles with α_{95} of solid line) in Fig.1. Six poles from Tohoku Region roughly lie on a segment which almost coincides with that of West Hokkaido. The two pole groups overlap completely and obviously this must be an evidence for the usual idea that West Hokkaido and Tohoku Region form the same block as Northeast Japan.

The pole distribution, however, has some problems if we carefully observe Fig.1. Sampling localities of pole 1 (8 Ma) by Tsunakawa et al. (1985) from Shimokura dike swarm and pole 3 (16 Ma) by Yamazaki (1989) from Matsushima and Otsuka Formation are close to each other of within 30 km, and yet their implications are very much different. Although Shimokura dike swarm give only one polarity, it is unlikely that the dikes intruded during only short time. Tsunakawa et al (1985) carefully examined the angular standard deviation (ASD) of dike's remanence directions. The calculated ASD is reasonably large to suppose that the duration of volcanic activity was long enough to average out the secular variation effect. Then possible explanation would be that there was a very local tectonic movement in Matsushima region. It is noted that our preliminary result from Upper Miocene mudstone sampled near this region also shows westerly deflected paleomagnetic direction.

On the timing of the rotation of Northeast Japan, we suspect Northeast Japan might have rotated at an earlier time than Southwest Japan. The reason is that Shakotan Peninsula (S) whose lowest member is older than 15 Ma (K-Ar) or 17 Ma (fission track) and Matsushima and Otsuka Formations (3) by Yamazaki (1989) of around 16 Ma show north-south paleomagnetic directions. Another aspect we also suspect is that the rotation velocity of Northeast Japan might have been slower than that of Southwest Japan.

REFERENCES

Fujiwara, Y. and R. Sugiyama (1986) Rock Mag. Paleogeophys. 13, 15.

Otofuji, Y., T. Matsuda, and S. Nohda (1985) Earth Planet. Sci. Lett. 75, 265.

Tosha, T. and Y. Hamano (1988) Tectonics 7, 653.

Tsunakawa, H., K. Heki, and K. Amano (1985) J. Geomag. Geoelectr. 37, 979.

Yamazaki, T. (1989) submitted to J. Geomag. Geoelectr.

PALEOMAGNETIC STUDY OF EASTERN TIBET
- DEFORMATION OF THE THREE RIVERS REGION -

Yo-ichiro OTOFUJI*, Yasuko INOUE*, Shoubu FUNAHARA*, Fumiyuki MURATA* and Xilan ZHENG**

* Department of Earth Sciences, Faculty of Science, Kobe University, Kobe 657, Japan
** Institute of Geology, Academia Sinica, Beijing, China

INTRODUCTION

Peculiar kink shape is observed in geomorphology at eastern Tibet which is bounded on the west to the Tibetan Plateau and on the east to the Yangtze block. Large three rivers, the Saluween, the Mekong and the Yangtze, flow southeastward in the Tibetan Plateau. These rivers are once concentrated in the narrow zone with width of about 200 Km, and change their flows to North-south direction in eastern Tibet. The large kink shape in this area is probably reflection of a large tectonic deformation of the Asian continent.

We had an expedition to traverse eastern Tibet along the latitude of about 30°N from Lhasa to Chengdu for 2800 Km (Fig. 1). More than 150 oriented samples were collected in an attempt to determine the deformation aspect of eastern Tibet.

Samples were collected at 40 sites from three geological tectonic provinces (Geological map of the Tibetan Plateau, 1981); the Lhasa block (23 sites), the Three rivers region (8 sites), and the Sichuan province (9 sites). Samples consist of Jurassic-Cretaceous red sand stone of 19 sites and Jurassic-Tertiary granite of 21 sites.

DEMAGNETIZATION

In the laboratory, individual specimens, 25 mm in diameter and 25 mm long, were prepared from each sample. Natural remanent magnetizations (NRMs) were measured with a ScT cryogenic magnetometer. The stability of the NRM was investigated by thermal demagnetization method. Specimens were demagnetized progressively in more than 17 steps up to 700 °C. Zijderveld component plots were used to assess the directional stability and coercivity spectrum of each specimen.

[Red sandstone]

All samples were found to be magnetically stable, and had unicomponent magnetizations. Demagnetization vectors of all 19 sites reached the origin at around 700 °C, indicating that the NRM resided in hematite.

[Granite]

Samples from Pa-shui area reveled two components of magnetization, whereas a demagnetization trajectory of the high temperature component above 300 °C converged toward the origin. Their NRMs showed a restricted blocking temperature range at around 580 °C, indicating that the high temperature component resided in titanium poor magnetite.

The other samples had unicomponent magnetizations, although they showed a broad blocking temperature range between 100°C and 500°C. The magnetization of more than 50 % of initial NRM was removed up to 250 °C. The low temperature component is probably due to the thermoviscous remagnetization acquired in a recent time (Pullaiah et al., 1975; Kent, 1985).

PALEOMAGNETIC RESULTS

Paleomagnetic directions of unicomponent and those of high temperature component of two components were accepted to be reliable characteristic directions (see Fig. 2). We arbitrarily discarded results from any site for which the precision parameter k was less than 12.

[Sichuan province]

Eight sites of red sand stone remain. Normal and reversed polarities are present. Since we collected from both shoulders of the synclinal structure in Ya'an, the fold test is applied. The precision parameter k increases from 10 to 24 after tilt correction: the fold test is significantly positive at 95 % level (McElhinny, 1964). Characteristic direction after tilt correction (D=2°, I=29°. α_{95}=11°) is accepted to be a primary paleomagnetic direction.

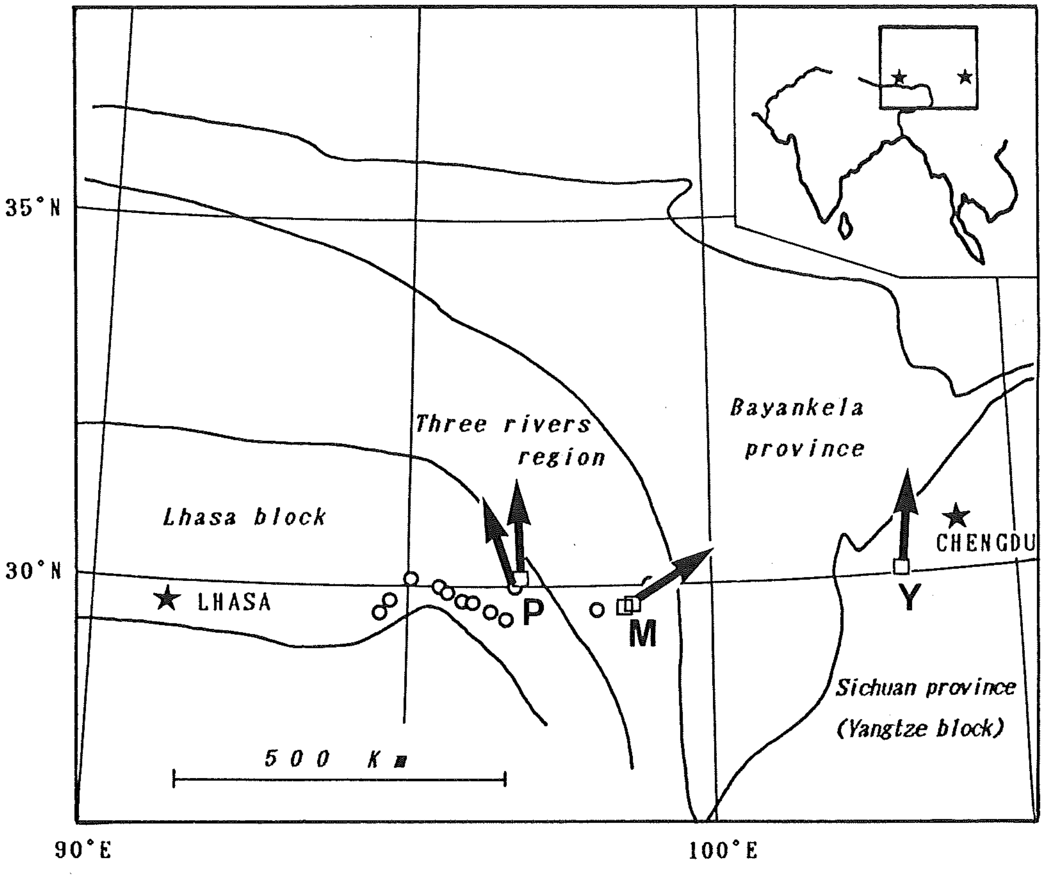

Fig. 1. Sketch map of sampling localities along Lhasa-Chengdu road. Sampling localities of red sandstones and granites are indicated by squares and open circles, respectively. Arrows indicate the declinations of the reliable paleomagnetic directions from three geological provinces. P: Pa-shui, M: Markam, Y: Ya'an.

[Three rivers region]

Five sites of red sandstone remain. Since the Jurassic formation show a homoclinal structure in Markam, we cannot apply the fold test. The characteristic directions before tilt correction deviates by 20° from the present direction. The demagnetization behavior of these red sandstones is as stable as that of red sandstones of Sichuan. These imply that their characteristic directions are due to primary component. Characteristic direction after tilt correction (D=48°, I=51°, α_{95}=11°) is accepted to be a marginally reliable paleomagnetic direction of Jurassic to Cretaceous time.

[Lhasa block]

Five sites of red sandstones and twelve sites of granite remain.

The fold test is not applied because we collected red sandstone from a homoclinal structure in Pa-shui. Characteristic direction has westerly direction and deviates by 37° from the present direction before tilt correction. The NRMs showed monotonous convergence to the origin in the orthogonal plot during thermal demagnetization. Based on these facts, we accept these characteristic directions of red sand stone after tilt correction (D=-1°, I=33°, α_{95}=24°) as a marginally reliable data for a primary paleomagnetic direction.

Except for two sites from Pa-shui, the directions of granite have normal polarity and are parallel to the present geomagnetic direction (D=3°, I=40°, α_{95}=9°; D=-1°, I=44°). These directions may be attributed to a secondary origin, probably produced in Brunhes Epoch. These directions are excluded from further paleomagnetic investigation.

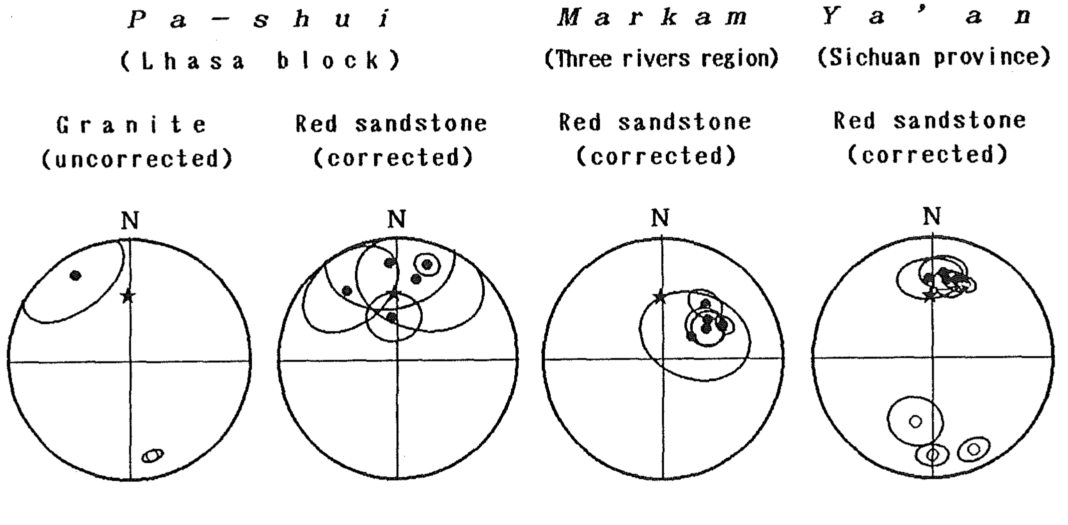

Fig. 2. Mean magnetic directions and 95 % confidence circles from three geologic provinces of the Lhasa block, the Three river regions, and the Sichuan province. Projections are equal area, solid (open) symbols on the lower (upper) hemisphere. Stars: present geomagnetic field direction.

Two sites from Pa-shui consist of NRM directions with both normal and reversed polarities. Their directions are antipodal each other. Their directions enough deviate from the present geomagnetic field direction, and are fairly parallel to the paleomagnetic directions of red sandstone after tilt correction. We accept these direction (D=-22°, I=15°) as a marginally reliable paleomagnetic direction.

DISCUSSION

Paleomagnetic directions of the Lhasa block and the Sichuan province are comparable with those previously reported from the same geological provinces.

Paleomagnetic direction was observed from Albian-Aptian Takena Formation in the Lhasa block (Achache et al., 1984). This formation has a paleomagnetic direction of D=-12.3°, I=24.0°, α_{95}=6.6 in the northern part of Lhasa. The expected direction from the data of Lhasa is D=-10.4° and I=21.7° at Pa-shui. Difference between observed paleomagnetic directions and expected ones at Pa-shui is ΔD=9.3° ± 29.7° and ΔI=11.1° ± 24.8°. This implies that the Pa-shui and the Lhasa areas have undergone any little relative movement, indicating that the Lhasa block including the Lhasa and the Pa-shui areas has behaved as a rigid unit block.

Kent et al. (1986) reported the Cretaceous paleomagnetic pole (80.9°N, 296.8°E, α_{95}=7.7°) from Western Sichuan at 102.3°E, 26.5°N. The expected direction calculated from this pole is D=-2.3° ± 8.3°, I=38.0° ± 11° at Ya'an, whereas our observed data in Ya'an is D=2°, I=29°, α_{95}=11°. Difference between expected and observed directions is ΔD=4.3° ± 14.6°, ΔI=9.0° ± 16.0°. This comparison clearly shows that the Sichuan province has been also behaved as a rigid block since Cretaceous.

The most striking result from this work is a large clockwise deflection in the paleomagnetic direction in the three rivers region. The amount of rotation is estimated from the comparison between the observed declination value and expected one calculated from 140 Ma pole of Northern Eurasian APWP of Irving (1977): R=28° ±20°. Inclination data indicate little significant north-south ward displacement, because the deference is only 2° ±14° between the observed and expected inclination values (51° ± 11° vs. 53° ± 8°). Three river region has undergone a clockwise rotation of about 30° without any north-south translation since Cretaceous time.

Clockwise rotation of about 30° is consistent with the amount of the flow change of the large three rivers. The Saluween river changes its flow direction from southeast to south by 36 degrees in eastern Tibet, the Mekong river changes by 21° and the Yangtze river changes by 35°. Clockwise paleomagnetic rotation of 28° is a geophysical evidence for tectonic origin of the large kink shape of the three river region.

Paleomagnetic data of eastern Tibet suggest that the tectonic deformation occurred only at the area between two rigid blocks of the Lhasa and the Sichuan. Since inclination of the Lhasa block is shallower by about 20 degrees than that of the Three rivers region, the kink shape observed in the Three river region is probably created by the northward translation of the rigid Lhasa block. After collision of Indian continent with the Lhasa block at about 50 Ma (Patriat and Achache, 1984), northward rush began in the Lhasa block by about 2000 Km associated with the indentation of India (Tapponnier et al., 1982). Since then deformation has occurred in eastern Tibet and the Three river region has undergone the clockwise rotation by the northward movement of the India and the Lhasa block.

REFERENCES

Achache, J, V. Courtillot and Z.Y. Xin (1984), J. Geophys. Res., 89, 10,311.

Geological map of the Tibetan Plateau (1981), 1/1,500,000, Chengdu, China.

Irving , E. (1977), Nature, 270, 304.

Kent, D.V. (1985), Geophys. Res. Lett., 12, 805.

Kent, D.V., G. Xu, K. Huang, Z. Wen-You and N.D. Opdyke (1986) Earth Planet. Sci. Lett., 79, 179.

McElhinny, M.W. (1964), Geophys. J. R. astr. Soc., 8, 338.

Patriat, P. and J. Achache (1984), Nature, 311, 615.

Pullaiah, G., E. Irving, K.L. Buchan and D.J. Dunlop (1975), Earth. Planet. Sci. Lett., 28, 133.

Tapponnier, P., G. Peltzer, A.Y. Le Dain, R. Armijo and P. Cobbold (1982), Geology, 10, 611.

PRELIMINARY PALEOMAGNETIC DATA FROM THE PALEOZOIC AND MESOZOIC ROCKS OF THE BILLEFJORDEN AREA, SOUTHWEST SPITSBERGEN

Akira HAYASHIDA and Hiroyuki SUZUKI

Laboratory of Earth Science, Doshisha University, Kyoto 602, Japan

Magnetic measurement was carried out on samples from post-Caledonian sedimentary rocks and intrusive rocks distributed in the Billefjorden area, Southwest Spitsbergen. Our sampling sites are located in east of the Central West Fault Zone, where the middle Paleozoic to late Mesozoic strata including Jurassic or Cretaceous dolerite sills strike NNW and dip almost vertically. Remanent magnetization of the samples were measured on spinner and cryogenic magnetometers, and magnetic components were identified through stepwise thermal and alternating field demagnetization.

Characteristic magnetic components were found in Upper Carboniferous red sandstones (2 sites) and a Mesozoic dolerite sill (1 site). Results of the demagnetization experiment suggest that magnetic carriers are hematite in the red sandstones and magnetite in the dolerite sill. Tilt-corrected magnetic directions, which were obtained assuming a simple rotation of the strata around horizontal axes, have low inclination values. The estimated paleolatitude for the late Carboniferous is about 15°N, which is concordant with the low-latitude paleoposition of Paleozoic Spitsbergen (e.g. Steel and Worsley, 1984). The virtual geomagnetic positions determined from the Upper Carboniferous red sandstones and the Mesozoic dolerite sill (Figure 1) are all discordant with the paleomagnetic poles reported from less deformed strata of Spitsbergen (e.g. Vincenz and Jelenska, 1985).

The deflected paleomagnetic poles from the Billefjorden area can be explained by clockwise rotation through about 60° around a vertical axis and a subsequent vertical tilt towards ENE around a horizontal axis. Combination of the two rotations are comparative to a single rotation around the axis oriented NEE and about 25° upward. This rotation is possibly attributed to the early Tertiary deformation along a dextral transform fault zone, to the west of Spitsbergen, which separated the Svalbard Archipelago from Greenland during the opening of the Norwegian and Greenland Sea in the northern Atlantic Ocean.

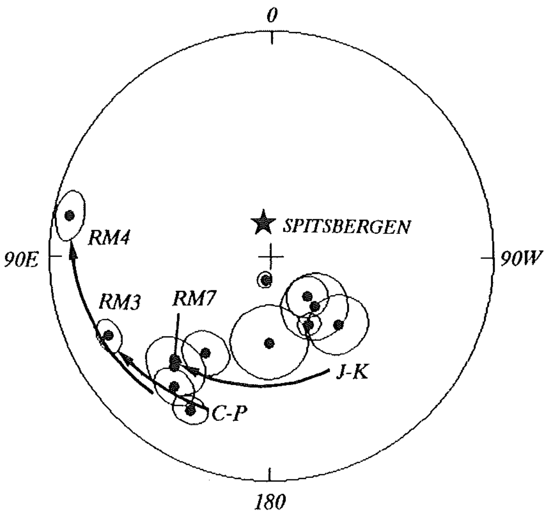

Figure 1. Paleomagnetic poles of Paleozoic sediments and Mesozoic igneous rocks of Spitsbergen (Northern Hemisphere of equal-area projection). RM3 and RM4: Upper Carboniferous red sandstone, RM7: Jurassic/Cretaceous dolerite sill (This study). CP: Carboniferous-Permian poles, JK: Jurassic-Cretaceous poles (from Piper, 1988). Clockwise deflection of the RM3, RM4 and RM7 poles are shown by arrows.

References

Piper, J. D. A. (1988) *Paleomagnetic Database*, (Open University Press), 304 pp.

Steel, R. J. and Worsley, D. (1985) *Petroleum Geology of the North European Margin*, (Graham & Trotman), 109.

Vincenz, S. A. and Jelenska, M. (1985) *Tectonophys.*, **114**, 163.

GRAVITY ANOMALY ACROSS THE PERUVIAN ANDES

Yoshio FUKAO and Akihiko YAMAMOTO

Department of Earth Sciences, Nagoya University, Nagoya 464, Japan

Masaru KONO

Department of Applied Physics, Tokyo Institute of Technology, Tokyo 152, Japan

1. Introduction

The Andes is a huge mountain belt running along the western border of the South American continent and having a length of more than 8000 km. The Andean margin is a place of plate subduction and shares many characteristic features with other subduction zones, such as deep-sea trenches, intermediate to deep focus earthquakes, and active volcanoes. The Peruvian Andes constitute the middle part of the Andean belt. In this area, several gravity studies have already been made, but available data are sparse; usually only gravity maps or gravity profiles were reported. Such smoothed versions of survey results are not often useful for quantitative discussion. Besides these gravity maps several gravity profiles are available in Peru. However, most of the reported gravity profiles are either offshore or coastal and do not extend over the Andean mountain belt except for those of Ocola and Meyer (1973).

To improve the gravity coverage of the Andes, we conducted gravity surveys across several sections of the Peruvian Andes in 1980 and 1984. Our aim in this paper is (1) to report the measured gravity values and Bouguer anomaly values in a hope that they serve as some of the most fundamental information about the Andean structure and tectonics, (2) to construct crustal models along several profiles across the Peruvian Andes from our gravity data, and (3) to compare these crustal models with the distribution of earthquake foci to get insight into the mantle wedge structure beneath the active margin of the South American continent.

2. Peruvian Andes

Peru is geomorphologically divided into three regions: the desert coastal lowlands (below 2000 m), the Andes, and the jungle-covered lowland (below 2000 m) of the upper Amazon Basin. The main geologic units in the coastal lowlands are, from trench eastward, the Arequipa massif in southern Peru, the eugeosynclinal marine volcanics of Mesozoic age in the coastal plains of central and northern Peru, and the coastal batholith of late Cretaceous to early Tertiary ages.

The Andes form a high and rugged barrier between the coastal lowlands on the west and the jungle lowlands on the east. North of about 10°S, the Andean mountain belt consists essentially of a single chain of closely spaced mountain ranges trending parallel to the coast. To the south the mountains branch: the western belt (Western Cordillera) continues parallel to the coast, while the eastern belt (Eastern Cordillera) trends southeast. The crests of both the eastern and western ranges are generally above 5 km. A flat plateau about 4 km in elevation separates the two mountain belts. The width of this plateau is several tens of kilometers in central Peru and increases considerably in the south to nearly 350 km near Lake Titicaca in the Altiplano. The Western Cordillera consists mainly of folded and faulted Mesozoic sequences cut by late Cretaceous and early Tertiary intermediate volcanics, which are covered, especially in southern Peru, by Tertiary volcanics of great thickness (James, 1971b). The Eastern Cordillera, on the other hand, consists of thick metasedimentary rocks of mainly early Paleozoic age. Intrusives of mostly Mesozoic age cut these older rocks. During the Cenozoic the Altiplano has been a depositional basin for continental clastic sediments derived from both cordilleras (James, 1971b).

The jungle-covered lowland to the east of the Andes is the sub-Andes foreland basin, where Cenozoic continental clastic rocks of great thickness rest on a sequence of marine Paleozoic and marine and continental Mesozoic strata. A persistent system of west dipping thrust or reverse faults separates the Andes from the sub-Andes foreland basin. Foreland folds decrease in amplitude eastward toward the Brazilian shield (Suarez et al, 1983).

3. Gravity Data

We made gravity measurements at bench marks of leveling of Instituto Geografico Militar (IGM), in September to November of 1980 and in July and August of 1984. Fig. 1 shows the survey routes, some of which traverse from the coast across the high Andes down to flat lands of tributaries of the Amazon.

The reference stations used to calibrate gravity values are Lima-O and Arequipa-K (International Association of Gravity (IAG), 1974) for the 1980 survey, and Lima-O (Nakagawa et al., 1983), Arequipa-K (IAG, 1974), and Cuzco-B228 (Nakagawa et al., 1983) for the 1984 survey. For the 1984 survey it was fortunate to have three reference stations near the coast and the western and eastern margins of the high Andes, with which we were able to correct for the change of drift rate with altitude (see Nakagawa et al., 1983). We estimated the accuracy of the tie to be better than 0.2 mGal. A similar accuracy was also estimated for the 1980 survey.

Terrain corrections are very important in obtaining accurate Bouguer anomaly values since many of the measuring stations are situated in places of rugged topography in a height range between 0 and 5000 m. Unfortunately the terrain correction cannot be applied to all the data in a uniform way because of the limited coverage of large-scale topographic maps in Peru. Many

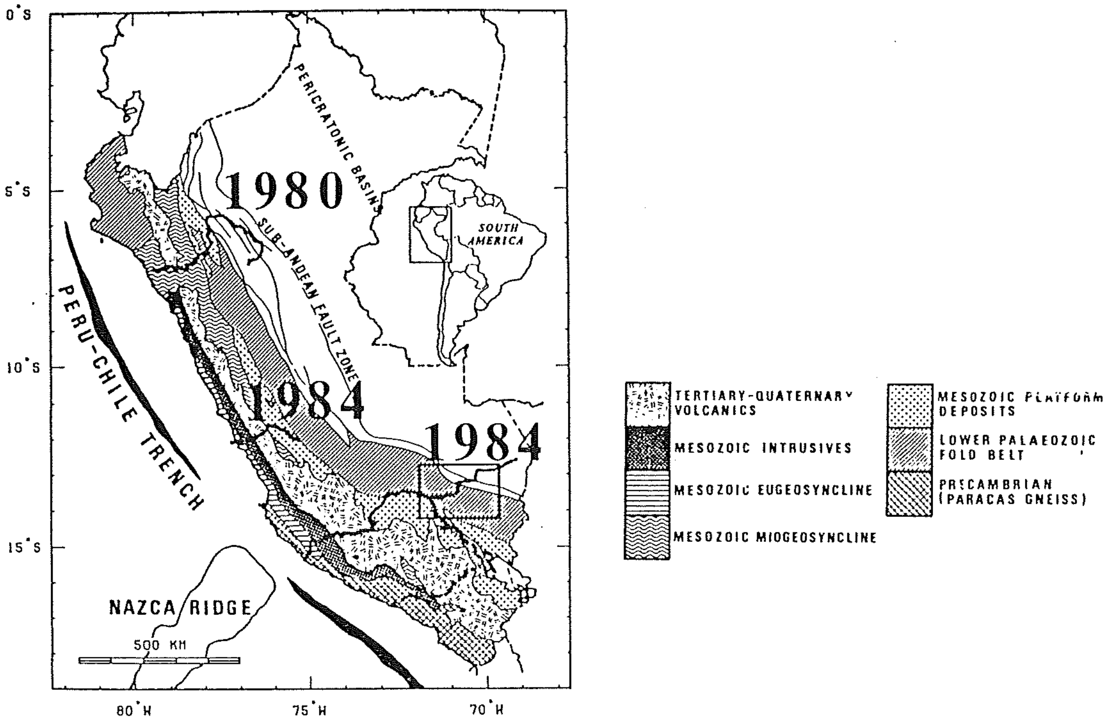

Fig. 1. Simplified geological map of Peru and locations of 1980 and 1984 gravity surveys.

of the 1/100,000 scale maps for the eastern parts of Peru have not yet been published. The 1/1,000,000 scale maps are available with contours, but they are too crude for corrections near the gravity stations. The largest contribution to terrain correction comes from topography within the range of 40 km or even 20 km from the station. The use of the 1/1,000,000 scale maps in this range in a hope of consistent correction for topography can result in a grossly erroneous Bouguer anomaly. To avoid the nonuniformity in reduced gravity values we were obliged at present to use simple Bouguer anomalies, admitting possible maximum errors of the order of 50 mGal. Although the relavant errors are considered much smaller than 50 mGal at most stations, there is always a possibility for the short-wavelength variation with maximum amplitude less than 50 mGal due to terrain effect. Such short-wavelength variation will be ignored in the following discussion.

Fig. 2 shows the profile along the Nazca route. Free air gravity values at sea were taken from Hayes (1966). The topographic profiles include not only the heights of the measuring points but also those of the mesh points read from the 1/1,000,000 map in a band 20 km length along the survey route. The scatter of the plots therefore gives a measure of ruggedness of topography, and their upper envelope defines the summit level.

Bouguer anomalies along the Juanjui route show two different trends to the east of the Andes. These two trends are the result of the complexity of the Juanjui route in its eastern part, where the Bouguer anomaly, as well as topography, changes rapidly in a direction parallel to the mountain axis. This section, therefore, must be interpreted with caution.

The Nazca profile (Fig. 2) is one of the best examples of a Bouguer anomaly profile across a mountain system, because of its extensiveness and straightness. This profile is characterized by (1) a sharp inlandward decrease of Bouguer anomaly at a rate of 3 mGal/km from the coast, (2) a large negative anomaly of about –400 mGal near the axis of the Western Cordillera, (3) a

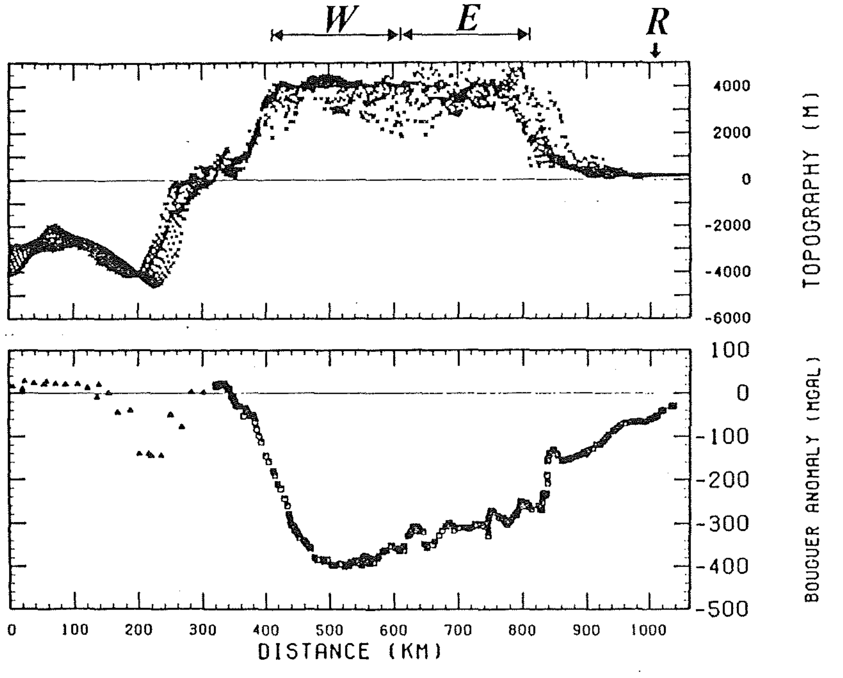

Fig. 2. Cross sections of Bouguer anomaly (square) and topography (cross) along the Nazca route. The anomaly at sea is free air anomaly (triangle). Note the symmetric feature of the Andes topography and the asymmetric feature of the gravity profile in the corresponding portion.

gradual increase at a rate of 0.5 mGal/km from the Western Cordillera to the Eastern Cordillera, (4) an abrupt increase of about 100 mGal across the western edge of the sub-Andes at the foot of the Eastern Cordillera, and (5) a slow increase at a rate of 0.8 mGal/km in the sub-Andes toward the Brazilian shield. The whole profile is thus quite asymmetric in spite of the approximately symmetric shape of the topographic profile.

The Arequipa profile landward of the coastal line is remarkably similar to the Nazca profile in the corresponding portion. The Cuzco profile approximately parallels the mountain axis and intersects the Nazca and Arequipa profiles at its northern and southern ends. The relative flatness of the Cuzco profile and the similarity between the Nazca and Arequipa profiles indicate that the Bouguer anomaly trends approximately parallel to the mountain axis in southern Peru. The maximum amplitude of negative anomaly of about –400 mGal in this region is significantly greater than that in northern Peru (–280 mGal), yet the rate of inlandward decrease from the coast is approximately the same, 3 mGal/km. The rate is anomalously high in central Peru along the Lima route, 5 mGal/km, a value consistent with that obtained by Bussel and Wilson (1985). The profile along this route is less complete because of fewer data points and a shorter stretch of the route.

4. Crustal Structure

The crustal structure beneath the Andes has already been studied by several authors; for example, by James (1971a) using surface wave dispersion data and by Ocola and Meyer (1973) and Couch et al. (1981) using gravity and seismic refraction data. Wilson (1985) reviewed seismic refraction surveys and surface wave studies in Peru and compiled six crustal models in the Peruvian Andes.

One may argue that the Nazca profile runs quite close to the northern end of the wide part of the Altiplano, so that the eastern part of the gravity profile could be strongly affected by the possible crustal thinning along strike to the northwest. Model calculation, however, indicates that such an effect is relatively small. The effect of cutoff was estimated in the following manner. The excess of the crustal thickness is assumed to be 20 km, a value appropriate for the Eastern Cordillera. The crust is 0.4 g/cm^3 lighter than the mantle. The thickened portion of the crust changes its width abruptly from 350 to 175 km across the crustal cutoff. Measurement is made along line AB at a distance of s km southeast of this cutoff. Calculations indicate that if line AB is about 60 km away from the cutoff, the asymmetry in gravity profile due to the edge effect becomes as small as 5 mGal. We define the actual cut-off location by the summit level of 3000 m at the NW end of the wide part of the Altiplano so as to be consistent with the definition of the crustal boundaries in the NE-SW direction. According to this definition the Nazca route is located certainly more than 60 km southeast of the crustal cutoff. This distance guarantees that the Nazca profile will vell interpreted with a two-dimensional model such as the one that will be developed below.

Before going into the model construction for the crust, however, we require some consideration of the effect of lithospheric plates. Fig. 3a shows the model of lithospheric plates. The mantle part of the Nazca plate has an excess density of 0.05 g/cm^3 and extends from a depth of 10 to 60 km under the ocean. The upper surface of its subducted portion is delineated by that of the Wadati-Benioff zone beneath the Andes. It is more difficult to model the South American plate beneath the Amazon, since few data, independent of gravity, are available. We assume that the South American plate is underthrusting beneath the Eastern Cordillera, following the suggestion by various authors (e.g., Suarez et al., 1983). The amount of plate bending at the sub-Andes may then be inferred from the thickness of the sedimentary cover there (Lyon-Caen et al., 1985). The sedimentary prism in the central and northern Peru consists of about 8000 m of Mesozoic-Cenozoic strata that overlie Paleozoic strata at least 1000 m thick (Megard, 1984). In

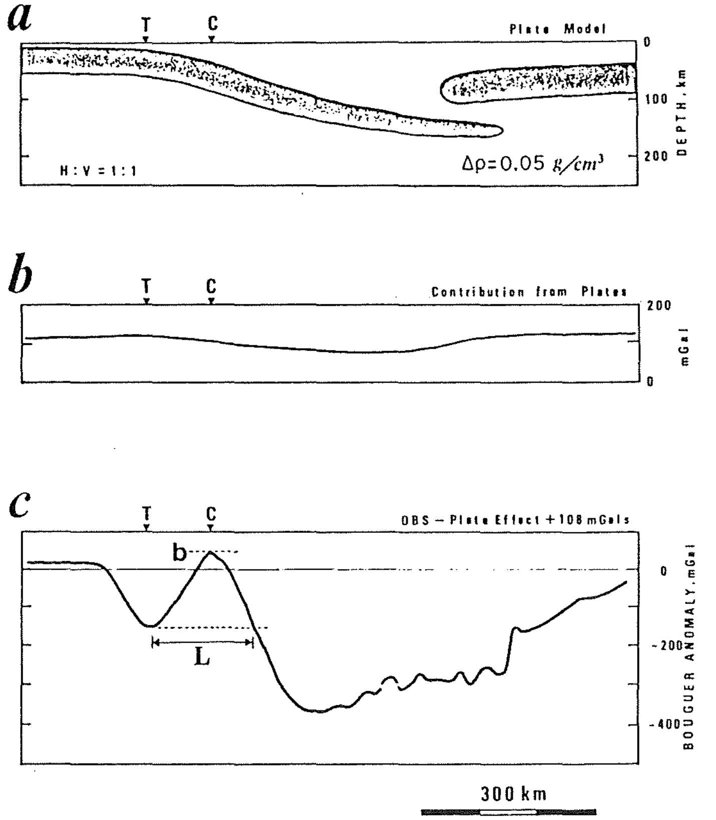

Fig. 3. (a) Model of the Nazca plate and the South American plate. Only their mantle parts are shown. T and C represents the positions of trench and coast, respectively. (b) Effect of the plates on gravity. (c) Observed Bouguer anomaly along the Nazca profile after the removal of the plate effect. Distance L is defined in this diagram, and b represents the gravity value at the coast.

some basins of northern Peru where exploration for oil has been active, depths up to 10 km have been reported (see Suarez et al., 1983). This line of evidence suggests that the plate bends beneath the sub-Andes with a vertical deflection of the order of 10 km, a value somewhat smaller than the corresponding value of 14 km in the Bolivian Andes (Lyon-Caen et al., 1985). It is not known how the plate extends further westward. Lyon-Caen et al. (1985) estimated a westward extension of at least 150 km for the Bolivian Andes based on a flexure model. We assume, for the Peruvian Andes, that the plate extends 100 km beneath the Eastern Cordillera with a vertical deflection of 20 km. We also assume that the deflection becomes negligibly small beneath the Brazilian shield at a distance of 200 km to the east of the sub-Andes. There would be no controlling data for or against these assumptions, which are made simply to obtain a very rough idea of the plate effect. The crustal thickness of the Brazilian shield is assumed to be about 35 km (Lyon-Caen et al., 1985), and the plate thickness is adjusted to have the gravity effect similar to that from the Nazca plate under the deep Pacific Ocean. The bottom of the South American plate then lies at a depth of about 90 km. The overall feature of this model is shown in Fig. 3a, and its gravity effect is given in Fig. 3b. The gravity efffect has a broad relative minimum of about –50 mGal in the Altiplano. To construct a crustal model, in principle, the effect has to be removed from the observed Bouguer anomaly profile as shown in Fig. 3c. There are, however, so many ambiguities in modeling the lithospheric plates quantitatively that the effect is relatively small. In what follows we construct crustal models ignoring the possible plate effect. The effect will be considered qualitatively when interpreting the resultant crustal models.

Fig. 4 shows our preliminary models of the crust beneath the Peruvian Andes. The computed gravity profiles are compared with the observed ones. To derive these models we assumed that the densities of the upper crust, lower crust, and mantle are 2.7, 2.9, and 3.2 g/cm^3, respectively, and that the thicknesses of the upper crust and lower crust are roughly equal. Only when necessary was the surface layer laterally divided into at most a few segments by referring to the geologic map published by Instituto Geologico Minero y Metalurgico (INGEMMET) (1977).

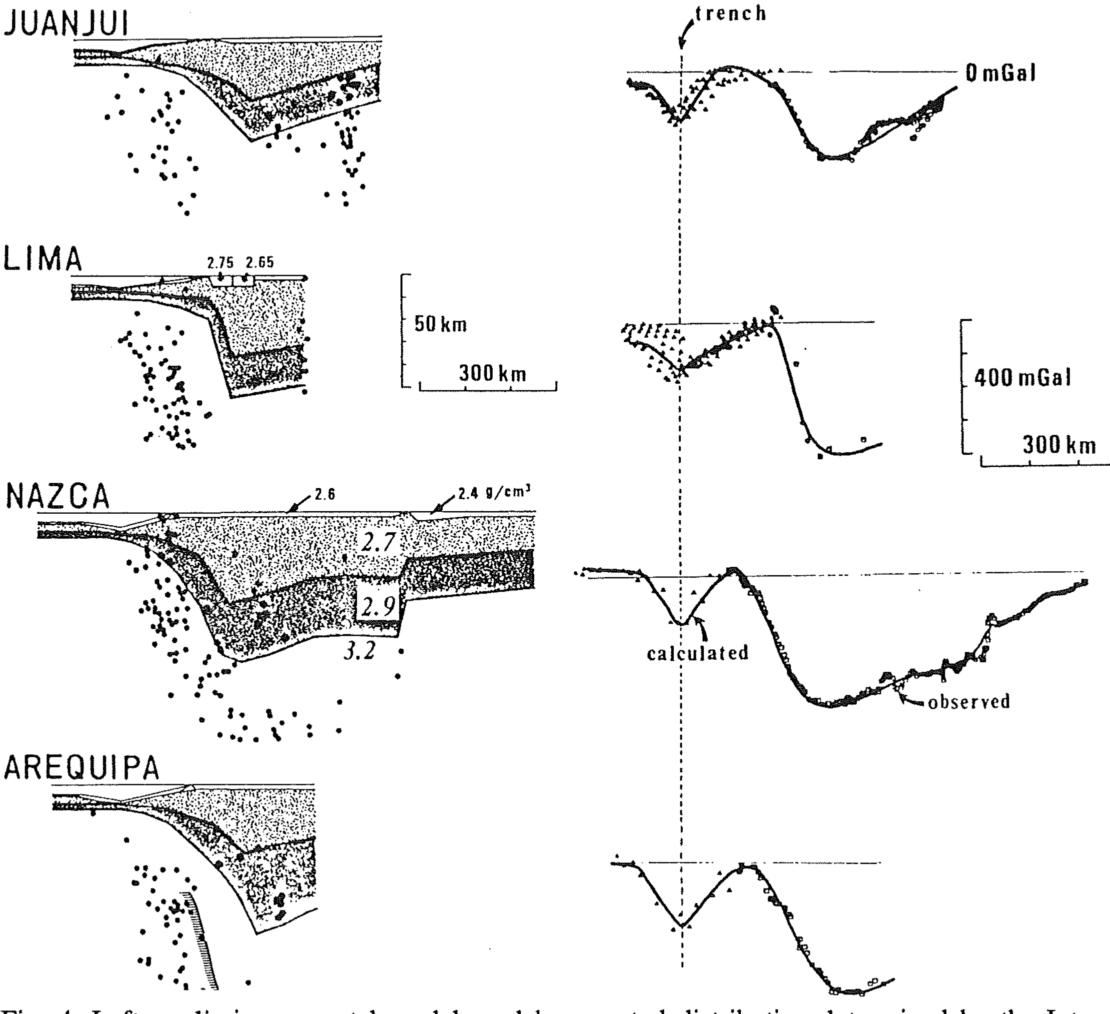

Fig. 4. Left: preliminary crustal models and hypocentral distribution determined by the International Seismological Centre (ISC) during the period from 1964 to 1981. The earthquakes were selected such that their hypocenters were determined by more than 30 stations with depth constraint. Superposed on these earthquake plots is the top of the Wadati-Benioff zone determined from the local network data (Boyd et al., 1984). For the locations of these four crustal sections, see Fig. 14. Densities of the surface layer, upper crust, lower crust and upper mantle are 2.6, 2.7, 2.9, and 3.2 g/cm^3, respectively, common to the four models. The surface layer density is changed when necessary by referring to the geologic map by INGEMMET (1975). Right: computed gravity anomaly (solid line) superposed on the observed anomaly (symbol).

The crustal models under the sea, which are not our major concern, are simplified versions of Couch et al. (1981).

We first obtained a model for the Nazca section, the most complete cross section extending from the coastal lowlands, across the Andes, to the jungle-covered lowland. The gravity profile computed for this model was then compared to the other sections. The model was successively changed so as to achieve a better fit. For the Juanjui section the model was constructed so that the synthetic profile passes through the midpoint between the N and S trends of the observed profile. The resulting model is therefore less reliable in its eastern part. For the Lima section we introduced a pair of slightly heavy and light blocks ($\pm$ 0.05 g/cm^3) in a transition zone from the coast to the Western Cordillera to account for the anomalously steep gradient in Bouguer anomaly. These blocks simulate the basic plutons and the coastal batholith, respectively (Bussel and Wilson, 1985).

The characteristic features of the models so derived are as follows.

1. The crustal thickness takes a maximum beneath the topographic maximum of the Western Cordillera. The maximum thickness is about 45 km in northern Peru, 55 km in central Peru, and 65 km in southern Peru, in contrast to the assumed thickness of about 35 km for the crust at the eastern end of the sub-Andes foreland basin. Although these absolute values are somewhat model-dependent, their relative magnitudes would be less so. The Peruvian Andes progressively thicken their crustal root as they go down to the south. This tendency is consistent with the Moho depth contour derived from a surface wave dispersion study (James, 1971a).

2. The Moho, at a depth of less than 25 km near the coast, is steeply dipping inlandward as emphasized by Ocola and Meyer (1973). For example, the Moho in southern Peru deepens by 40 km over a horizontal distance of 150 km along the western slope of the Andes. The Moho in central Peru may be even more steeply dipping (but see also Bussel and Wilson (1985)).

3. The Western Cordillera and the Eastern Cordillera are dissimilar in crustal structure. The crust is thicker to the west than to the east beneath the Andes. Such an asymmetry in crustal structure is in contrast to the remarkable symmetry in topography. The asymmetric crustal structure is also seen in the model of Ocola and Meyer (1973), but a significant inconsistency between the model and the observation makes this point less convincing.

4. There is a steplike change in Bouguer anomaly along the eastern slope of the Eastern Cordillera (see Fig. 2). It is difficult to interpret this large step solely by a shallow structure. The steplike change occurs between two villages, Marcapata and Quince Mil, along the eastern slope of the Eastern Cordillera where it consists of the early Paleozoic metamorphics. To the east of Quince Mil the sub-Andes foreland basin extends eastward, where it is covered by thick Tertiary to Quaternary sediments. Quince Mil thus separates denser rocks to the west from lighter rocks to the east in a sense opposite to that expected from the observed steplike change in gravity anomaly.

The short-wavelength component of the observed step may be due to the terrain effect. The long-wavelength component, however, cannot be attributed to this effect. We interpret the observed step as the composite effects of the surface topography and the deep structure. In our model there is a discontinuous change in crustal thickness across the sub-Andes, which contributes to the long-wavelength component of the observed step (Fig. 4). The remaining short-wavelength component is significant along the steep slope at the eastern side of the Eastern Cordillera, with a maximum value of the order of 50 mGal at the midpoint near Marcapata. This feature is remarkably consistent with what is expected as a terrain effect. Unfortunately no detailed topographic maps are available in this most critical region. Our interpretation must be finally checked when such maps become available. The possibility of a lithospheric plate effect does not help the difficulty associated with a smooth model. The correction for the plate effect further enhances the tendency of relative flatness over the Eastern Cordillera and the tendency of eastward increase over the foreland basin. The steplike change across the sub-Andes remains essentially unchanged. The Nazca profile thus strongly suggests that the sub-Andes is the first-order discontinuity extending down to a depth as deep as 60 km.

5. The sub-Andes foreland basin is covered by Cenozoic clastic rocks of great thickness resting on a sequence of Paleozoic and Mesozoic strata, the total thickness being roughly 10 km (Suarez et al., 1983; Megard, 1984). This layer gradually thins toward the Brazilian shield as suggested by Lyon-Caen et al. (1985) for the Bolivian Andes. Such an eastward thinning of the basin sediment is a required feature if we wish to keep the crustal thickness at the eastern end of the basin greater than 30 km.

Our modeling strategy was to vary layer thicknesses rather than layer densities. Within this framework we consider that the characteristic features described above would remain unchanged upon further improvement of the model. Nevertheless it must be borne in mind that the result of our strategy is an extremum and that lateral density variation is likely to exist. If the average crustal density of the Brazilian shield is, as is quite likely, greater than that of the Andes, for example, then the Andean crust need not be so thick as in our model. Similarly the discontinuity in crustal thickness across the sub-Andes may not be so large as in our model. The Andean crust can also be thinner than our model if a plate effect such as that shown in Fig. 3 is taken into account. Gravity data poorly control the density and layer thickness independently but better constrain their product. Note that a possible lateral variation of crustal densities and a possible effect of subducting plates both tend to reduce the crustal thickness estimated for the Andes.

Further discussion about the mechanism of mountain building in the Central Andes is treated elsewhere (Kono et al., 1989).

References

Boyd, T., A. Snoke, I. S. Sacks, and A. Rodriguez, *Bull. Seismol. Soc. Am., 74*, 557–566, 1984.

Bussel, M. A., and C. D. V. Wilson, *J. Geol. Soc. London, 142*, 633–641, 1985.

Couch, R., R. Whitsett, B. Huehn, and L. Briceno-Guarupe, in *Nazca Plate, Mem. Geol. Soc. Am., 154*, 703–726, 1981.

Hayes, D. E., *Mar. Geol., 4*, 309–351, 1966.

IAG, International Gravity Standardization Net 1971, *Spec. Publ., 4*, IAG, Paris, 1974.

Kono, M., Y. Fukao, and A. Yamamoto, *J. Geophys. Res.*, in press, 1989.

IGM, Mapa fisico politico, scale 1:1,000,000, Lima, Peru, 1978.

INGEMMET, Mapa geologico del Peru, scale 1:1,000,000, Lima, Peru, 1975.

James, D. E., *J. Geophys. Res., 76*, 3246–3271, 1971a.

James, D. E., *Geol. Soc. Am. Bull., 82*, 3325–3346, 1971b.

Lyon-Caen, H., P. Molnar, and G. Suarez, *Earth Planet. Sci. Lett., 75*, 81–92, 1985.

Megard, F., *J. Geol. Soc. London, 141*, 893–900, 1984.

Nakagawa, I., S. Nakai, R. Shichi, H. Tajima, S. Izutuya, Y. Kono, T. Higashi, H. Fujimoto, M. Murakami, K. Tajima, and M. Funaki, Preprint, 117 pp., Kyoto University, Kyoto, 1983.

Ocola, C. L., and R. P. Meyer, *Geol. Soc. Am. Bull., 84*, 3387–3404, 1973.

Pilger, R. H., Jr., *Geol. Soc. Am. Bull., 92*, 448–456, 1981.

Suarez, G., P. Molnar, and B. C. Burchfiel, *J. Geophys. Res., 88*, 10403–10428, 1983.

(in press in Journal of Geophysical Research)

MOUNTAIN BUILDING IN THE CENTRAL ANDES

Masaru KONO
Department of Applied Physics, Tokyo Institute of Technology, Tokyo 152, Japan

Yoshio FUKAO and Akihiko YAMAMOTO
Department of Earth Sciences, Nagoya University, Nagoya 464, Japan

1. Introduction

The formation of the Andes is an important and interesting problem in global tectonics as it is a very large mountain chain in length (more than 8000 km), and in width (sometimes more than 400 km), as well as in height (close to 7000 m). Between about 13°S and 27°S, the mountain ranges are most well developed forming parallel chains of highest mountains. The "Central Andes" in this paper refers to this area of the Andean chain, which covers parts of Peru, Chile, Bolivia, and Argentina. In contrast to the Himalaya, which is a continent-continent collision boundary, the Andes is a mountain chain associated with the subduction of an oceanic lithosphere below the continental plate, similar to the island arcs on the western edge of the Pacific. In this respect, the Andes is often called a continental arc. Both the island arcs and continental arcs are characterized by deep trenches, active volcanoes and deep earthquakes. However, there are marked differences between the two arcs, which should be related to the different tectonic processes occurring in these arcs.

The highest peaks in the Central Andes form distinct parallel chains several hundred kilometers apart; the Western and Eastern Cordilleras. The highest peaks in both chains attain heights of more than 6500 m. But the most prominent feature of the Central Andes is not the parallel mountain chains themselves but the very flat plateau between them: the Altiplano of Bolivia and southern Peru and the Puna of Argentina, which have a nearly constant height of about 4000 m. In other words, the most fundamental landshape in this area is the trapezoidal form of the Altiplano-Puna, while the Western and Eastern Cordilleras may be thought of as the volcano chain on the western edge of the plateau and dissected eastern edge of the plateau, respectively. The high peaks occupy only small areas in both Cordilleras, and so the hypsometry is dominated by the altitude of the plateaus. Accordingly, if we project the topography along the trend of the mountain chain, the mountains themselves are not very prominent feature. This can be compared with the similar situation in the Himalaya-Tibet section (e.g., Kono, 1974). The maximum width of the Altiplano-Puna is about 450 km and is not as large large a feature as the Tibetan plateau where the width is of the order of 1000 km and the mean height is 5000 m. However, it is a big question how this large-scale crustal feature is produced and supported. In the following, we present summary of various observations related to the process of formation of the Central Andes, and then try to construct a tectonic model which is consistent with these observations.

2. Observational Data from the Central Andes

Seismicity and Earthquake Mechanisms. In the Central Andes region, shallow earthquakes are most abundant between the coast and the Peru-Chile trench. This is certainly expected as a strong coupling is suspected between the oceanic (Nazca) and continental (South American) lithospheres. Once in the continent, the number of shallow earthquakes gradually decreases to a low level. However, as pointed out by many authors (Fukao, 1982; Suarez et al. (1983; Chinn and Isacks, 1983; Jordan et al., 1983; Froidevaux and Isacks, 1984), considerable number of earthquakes are again observed where the Eastern Cordillera ends and the Amazon basin begins. The shallow earthquakes abruptly end here, and no more events are observed in the continental crust of the Amazon Basin in the Brazilian shield. In contrast, considerable activity is observed in the central Peru even below the mountain area. The almost bimodal distribution of the shallow earthquakes is a peculiar characteristic of the Altiplano-Puna. In the continent-continent collision zones such as the Himalaya, the distribution of the shallow events are more diffuse and there is no indication of bimodality. This is an interesting feature when we consider the tectonic situation prevailing in the Central Andes.

Stauder (1973, 1975), Suarez et al. (1983), and Chinn and Isacks (1983) obtained source mechanisms of shallow earthquakes in this area. The earthquakes near the trench are of shallow-angle reverse fault type with slip direction of east by northeast, which is nearly parallel to the present direction of the movement of the Nazca plate relative to the South American plate. These mechanisms undoubtedly represent the relative motion between the oceanic and continental lithospheres at present. As their coupling is very strong (Uyeda and Kanamori, 1979), very big earthquakes such as the Chilean earthquake of 1960 take place. On the other hand, most of the shallow earthquakes below the Eastern Cordillera show source mechanisms of reverse fault type with compressive axis in east-west direction. The fault planes associated with these earthquakes are considered to be the one which dips to the west, as such faults actually occur abundantly in surface outcrops in this region (e.g., Bellido, 1979; Suarez et al., 1983). They form a conspicuous zone of reverse faults in the foreland basin to the east of the Eastern Cordillera.

Deformation of Layers on the Altiplano. A remarkable fact about the Altiplano, especially in the central and western part, is that, despite its high altitude and vast horizontal extent, significant amount of deformation cannot be found for geologic formations producing the Altiplano. Where sections of geological strata are exposed due to cutting by rivers or by the cliffs at the central and western parts of the Altiplano, the strata are astonishingly flat and deformations (faulting and folding) are minimal.

The lack of deformation is not restricted to the southern Peru portion, but seems to be a peculiar characteristic of the Altiplano. Noble et al. (1979) reported that, although the Mesozoic Yura formation is moderately deformed, the Nazca tuffs with K-Ar age of 18-22 Ma capping the altiplano were completely undeformed. Rutland (1971) noted that folding became less intense in the Tertiary and folds have large wavelength in the Altiplano of northern Chile. The lack of severe deformation can be appreciated by the inspection of small scale geologic maps of this area; the distribution of formations are quite simple in the Altiplano-Puna compared to the Eastern Cordillera where many formations with different ages are exposed, sometimes with significant amount of deformations. Thus the surface layers, at least in the center and west of the Altiplano, seem to have been elevated to the present height without much distortion affecting the layers. The situation may be slightly different between the northern and southern Central Andes. Allmendinger (1986) pointed out that the Altiplano and the northern Puna generally show little neotectonic activity, while the southern Puna is neotectonically active and a few crustal earthquakes are observed there.

Other geomorphological evidences also suggest that at least the surface layers of the Altiplano have not experienced heavy deformation since their formation. In conjunction with this, it is interesting to note that the mountains of the Western Cordillera are not under compression. Extensional deformation such as normal faults were reported form this area. Some of the extensional features may correspond not exactly to the present stress state but to that of earlier period. We conclude that the stress regime in the western part of the Altiplano and the Western Cordillera is almost neutral, with local tensional patches as indicated by normal faults.

The mountain ranges are also well developed in the Eastern Cordillera, but the stress state seems to be completely different; abundant reverse faults are observed while normal faults do not exist in this area. This is confirmed by surface observations as well as from the study of seismicity and earthquake source mechanisms (Stauder, 1973, 1975; Suarez et al., 1983; Chinn and Isacks, 1983). Therefore, the compressional regime seems to play an essential role in the Eastern Cordillera. We note, in passing, that the fault system is most developed in the foreland basin. Few faults exist on the western side of the Eastern Cordillera.

Gravity Anomalies and the Crustal Structure. Several seismic refraction experiments have been performed in the Central Andes, but crustal structures beneath the Central Andes are not well constrained by these studies, because of high attenuation and noisy record associated with the Altiplano. James (1971a) studied dispersions of surface wave traveling across and along the Andes chain and estimated the depths to the Moho. His contours show that the crustal thickness is over 70 km beneath the Western Cordillera and gradually diminishes to the east to a value of 55 to 60 km below the Eastern Cordillera.

In 1980 and 1984, we performed traverses crossing the Central Andes in Peru, measuring gravity values at bench marks with precise altitude information at a separation of one to three kilometers. Details of gravity measurements, calibration, and gravity corrections are described in the accompanying paper (Fukao et al., 1989). The longest of these profiles is the one connecting Nazca on the Pacific coast with Puerto Maldonado on the Amazon Basin, passing through Puquio, Chalhuanca, Abancay, Cuzco, and Mazuco. This route crosses the entire section of the coast–Western Cordillera–Altiplano–Eastern Cordillera–Amazon Basin. As the topography is essentially two-dimensional to the southeast of this route, we may take this as a gravity profile characteristic to the Central Andes.

The prominent features of the gravity anomalies obtained by Fukao et al. (1989) from the traverse crossing the Altiplano, from west to east, can be summarized as follows. From the coast to inlands, the Bouguer anomaly decreases steeply, and the minimum value of about –400 mGal is reached just below the mountains of the Western Cordillera. Although the surface topography is almost symmetric and suggests a similar structure below the Eastern Cordillera, gravity data show that it is not the case. The magnitude of the negative Bouguer anomaly gradually decreases from west to east and reaches to a value of about –280 mGal below the Eastern Cordillera. The crustal model consistent with the gravity anomalies has a Moho depth of 65 km below the sea level under the Western Cordillera and 55 km under the Eastern Cordillera (Fukao et al., 1989). The thinning of the crust from west to east suggested from the Bouguer anomaly profile is in good agreement with the structure obtained by dispersion of surface waves (James, 1971a). A discontinuous jump of Bouguer anomaly occurs where the Eastern Cordillera rapidly lose height to reach the flat lands of the Amazon Basin. This step is nearly 150 mGal in magnitude, and suggest a sudden change in the crustal thickness at the junction of the Andes and the stable continent. In the Amazon Basin, the Bouguer anomaly gradually approaches to the zero level.

The asymmetry of the Bouguer anomaly in spite of the apparent symmetry of the topography is a fundamental feature of the Central Andes and suggests that the formation process may also be asymmetrical.

Distribution of Volcanoes and Recent Volcanic Rocks. An enormous amount of Cenozoic volcanic rocks distribute in the Central Andes of Peru, Bolivia, Chile, and Argentina. In the central and northern Peru, the volcanic rocks are distributed in a narrow zone and intermittently. The amount of surface outcrops of young volcanics shows an abrupt increase in the southern Peru, coincident with the start of the Altiplano. In the Altiplano-Puna ranging from Peru through Bolivia to Chile and Argentina, young volcanic rocks are found very abundantly and in a wide spatial extent.

In the present Central Andes, the active volcanoes align in a single line forming a distinct volcanic front in the southern Peru and the northern Chile. However, if we look back for the entire Neogene period, the volcanic centers are not restricted to a narrow zone as it is today. The post-Miocene volcanoes are distributed almost all over the Altiplano, especially in Bolivia. One of the largest ignimbrite field (Frailes Plateau with an area of 13,000 km^2) is displaced from the present-day volcanic front by almost 300 km toward the continental side (Baker, 1981).. We suggest that the concentration of the active volcanoes at the volcanic front today is an exception rather than a rule for the distribution of the volcanic centers in the Central Andes. A much wider region has been under the influence of the volcanic activity, and a considerable amount of magmatic material should have been supplied to the crust beneath the Western Cordillera as well as the Altiplano. A wide distribution of volcanism is also consistent with high heat flow values observed not only near the Western Cordillera but in most part of the Altiplano (Uyeda and Watanabe, 1982).

We suggest that the volcanic activity in the Central Andes is perhaps distributed over a wide geographical extent covering most of the Altiplano, and that the Altiplano corresponds roughly to the area of magma generation associated with the subduction of the Nazca plate beneath the South American continent.

Timing of the Uplift of the Plateau. From a study of the ages of the ignimbrites in northern Chile, Rutland et al. (1965) concluded that the main phase of the uplift took place in the 6 Ma period between 4 and 10 Ma. They further suggested that the average rate of uplift is less than 0.5 mm/y based on the assumption that the Puna surface attained 4000 m in the 10 Ma period, and that this rate is similar to the other Tertiary mountain chains, such as the Himalaya or the Alps.

The ignimbrite activity must have been a spectacular one. After a relatively quiet period of Oligocene (Lahsen, 1982), the volcanic activity continued almost continuously between 24 Ma and present (Kussmaul et al., 1977). The Miocene and Pliocene ignimbrites distribute in the entire north-south extension of the Central Andes (Baker, 1981), and some of the ignimbrite plateaus cover an area of as much as 13000 km^2 (Francis et al., 1983). The total thickness of these ignimbrites are generally unknown (Kussmaul et al., 1977), but one estimate places it at about 1 km (Francis et al., 1983). As the Miocene volcanic activity is very extensive, it is quite natural to assume that it is a part of the most active phase of the mountain building.

That the uplift in the Central Andes is a very recent phenomenon is supported from other directions. Sebrier et al. (1985) showed from neotectonic studies of active faults that the mountain building process is going on at a high speed in the Quaternary. Even more direct estimate of the uplift rate was obtained by the fission-track dating method. Crough (1983) and Benjamin et al. (1987) dated Triassic plutonic rocks in Zongo valley of Cordillera Real in Bolivia and obtained the apatite ages of 5–15 Ma and zircon ages of 25–45 Ma for rocks with K-Ar ages of about 210 Ma (McBride et al., 1983). Since the tracks in apatite and zircon are annealed at about 100°C and 200°C, it is possible to estimate the uplift or erosion rate by assuming an appropriate geothermal gradient. From the detailed study of rocks at various altitude in Zongo valley, Benjamin et al. (1987) concluded that the uplift rate was small in the 20-40 Ma period (0.1–0.2 mm/y), but sharply increased between 10 and 15 Ma and attained a high rate of 0.7 mm/y at 3 Ma.

It is therefore reasonable to conclude that the main phase of the mountain building was within the Cenozoic and that the uplift was most severe since Miocene. However, this refers only to the most recent cycle of mountain building in the Central Andes. We will confine our discussions to this last cycle which started in Cenozoic and became very vigorous since Miocene.

3. A Model of Mountain Building in the Central Andes

The key element in considering the mountain building in the Central Andes is why and how the high plateau of the Altiplano-Puna was formed there. The absence of backarc basin behind the Andes is another important feature, but we think that the latter problem is closely related to the former. It is well known that geologic features with sizes of about 200 km or larger cannot be supported completely by the elastic stress in the surfacial layers. Yet, a substantial part of the Central Andes is not in the equilibrium state now. Our gravity study showed that the Moho lies about 65 km below the Eastern Cordillera and 55 km below the Eastern Cordillera, and the crustal thickness changes smoothly between these two values below the Altiplano (Fukao et al., 1989). Since this indicates only the Western Cordillera and the western part of the Altiplano is compensated by the crust, some sort of support is needed for the eastern half of the Altiplano and the Eastern Cordillera.

The problem of formation of high plateaus is a problem of how to thicken the crust and how to support the excess load if compensation is not complete. In either way, excess mass should be supplied for the topography. A number of ways can be conceived for this purpose (Fig. 1). The three cartoons on the right side of Fig. 1 show thickening of crust due to shortening. The folding model is what is inferred for the Chilean type subduction by Uyeda and Kanamori (1979). However, this model is not consistent with the fact that the observed deformation is very small in the Altiplano and the east-west asymmetry shown by the gravity data.

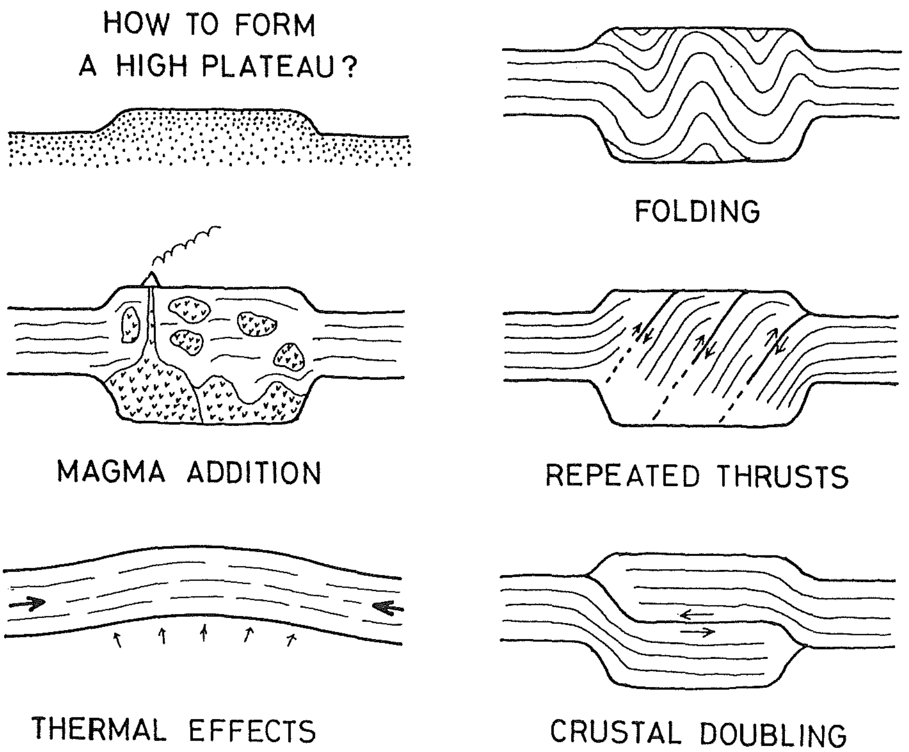

Fig. 1. Processes which can form an extended plateau of high altitude. The three on the right involve some sort of crustal shortening, while the two on the left relies on the supply of volcanic material or heat from below.

The crustal thickening by repeated underthrusting of the continental crust was the mechanism suggested by Suarez et al. (1983). However, such motions are unlikely in the western half of the Central Andes. The compressive stress regime only prevails in the Eastern Cordillera and the Amazonian foreland. Addition of subducted crustal material was proposed by Rutland (1971), but this proposal was based on the assumption of constant migration of the volcanic centers to the east with time. As this assumption was denied, we may discard this process from the possible crustal shortening mechanisms.

The two cartoons on the left side of Fig. 1 show ways to thicken the crust or at least to make the surface topography without shortening the crust. Volcanism is certainly a decisive factor in the Western Cordillera, but does not appear so in the east where the crust consists of Paleozoic to Mesozoic sedimentary and metamorphic rocks. Thermal expansion was studied by Froidevaux and Isacks (1984) by assuming that the Central Andes is essentially in equilibrium state. The idea is that the topography should be compensated either by the crust or by the lithosphere, because of the size of the Central Andes. However, we think this rather unlikely because of the east-west asymmetry; if the eastern part is supported by hot and lighter lithosphere underneath, similarly hot or even hotter lithosphere should exist under the Western Cordillera, leading to an over compasation of the surface load there.

We conclude that a single mechanism cannot create and support the topographic features of the Central Andes. Instead, we propose that two different mechanism operate simultaneously at the western and eastern halves: magma addition and crustal shortening (Fig. 2). Combination of these two are the main agents which contributed to make the Central Andes a unique mountain

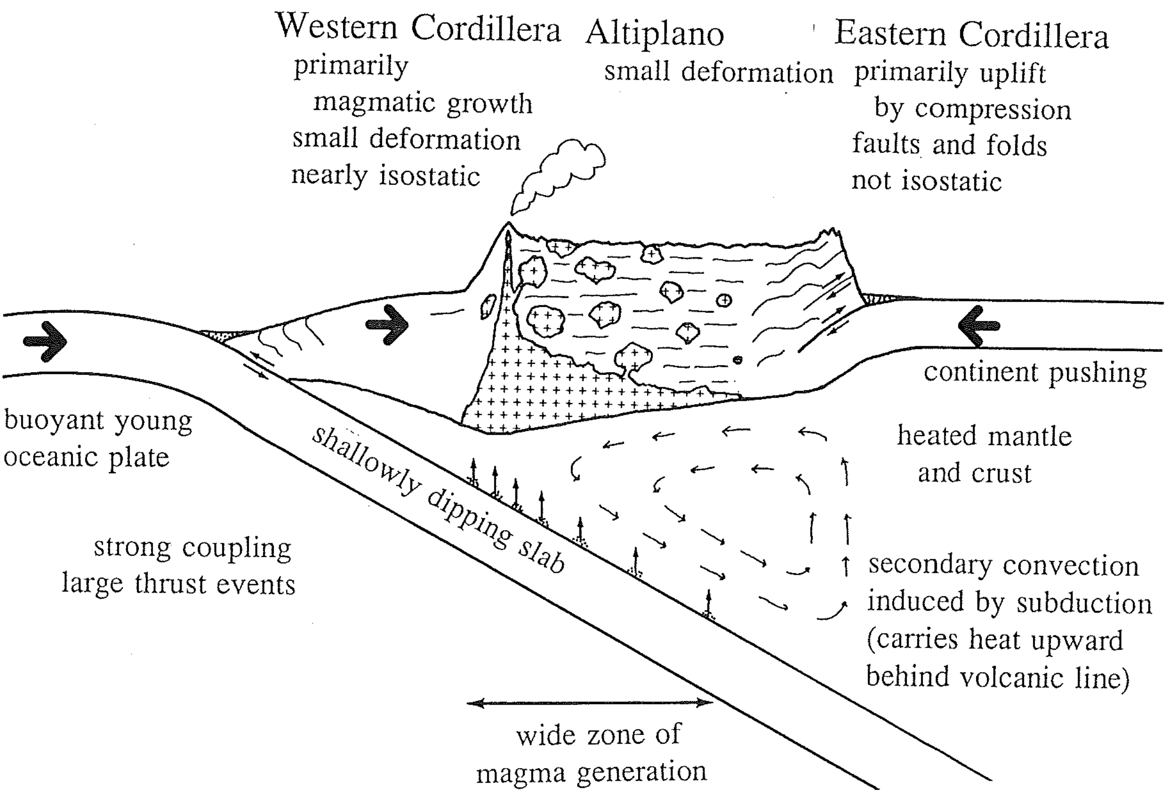

Fig. 2. A cartoon showing the processes operating in the formation of the Central Andes. Not to scale.

chain associated with a subduction zone; e.g., existence of high plateaus of wide extent and absence of backarc basins.

In the western half of the Central Andes, substantial amount of magma has been added to the crust from below, thickening the crust and raising the plateau without severely distorting the geologic formations. The reason for this is the shallow (10°–30°) and fast (about 10 cm/y) subduction of the young Nazca plate, a situation which must have continued since Miocene (Fig. 2). Subduction angle must have changed in the past reflecting the stress state of that time, but it stayed in the shallow range because of hot and buoyant nature of the Nazca plate, and the trenchward advance of South America (Uyeda and Kanamori, 1979). When the slab descends shallowly, magma may be generated in a wider zone across the arc, because the generation of magma is controled by the supply of water to the hot mantle by dehydration of hydrous minerals and thus dependent on depth of the slab (Tatsumi, 1986). The strong coupling between the down-going slab and the overlying mantle induces secondary convection in the mantle wedge (Toksoz and Bird, 1977), which helps magma generation to occur in a wide zone by dragging the water-bearing mantle material toward continental interiors (Tatsumi, 1986).

The continued shallow and fast subduction below the Central Andes since Miocene is consistent with the opening of the Atlantic Ocean and the ages of the sea floor inferred from the magnetic anomaly pattern analysis of the Nazca Plate (Couch and Whitsett, 1981; Couch et al., 1981).

When magma or mantle diapir ascends from the surface of the slab, only a small part of magma would reach to the surface. The rest are hindered to ascend to the surface by the compressive crust above and will either intrude in the crust or attach to the base of the lower crust and fatten it. This is because most of the Andean crust has continuously been under compressive stress regime since Miocene. In the present Western Cordillera, tensional field locally occurs and magma can reach the surface forming active volcanoes. Thus a clear volcanic front is formed parallel to the Pacific coast of South America. However, magma generation related to the formation of the Central Andes must have been more widely distributed. A hot or at least warm mantle must extend further eastward as suggested by the high heat flow observed there (Uyeda and Watanabe, 1982). Because of shallow subduction, magma will be produced considerably inland behind the volcanic front, although it does not appear on the surface due to the overlying compressive crust. Accretion of such volcanic materials is the main reason of the thickening of the crust observed in the Central Andes, especially in the Altiplano and the Western Cordillera.

In the Eastern Cordillera and Andean foreland basin, there is little evidence for extensive magma intrusion during Cenozoic age. Instead, thick Paleozoic rocks have been extensively folded and faulted. Crustal seismic activity shows horizontal compression almost perpendicular to the mountain axis. The sub-Andes foreland basin is formed by a series of folds and west dipping reverse faults active from at least Pliocene time to the present (Suarez et al., 1983; Allmendinger, 1986). Such evidence suggests that crustal shortening due to westward compression from the Brazilian Shield is a major agent of the mountain building in the Eastern Cordillera. Perhaps the Andean crustal block is heated from below even in its eastern part and it is on the whole hotter and softer than the Brazilian Shield block. When the soft Andes block is pushed by the hard block of the Brazilian Shield, intense deformation would occur in the Andes block but is concentrated to the region near the colliding boundary. A similar situation occurs in the Himalaya where deformation is concentrated near the boundary between hard and soft blocks (Molnar and Tapponier, 1979). We consider that the resultant crustal shortening and thickening with possible underthrusting of the Brazilian Shield block are the main reason for the uplifting of the Eastern Cordillera.

The two processes are strongest at both ends, but extends to the east or west losing their strengths gradually. The superposition of the two different processes is responsible for the creation and maintainance of the intermediate plateau, the Altiplano-Puna. Sediment fill from both eastern and western mountain ranges must have been substantial (James, 1971b), but this is secondary effect compared with the former two processes.

Thus our model of the mountain uplifting can be summarized as follows. Because of the relatively shallow subduction of the young oceanic plate, magma is generated in an extensive area above the descending slab. Accretion of magmatic material into the crust is most extensive at the volcanic front and progressively decreases eastward. The Andes block, even at its eastern end, is heated and softened by the extensive volcanism, and is pushed westward by the hard block of the Brazilian Shield. The deformation due to this push is severest at Amazonian foreland basin and the Eastern Cordillera, but also extends to the west with decreasing magnitude. These two mountain ranges thus represent two extreme cases in the process of mountain uplifting. The superposition of asymmetric processes to form relatively symmetric feature, the Altiplano-Puna, is the essential property of the Central Andes.

References

Allmendinger, R.W., *Geol. Soc. Am. Bull., 97,* 1070-1082, 1986.

Baker, M.C.W., *J. Volcanol. Geotherm. Res., 11,* 293-315, 1981.

Bellido, B.E., *INGEMMET Boletin, 22,* 54pp., 1979.

Benjamin, M.T., N.M. Johnson, and C.W. Naeser, *Geology, 15,* 680-683, 1987.

Chinn, D.S. and B.L. Isacks, *Tectonics, 2,* 529-563, 1983.

Couch, R. and R. Whitsett, in *Nazca Plate, Mem. Geol. Soc. Am., 154,* 569-586, 1981.

Crough, S.T., *Earth Planet. Sci. Lett., 64,* 396-397, 1983.

Francis, P.W., C. Halls, and M.C.W. Baker, *J. Volcanol. Geotherm. Res., 18,* 165-190, 1983.

Froidevaux, C. and B.L. Isacks, *Earth Planet. Sci. Lett., 71,* 305-314, 1984.

Fukao, Y., in Andes Science, edited by M. Kono, pp. 28-39, Tokyo Inst. Technology, 1982.

Fukao, Y., A. Yamamoto, and M. Kono, in press in *J. Geophys. Res.,* 1989.

James, D.E., *J. Geophys. Res., 76,* 3246-3271, 1971a.

James, D.E., *Geol. Soc. Am. Bull., 82,* 3325-3346, 1971b.

James, D.E., *Sci. Am., 229(2),* 60-69, 1973.

Jordan, T.E., B.L. Isacks, R.W. Allmendinger, J.A. Brewer, V.A. Ramos, and C.J. Ando, *Bull. Geol. Soc. Am., 94,* 341-361, 1983.

Kono, M., *Geophys. J. Roy. Astron. Soc., 39,* 283-299, 1974.

Kussmaul, S., P.K. Hormann, E. Ploskonka, and T. Subieta, *J. Volcanol. Geotherm. Res., 2,* 73-111, 1973.

Lahsen, A., *Earth-Sci. Rev., 18,* 285-302, 1982.

Molnar, P. and P. Tapponier, *Science, 189,* 419-426, 1975.

Noble, D.C., E. Farrar, and E.J. Cobbing, *Earth Planet. Sci. Lett., 45,* 80-86, 1979.

Rutland, R.W.R., *Nature, 233,* 252-255, 1971.

Rutland, R.W.R., J.E. Guest, and R.L. Grasty, *Nature, 208,* 677-678, 1965.

Sebrier, M., J.L. Mercier, F. Megard, G. Laubacher, and E. Carey-Gailhardis, *Tectonics, 4,* 739-780, 1985.

Stauder, W., *J. Geophys. Res., 78,* 5033-5061, 1973.

Stauder, W., *J. Geophys. Res., 80,* 1053-1064, 1975.

Suarez, G., P. Molnar, and B.C. Burchfiel, *J. Geophys. Res., 88,* 10403-10428, 1983.

Tatsumi, Y., *Geophys. Res. Lett., 13,* 717-720, 1986.

Toksoz, M.N. and P. Bird, *Island Arcs, Deep Sea Trenches, and Back-Arc Basins,* Maurice Ewing Ser., vol. 1, 379-393, Am. Geophys. Union, Washington, D.C., 1977.

Uyeda, S. and H. Kanamori, *J. Geophys. Res., 84,* 1049-1061, 1979.

Uyeda, S. and T. Watanabe, *Tectonophysics, 83,* 63-70, 1982.

(in press in Journal of Geophysical Research)

AUTHOR INDEX

ARAKI, Makoto see Itoh et al.

CHANNELL, James E.T. and M. Torii 28

DANHARA, Tohru see Itoh et al.

FUKAO, Yoshio, A. Yamamoto, and M. Kono 65

FUKAO, Yoshio see Kono et al.

FUNAHARA, Shoubu see Otofuji et al.

FURUKAWA, Masahide see Shima et al.

HAYASHI, Kenichiro see Ueno et al.

HAYASHIDA, Akira and H. Suzuki 64

HORIE, Ikuko see Liu et al.

HORIE, Ikuko see Morinaga et al.

HYODO, Masayuki, W. Sunata, E.E. Susanto, and H. Wahyono 31

IMAMURA, Hiroshi see Morinaga et al.

INOKUCHI, Hiroo see Miki et al.

INOKUCHI, Hiroo see Morinaga et al.

INOUE, Yasuko see Otofuji et al.

ISEZAKI, Nobuhiro see Miki et al.

ISEZAKI, Nobuhiro see Shima et al.

ITOH, Yasuto, M. Araki, I. Katsura, and T. Danhara 4

KANEOKA, Ichiro and M. Yuasa 53

KATSURA, Ikuo see Itoh et al.

KATSURA, Ikuo see Yamazaki and Katsura

KITAZATO, Hiroshi see Koyama and Kitazato

KONO, Masaru, Y. Fukao, and A. Yamamoto 73

KONO, Masaru see Fukao et al.

KOYAMA, Masato 39

KOYAMA, Masato and H. Kitazato 35

KURAMOTO, Tadashi see Morinaga et al.

LIU, Yu Yan, H. Morinaga, I Horie, H. Murayama, and Y. Yaskawa 21

MATSUDA, Jun-ichi see Miki et al.

MATSUMOTO, Kiyoto see Shima et al.

MIKI, Masako, H. Inokuchi, T. Matsuda, S. Yamaguchi, N. Isezaki, and K. Yaskawa 25

MORINAGA, Hayao, H. Imamura, H. Inokuchi, and K. Yaskawa 11

MORINAGA, Hayao, I. Horie, H. Murayama, Y.Y. Liu, T. Kuramoto, and K. Yaskawa 15

MORINAGA, Hayao see Liu et al.

MURATA, Fumiyuki see Otofuji et al.

MURAYAMA, Haruko see Liu et al.

MURAYAMA, Haruko see Morinaga et al.

NAKAJIMA, Tadashi 23

NEDACHI, Munetomo see Ueno et al.

NISHITANI, Tadashi and S. Sasaki 1

OTOFUJI, Yo-ichiro, Y. Inoue, S. Funahara, F. Murata, and Z. Zheng 59
SASAKI, Senichi see Nishitani and Sasaki
SHIMA, Nobukazu, K. Matsumoto, M. Furukawa, and N. Isezaki 50
SUNATA, Whyu see Hyodo et al.
SUSANTO, Eko Edi see Hyodo et al.
SUZUKI, Hiroyuki see Hayashida and Suzuki
TANAKA, Hidefumi and H. Tsunakawa 56
TORII, Masayuki see Channell and Torii
TSUNAKAWA, Hideo see Tanaka and Tsunakawa
UENO, Hirotomo, K. Hayashi, and M. Nedachi 41
WAHYONO, Hendro see Hyodo et al.
YAMAGUCHI, Satoru see Miki et al.
YAMAMOTO, Akihiko see Fukao et al.
YAMAMOTO, Akihiko see Kono et al.
YAMAZAKI, Toshitsugu 47
YAMAZAKI, Toshitsugu and I. Katsura 7
YASKAWA, Katsumi see Liu et al.
YASKAWA, Katsumi see Miki et al.
YASKAWA, Katsumi see Morinaga et al.
YUASA, Makoto see Kaneoka and Yuasa
ZHENG, Xilan see Otofuji et al.

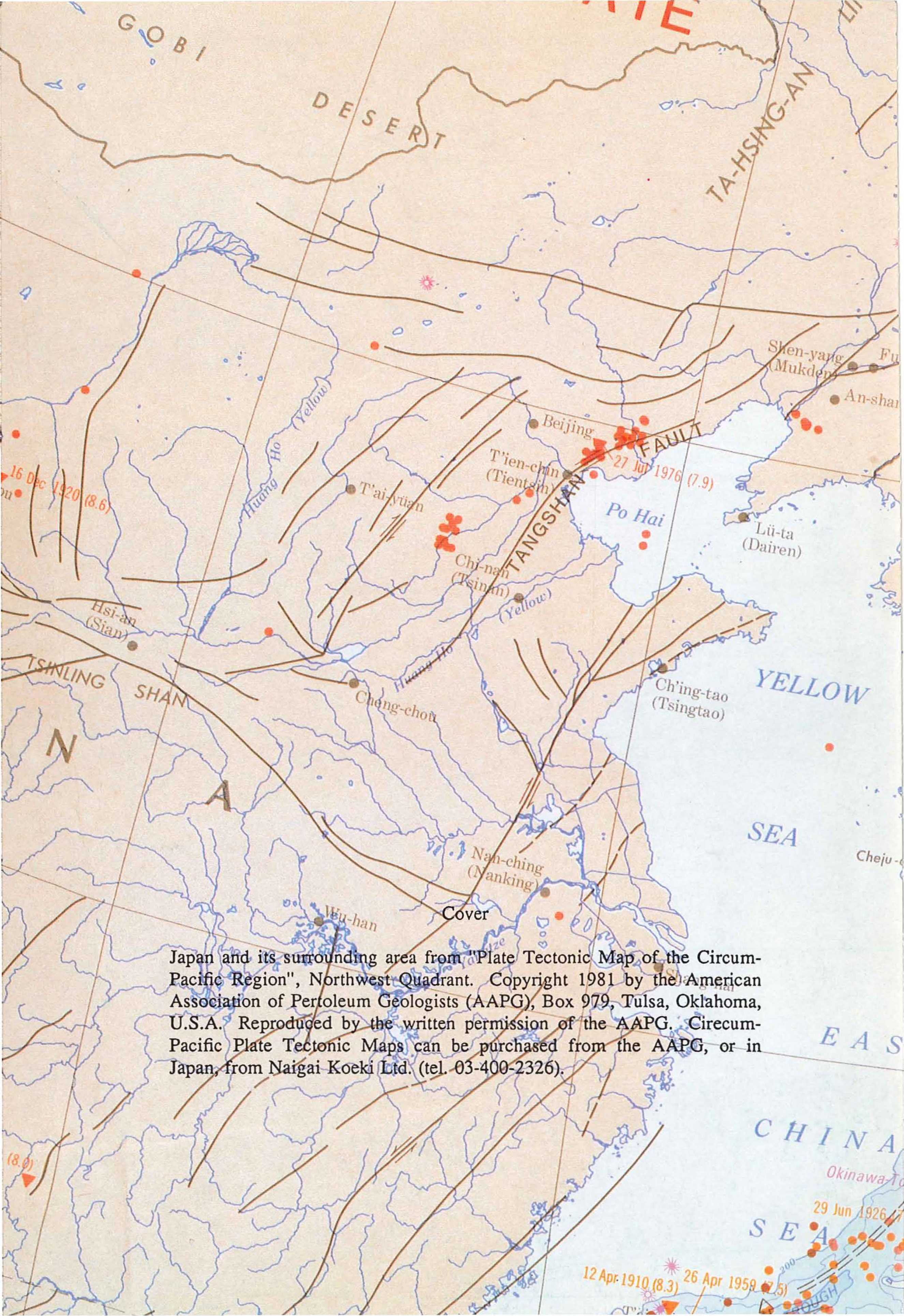

Cover

Japan and its surrounding area from "Plate Tectonic Map of the Circum-Pacific Region", Northwest Quadrant. Copyright 1981 by the American Association of Pertoleum Geologists (AAPG), Box 979, Tulsa, Oklahoma, U.S.A. Reproduced by the written permission of the AAPG. Cirecum-Pacific Plate Tectonic Maps can be purchased from the AAPG, or in Japan, from Naigai Koeki Ltd. (tel. 03-400-2326).